FOI-R--1179--SE
February 2004
ISSN 1650-1942
Technical report

SWEDISH DEFENCE RESEARCH AGENCY

Vanesa Isovic

Investigation of the Equivalence between Susceptibility Testing Performed With Many Angles of Incidence and Susceptibility Testing Performed With Many Frequencies

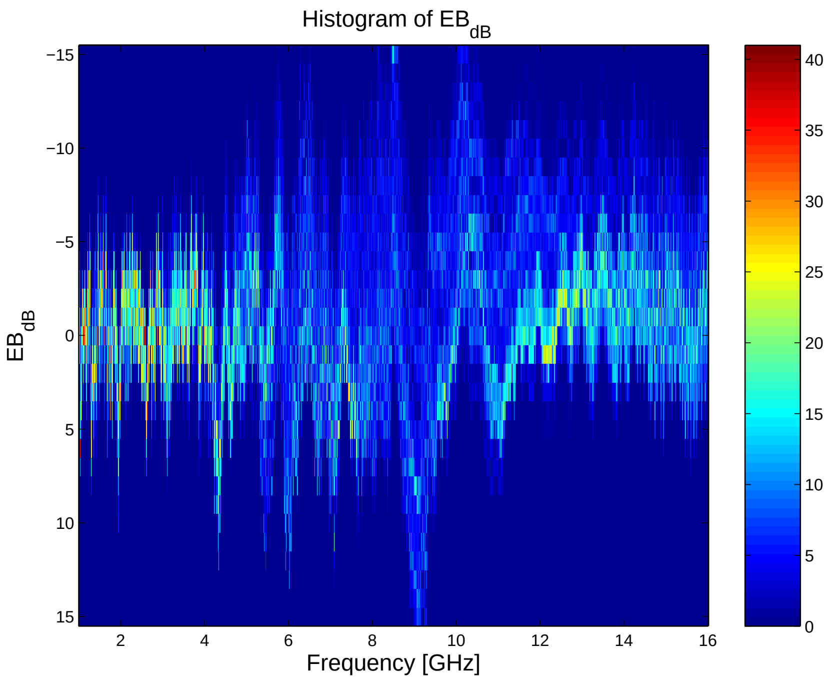

Sensor Technology
SE-581 11 Linköping

SWEDISH DEFENCE RESEARCH AGENCY

Sensor Technology
P.O. Box 1165
SE-581 11 Linköping

FOI-R--1179--SE

February 2004

ISSN 1650-1942

Technical report

Vanesa Isovic

Investigation of the Equivalence between Susceptibility Testing Performed With Many Angles of Incidence and Susceptibility Testing Performed With Many Frequencies

Issuing organization FOI – Swedish Defence Research Agency Sensor Technology P.O. Box 1165 SE-581 11 Linköping	**Report number, ISRN** FOI-R--1179--SE **Report type** Technical report **Research area code** 6. Electronic Warfare **Month year** February 2004 **Project no.** E3031 **Customers code** 5. Commissioned Research **Sub area code** 61 Electronic Warfare including Electromagnetic Weapons and Protection
Author/s (editor/s) Vanesa Isovic	**Project manager** Mats Bäckström **Approved by** Magnus Höijer **Sponsoring agency** Swedish Armed Forces **Scientifically and technically responsible** Magnus Höijer

Report title

Investigation of the Equivalence between Susceptibility Testing Performed With Many Angles of Incidence and Susceptibility Testing Performed With Many Frequencies

Abstract (not more than 200 words)

Electromagnetic radiation can cause disturbances in electronic systems. Considering the increased use of electronics in modern safety systems and the possible development of high-power microwave weapons (HPM), great concern is attached to Radiated Susceptibility (RS) testing and shielding of electronic equipment.

In RS testing of electronic equipment for microwave frequencies, thousands of different angles of incidence/polarisations may be needed to find the angle of incidence that corresponds to the worst susceptibility. However, in practice, one can often only afford to perform a test with a few angles of incidence.

In this Master of Science thesis, the results from low level coupling measurements, performed on three different objects, are used to investigate a method which could relieve the requirement of high angular resolution. The method uses only a few angles of incidence and polarisations, but a frequency interval consisting of frequencies that are adjacent to the frequency of interest. Statistical analysis of the electromagnetic coupling is performed as well.

The frequency substitution method seems to work for all frequencies, except at the tested objects' resonance frequencies. The χ^2-distribution with one degree of freedom can be used as a rough estimate of the distribution function of the coupling data.

This work was performed within the project *High Power Microwave Protection Methods for Network Based Defence.* The project was financially supported by the Swedish Armed Forces.

Keywords

RS-testing (Radiated Susceptibility), Directivity, Error bias, High Power Microwaves, Anechoic Chamber, Cumulative distribution function

Further bibliographic information The report is also published at Linköping University.	**Language** English
ISSN 1650-1942	**Pages** 108 p.
	Price acc. to pricelist

Utgivare	Rapportnummer, ISRN	Klassificering
Totalförsvarets Forskningsinstitut – FOI Sensorteknik Box 1165 581 11 Linköping	FOI-R--1179--SE	Teknisk rapport
	Forskningsområde 6. Telekrig	
	Månad, år Februari 2004	**Projektnummer** E3031
	Verksamhetsgren 5. Uppdragsfinansierad verksamhet	
	Delområde 61 Telekrigföring med EM-vapen och skydd	
Författare/redaktör Vanesa Isovic	**Projektledare** Mats Bäckström	
	Godkänd av Magnus Höijer	
	Uppdragsgivare/kundbeteckning Försvarsmakten	
	Tekniskt och/eller vetenskapligt ansvarig Magnus Höijer	

Rapportens titel (i översättning)

Undersökning av ekvivalensen mellan susceptibilitetstest utförda med många infallsriktningar respektive många frekvenser

Sammanfattning (högst 200 ord)

Elektromagnetisk strålning kan störa elektronik-utrustning. Med tanke på att elektronik i ökande utsträckning används i moderna säkerhetssystem, har EMC-provning (Electromagnetic Compatibility) och skärmning av elektronisk utrustning mycket stor betydelse. En annan faktor som har bidragit till detta är utvecklingen av HPM-vapen (Högeffektpulsad Mikrovågsstrålning).

Vid EMC-provning av elektronisk utrustning i mikrovågsområdet kan det krävas tusentals olika infallsriktningar/polarisationer för att träffa den infallsriktningen där känsligheten mot elektromagnetisk strålning är störst. I praktiken har man emellertid oftast endast råd att prova med ett litet antal infallsriktningar och polarisationer.

I detta examensarbete för civilingenjörsexamen undersöks resultaten från mätningar av skärmverkan på tre olika objekt. Detta för att finna en metod som kan ersätta kravet på hög vinkelupplösning. Vi föreslår en frekvenssubstitutionsmetod som bara använder ett fåtal infallsriktningar och polarisationer, men ett frekvensintervall runtomkring den aktuella frekvensen. En statistisk modell för den elektromagnetiska kopplingen studeras också.

Frekvenssubstitutionsmetoden verkar fungera för alla frekvenser förutom vid testobjektens resonansfrekvenser. χ^2-fördelningen med en frihetsgrad kan användas som en grov skattning av fördelningsfunktionen för den elektromagnetiska kopplingen.

Arbetet är genomfört inom projektet *HPM-skyddsmetoder för NBF*. Projektet är finanserat av Försvarsmakten.

Nyckelord

EMC-provning, Direktivitet, Error bias, Ekofri mäthall, HPM, Fördelningsfunktion

Övriga bibliografiska uppgifter — **Språk** Engelska

Rapporten är även utgiven på Linköpings universitet.

ISSN 1650-1942 — **Antal sidor:** 108 s.

Distribution enligt missiv — **Pris: Enligt prislista**

1 Introduction

1.1 Background

It is well-known that electromagnetic radiation may cause disturbances in electronic systems. Examples of this disturbance can be found in everyday life, e.g., disturbances in computers, TV and stereo systems caused by electromagnetic radiation from mobile phones. In a similar manner, the equipment in aeroplanes and hospitals may be affected by electromagnetic radiation which in worst case can cause serious functional disorders with crucial consequences.

Bearing in mind the increased use of electronics in modern safety systems in e.g. cars and aeroplanes, military as well as civil, it is not surprising that great concern has been attached to Radiated Susceptibility (RS) testing and shielding of electronic equipment in the recent years. Another factor that has contributed to this concern is the possible development of high – power microwave (HPM) weapons which transmit microwaves in order to disturb or damage electronics.

Different kind of measurements and test facilities are used to determine the shielding properties of a specific object. A measurement may be a high level RS testing or a low level coupling measurement. RS testing is performed in order to test the susceptibility of the Equipment Under Test (EUT) while low level coupling measurements are performed only to evaluate the fraction of the incident field that is coupled to the inside of the EUT. Three commonly used test facilities are the Anechoic Chamber (AC), the Reverberation Chamber (RC) and the Open Area Test Site (OATS). The test facilities, which can be used for performing a Radiated Susceptibility testing and a low level measurement respectively, are presented in Table 1 below.

	OATS	AC	RC
High level RS testing	**X**	*x*	**X**
Low level coupling measurements	*x*	**X**	**X**

Table 1. Test facilities for performing immunity testing. X – the test facility can be used, *x* – the test facility may be used but it is not preferable.

The combination RS testing – AC is marked with *x*. A Radiated Susceptibility test is difficult to perform in an Anechoic Chamber due to the large susceptibility of the absorbers to the high level fields (absorbers are destroyed). Nevertheless, RS testing is sometimes performed in an AC. One main reason is that RS testing with high electromagnetic field levels is not allowed to be performed outdoor in some countries. In those cases the absorbers are often cooled. The combination Low level coupling measurements – OATS is possible but often not preferable because of the noise from surroundings e.g. cellular phones, so this kind of measurement is more convenient to be performed indoor. However, the EUT is in some cases not moveable, e.g. a building and then the low coupling measurement has to be performed outdoor, and perhaps not even at an open area, but at a place with a lot of unwanted reflections.

In RS testing of electronic equipment for microwave frequencies, the susceptibility of the equipment differs between different angles of incidence and the polarisation of the incident field. The shielding varies typically with a factor of 100 – 10 000 between different angles of incidence and different polarisations (see Section 2). In general, it is not possible to decide in advance the polarisation and angle of incidence that causes the worst susceptibility. It can be shown, theoretically [1] as well as experimentally [2] that thousands of different angles of incidences might be needed in a test to find the worst angle of incidence with a reasonable uncertainty. However, one can often in practice only afford to perform the testing for a few polarizations and angles of incidence. Obviously, the probability is very small that the equipment will be irradiated in the most sensitive direction. Thus, there is a huge risk for undertesting, which might cause serious consequences.

Finding a method that would solve the problems of using only a few angles of incidence would be of great practical and economical interest. This has received a lot of attention in later discussions about RS testing at an Open Area Test Site or in an Anechoic Chamber. The worst angle of incidence, in general, varies with frequency. It seems reasonable to use this frequency dependence to, in some way, reduce the problem with the angular sampling requirement. An idea, being investigated in this Master of Science thesis, is to, instead of testing with many angles of incidence and polarisations use only a few angles of incidence and polarisations and vary the frequency around the chosen test frequency. One restriction in this method is that the susceptibility of electronic components does fundamentally vary with frequency which means that the frequency can not be varied too much.

A Reverberation Chamber (RC) is a test facility which can be used for doing susceptibility tests (Table 1). According to previous investigations, testing in a RC is not equivalent to the plane wave radiation in an AC [3], [4]. The results showed however a very good match between the RC data and the average AC data, taken over all angles of incidence and polarisations, so testing in a Reverberation Chamber gives the mean of the measurements in an Anechoic Chamber. Given this knowledge, there is an advantage with knowing the probability density function (pdf) for the Anechoic Chamber measurements data for different frequencies. Knowing the pdf would enable one to, after that a test is performed in the RC, calculate the probability of obtaining a value of a measurement data within some specific range of values, if the measurements in the Anechoic Chamber had been done for many different angles of incidence as well as many different polarisations.

1.2 This work

The potential in a testing methodology that uses the frequency dependence of the worst angle of incidence is investigated in this paper. The results from low level coupling measurements performed on three different objects are used for the investigation [3]. Low level coupling measurements are generally performed in order to evaluate the shielding effectiveness of electronic equipment. The coupling is given in terms of the receiving cross section.

From the measurements data, several fixed frequencies are selected for the investigation. For these frequencies, the maximum of the measurements data, taken over all used angles of incidence and polarizations, is determined. Then, consistent with the method that is to be investigated, instead of having a fixed frequency and all angles of incidence and polarisations, the frequency is varied around the chosen test frequency and only a few angles of incidence and polarisations are used. So now, we have a frequency interval which consists of frequencies that are adjacent to the chosen test frequency, and only a small number of angles of incidence and polarisations.

Statistical investigations of a quantity, that represents the measure of the agreement between the case when we have a frequency interval and only a few angles of incidence (the method that is to be investigated), and the case when we have a fixed frequency and many angles of incidence and polarisations (the ideal case) is done (see Section 3). In order to get useful statistics, 100 samples containing 3 angles of incidence each, are selected randomly. A theoretical statistical distribution, appropriate to describe the expected distribution of the resulting random outcomes is suggested. To decide whether our observed distribution is consistent with the expected theoretical distribution, the Chi squared Goodness-Of-fit test on the data is performed. If the results of this test show that the measurements are distributed as expected at some confidence level (e.g. 95%), then it could be possible to determine the probability of observing the given error bias, for an individual frequency, within given bounds. Some problems, like exposing the EUT to much lower (undertesting) or much higher (overtesting) stress levels than what is suitable to carry out a radiated susceptibility test, are discussed.

Later in the paper, an attempt to find a statistical model for the low level coupling measurements is done, using the same coupling measurements data as above, (see Section 4). The graphical statistical analysis resulted in a proposal of the distribution that fits the data best. The suggested distribution is χ^2-distribution with one degree of freedom. An evaluation of how well the measurements agree with the proposed distribution is done (with plots of variance and with the Chi squared Goodness-Of-fit test). The use of the probability density functions is also discussed in this work.

2 The method

2.1 Test objects and measurement method

The coupling measurements used in this paper have been performed on three different objects [3]. The measurements have been carried out in FOI's Anechoic (AC) Chamber. The objects were a test missile, an army radio and an avionics box. The tested objects were oriented in three perpendicular planes. For each plane the coupling measurements were done with both vertical and horizontal polarization. The frequency range was 0.5 – 18 GHz and the angular resolution was 1°. There were two probes, denoted as tp2 and tp4 in this paper, installed in each object for these measurements. The probes are assumed representative for the receiving properties of e.g. wires inside the tested objects. The tested object and the probe, as one, can be regarded as a receiving antenna. A simplified block diagram of the measurements setup is shown in Figure 1 and the picture of the probe is shown in Figure 2 below.

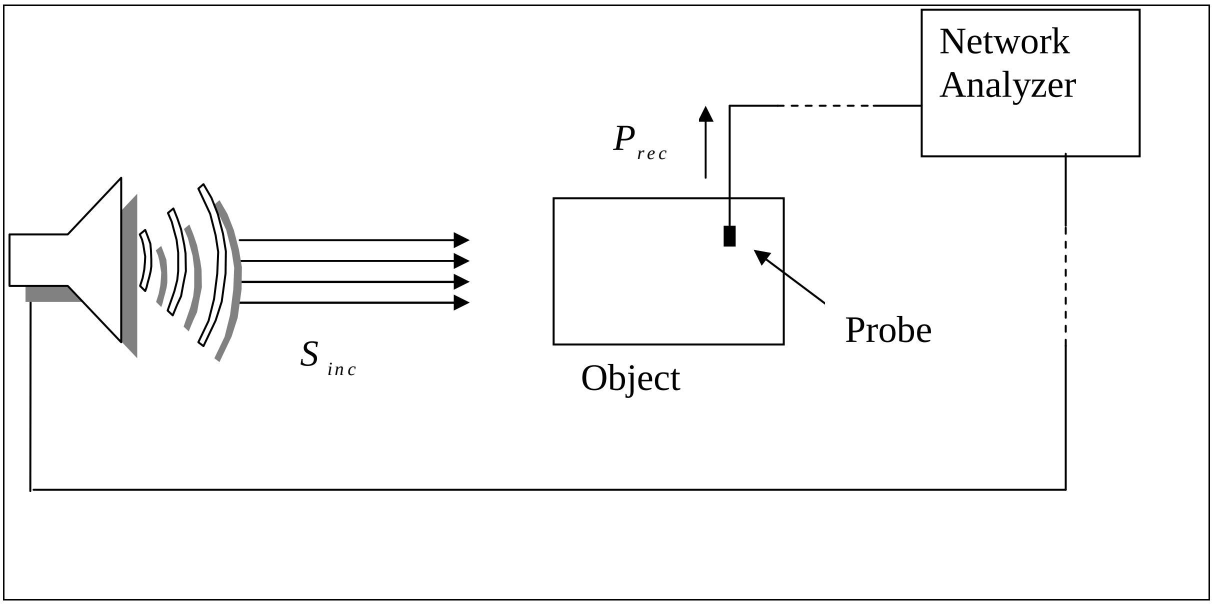

Figure 1. A sketch of the measurements set-up.

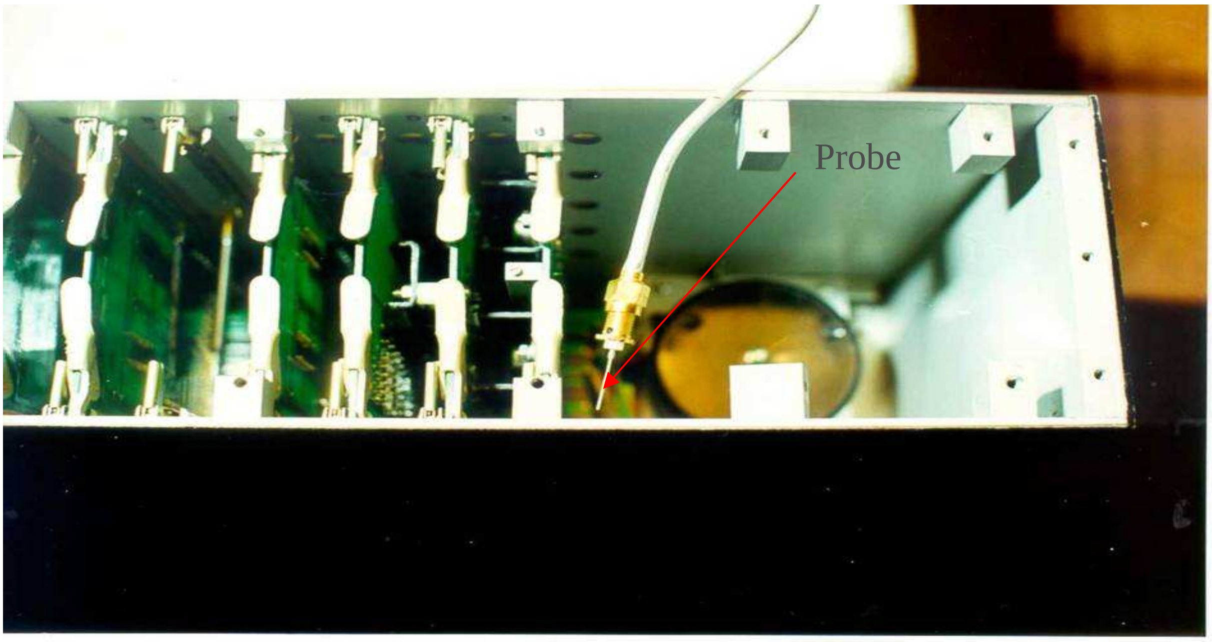

Figure 2. One of the two probes inside the Avionics Box.

The coupling is expressed in terms of the receiving cross-section, σ, of each of the two probes. The cross-section is the ratio between the power received by the load connected to the probe, P_{rec}, and the power density, S_{inc}, of the incident external plane wave:

$$\sigma = \frac{P_{rec}}{S_{inc}} \tag{1}$$

where S_{inc} in principle may be measured using a calibrated antenna. In reality the measurement is performed in a more complex way, including the Network Analyzer, see [5], [6]. In the measurements σ is given by:

$$\sigma = \frac{\lambda^2}{4\pi} G_{p,R} \tag{2}$$

where $G_{p,R}$ is the partial realized gain[1] and λ is the wavelength of the incident plane wave. The partial realized gain is the ratio of the received intensity in the direction $\Omega = (\theta, \varphi)$ [2] and the average received intensity taken over all directions (angles of incidence) and polarisations of the incident field.

If the probe inside the object is not matched to the impedance of the load connected to it, a part of the received power will be reflected. The impedance mismatch factor is the fraction of the received power not being reflected and is denoted with q. The variation of the impedance mismatch factor is in principle deterministic but in [4] it is shown that even for a very small change in frequency, the impedance mismatch factor may vary between typically 0.01 and 1. Hence, we have to take the risk of a complete impedance match into account. For that reason we compensate for the impedance mismatch factor of the probe. Consequently, the most used quantity in this paper is the impedance matched receiving cross-section:

$$\sigma_q = \frac{\sigma}{q} \tag{3}$$

which represents the maximum power that can be delivered to a load.

[1] Partial realized gain = realized gain times the polarisation mismatch factor.

[2] In general, an antenna pattern is three-dimensional and varies with the spherical coordinates θ and φ.

2.2 Angular dependence of σ_q

The receiving cross-section varies as function of angle of incidence which is the reason why it is important to have a small angular sampling interval to be sure that the test includes the worst case. Figure 3 below shows the plots of the angular dependence of the coupling for the Army Radio, tp2, for frequencies 0.5, 1, 2, 4, 8 and 18 GHz.

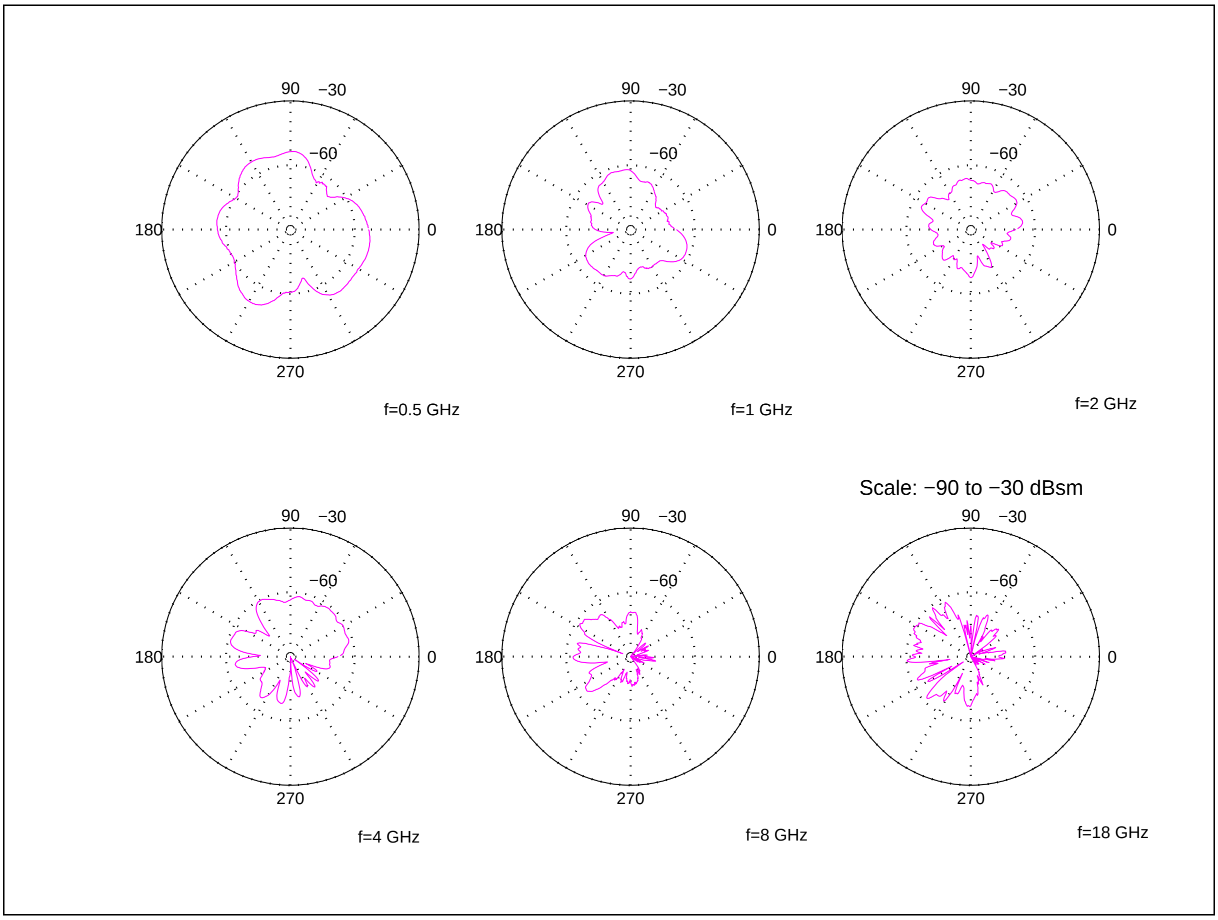

Figure 3. Angular dependence of σ_q. The Army Radio, plane 1, horizontal polarisation, tp2.

According to the figure above, it is obvious that the angle that gives the maximum coupling, i.e. the worst angle, in general varies with the frequency.

The corresponding plots for all combinations of objects, planes of incidence, polarizations and probes are given in Appendix, page 47–64. They all demonstrate the variation of the worst angle with the frequency.

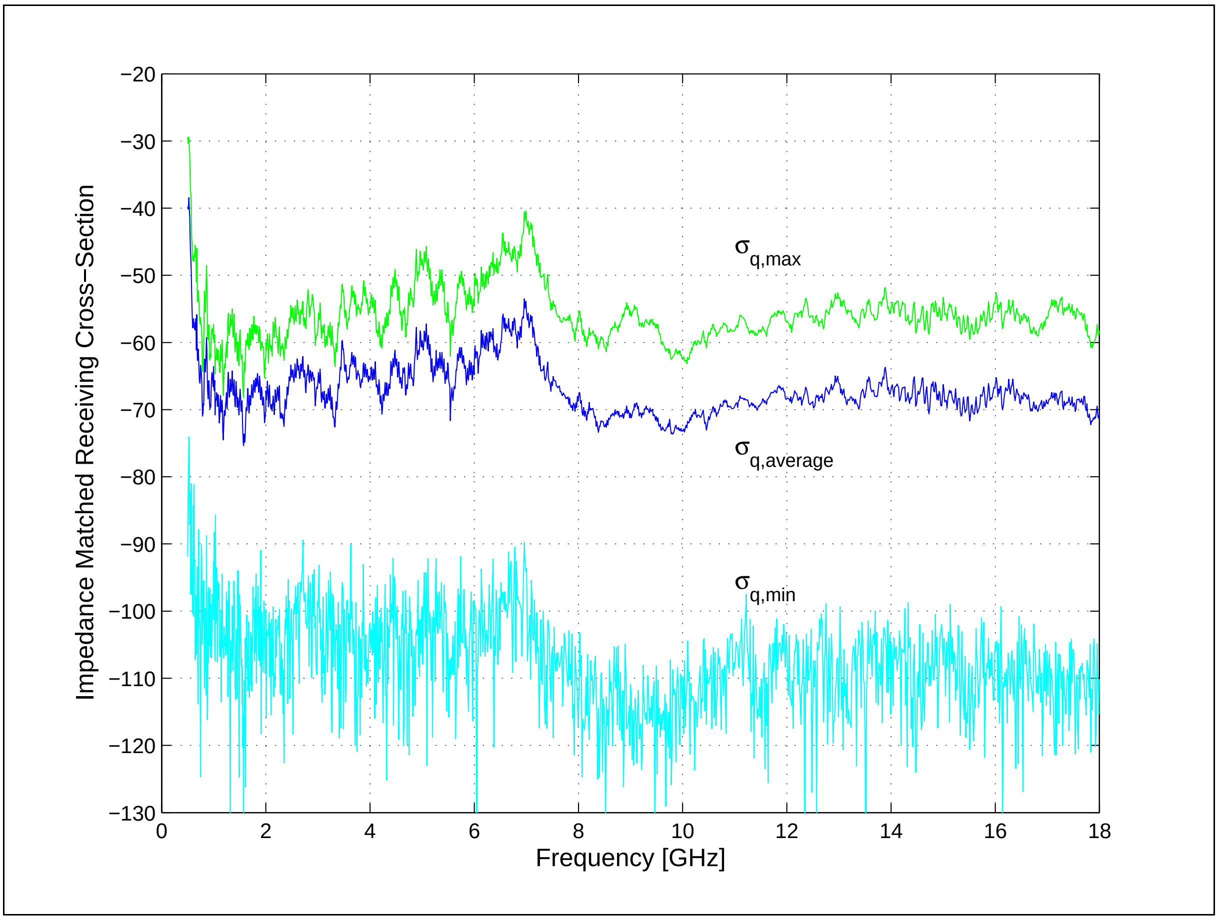

Figure 4. Impedance matched receiving cross-section σ_q for the Army Radio, tp2.

Outgoing from the measured σ_q for all angles of incidence and polarizations, Army Radio, tp2, the minimum, average and maximum values are calculated and shown in Figure 4. Difference between the maximum and minimum σ_q appears to be big, 40 – 50 dB, which is an illustration of difficulties in testing using, like in most cases in practice, only a few numbers of angles of incidence and polarizations. This difference is characteristic for other objects as well, see Appendix, page 65–67. As it is usually impossible to know beforehand which angle of incidence that corresponds to the worst susceptibility there is a large risk the equipment not being irradiated in the most sensitive direction which makes the risk for undertesting very most likely.

In order to facilitate the investigation of the method, the following quantities are defined:

σ_{true} – the maximum σ_q, taken for a fixed frequency and all angles of incidence over all three planes and two polarisations.

σ_f – the maximum σ_q, taken for a frequency interval and only a few angles of incidence and two polarisations.

A problem with this method of using only a few angles of incidence is that the measured value of the maximal receiving cross section, σ_f, will probably be downwards or upwards biased compared to the true value, σ_{true}. In other words, overtesting as well as undertesting is very likely. One more item to consider is that the frequency should not be varied to a great extent since the susceptibility of the electronic circuits varies with frequency as well. So, the question is if this method may enable a drastic reduction of the number of angles of incidence and polarisations. This possibility, the problems involved and an attempt to solve some of them, are studied in more detail below.

2.3 The error bias

The expected outcome of the investigated method is that σ_f will be downwards or upwards biased compared to the true value, σ_{true}. As a measure of the agreement between σ_{true} and σ_f, i.e. between the measurements including one fixed frequency and all used angles of incidence and polarizations and those who include several frequencies and only a few angles of incidence and polarisations, the quantity error bias, EB, is defined:

$$EB = \frac{\sigma_f}{\sigma_{true}} \tag{4}$$

However, it appeared that EB expressed in decibel was more fruitful for the analysis. Thus, the following quantity is defined:

$$EB_{dB} = 10\log_{10}\left(\frac{\sigma_f}{\sigma_{true}}\right) \tag{5}$$

where EB_{dB} stands for error bias expressed in decibel.

Noticeably, the expression given in (5) is equivalent to the difference of σ_f and σ_{true} if both these quantities were taken in decibels relative to a square meter (dBsm).

3 Statistical analysis

In Section 2 we defined the error bias which we use in this section for the analysis. Interpretation of the measurements results is done by means of statistical methods. Statistical investigation of EB_{dB} is done at several frequencies. The number of angles of incidence is reduced to three, one angle for each plane. Since the measurements were done with both vertical and horizontal polarisation for each angle of incidence, there are six samples for each frequency (two polarisations for every angle of incidence). To be able to perform a statistical analysis 100 samples containing three angles of incidence and two polarisations for each angle of incidence are chosen. This is done for every test frequency and every frequency interval (see below).

3.1 Random model

In order to get a random model, the method of selecting 100 samples, containing 3 angles of incidence each, must satisfy the rules of random selection [7, Chapter 5]. In other words, a method of selection that chooses three angles at a time and with equal probability is needed. The probability model used is the so-called urn model [7]. The number of angles in the urn is 360. 100 random samples, containing 3 angles each, are selected according to the capture-recapture method. Each sample constitutes a random sample from the total angle population. The distribution that arises from these kinds of experiments is the discrete uniform distribution because it puts equal weight on the integers from one to, in this case, 360. So, in practice, randomness is achieved by generating discrete uniform random numbers with maximum 360.

Three random numbers are generated 100 times. The angle samples are given in Appendix, page 96.

3.1.1 Frequency intervals

The frequency range in the coupling measurements was 0.5 – 18 GHz. The frequency interval was divided into three subintervals. The number of measurements points in each subinterval differed between the three different test objects, as seen in Table 2. The number of tested frequencies for the Army Radio is 1203, for the Avionics Box 319 and for the Test Missile 2670.

Test object	Frequency (GHz)	Points in the frequency interval	Accuracy (GHz)
Army Radio	0.5 – 2	1 – 201	0.0075
	2 – 6	202 – 602	0.01
	6 – 18	603 – 1403	0.015
Avionics Box	0.5 – 2	1 – 201	0.0075
	2 – 6	202 – 302	0.04
	6 – 18	303 – 403	0.12
Test Missile	0.5 – 2	1 – 801	0.0019
	2 – 6	802 – 1602	0.005
	6 – 18	1603 – 3204	0.0075

Table 2. Frequency points used in the coupling measurements for the three test objects. The accuracy is the distance between two consecutive frequency points, i.e. the frequency step.

For each test frequency several different intervals are chosen, all consisting of the test frequency and the frequencies adjacent to it. Intervals 1, 2, 3, 4, 5, 6, 7, 8, 9 and 10 are calculated according to the following equation:

$$\underbrace{freq\_v\,(f) - \frac{\frac{k \cdot f}{2}}{accuracy}}_{int\_low} \;:\; \underbrace{freq\_v\,(f) + \frac{\frac{k \cdot f}{2}}{accuracy}}_{int\_high}$$

$$\text{Interval } k = f - (freq\_v(f) - \text{int}\_low) \cdot accuracy : f + (\text{int}\_high - freq\_v(f)) \cdot accuracy$$

where:

$$\begin{aligned} f &= \text{the test frequency in use.} \\ freq\_v\,(f) &= \text{the point in the frequency vector where the frequency } f \text{ is found.} \\ k &= 0.1,\ 0.2,\ 0.3\ \ldots 1 \text{ corresponding to Interval } 1,\ 2,\ 3\ \ldots 10. \\ accuracy &= \text{the accuracy around the frequency } f. \end{aligned} \qquad (6)$$

In order to simplify the calculations the same accuracy has been used for all three intervals, 0.015 for the Army Radio, 0.12 for the Avionics Box and 0.0075 for the Test Missile. As an example, the frequency intervals for the frequency 3 GHz (2.9994 GHz), Army Radio, tp2, are calculated and given below:

$$\begin{aligned} f &= 2.9994 \text{ GHz} \\ freq\_v(f) &= 302 \\ k &= 0.1,\ 0.2,\ 0.3,\ \ldots 1 \\ accuracy &= 0.015 \end{aligned}$$

	[GHz]
Interval 1	2.8994:3.0994
Interval 2	2.7994:3.1994
Interval 3	2.6993:3.2995
Interval 4	2.5993:3.3995
Interval 5	2.4993:3.4995
Interval 6	2.3993:3.5995
Interval 7	2.2993:3.6995
Interval 8	2.1992:3.7996
Interval 9	2.0992:3.8996
Interval 10	1.9992:3.9996

For every combination of angles of incidence and frequency interval, σ_f is calculated. Then, EB_{dB} is determined for each σ_f. That means that, for each frequency interval, 100 random values of EB_{dB} are obtained. This procedure is repeated for all test frequencies. (The angle combinations are the same for all frequencies.)

3.2 Statistical model for the error bias

In discussing the results of the experiments it is essential to find a way to handle and display the obtained values. A convenient method is to use a histogram. If the number of the measurements of the error bias is large enough, the histogram will approach a continuous curve, often called the limiting distribution [8, pp. 126-129]. Knowing the limiting distribution for the error bias, EB_{dB}, is of great interest since it makes it possible to know the probability of obtaining an answer within a certain interval.

Knowing the distribution of EB_{dB}, one is able to determinate the probability of obtaining an error bias in logarithmic terms (dB) within some specific ranges, but the probability density function for EB can also be calculated, which make it possible to determinate the probability of obtaining an error bias in linear terms as well. The following illustrates how the distribution functions of EB_{dB} and EB are related. To facilitate the writing, EB_{dB} is denoted with y and EB with x, while F_Y and F_X stand for corresponding distribution function.

$$
\begin{aligned}
&F_X(x) = F_Y(10\log x) && \text{for } x > 0 \\
&F_X(x) = 0 && \text{for } x \le 0 \\
&x = EB \\
&y = EB_{dB}
\end{aligned}
\tag{7}
$$

3.2.1 Theoretical model

According to practical knowledge, measurements in dB are often distributed normally. This can be explained with the logarithmic results, dB, being treated as additive data.

So, the expectations are that the results follow a normal (sometimes called Gaussian) distribution $N(\mu,\sigma)$, where μ (the mean) and σ (the standard deviation) are to be find from measurements data. If EB_{dB} is normally distributed then EB is said to be lognormally distributed, which follows from the definition of the lognormal distribution [14] and which also can be seen in (7). To illustrate this relationship between the lognormal and normal variate, the Lognormal distribution, $L(0,1)$, and its conversion to the standard normal distribution, $N(0,1)$ or vice versa, is shown in Figure 5, [10].

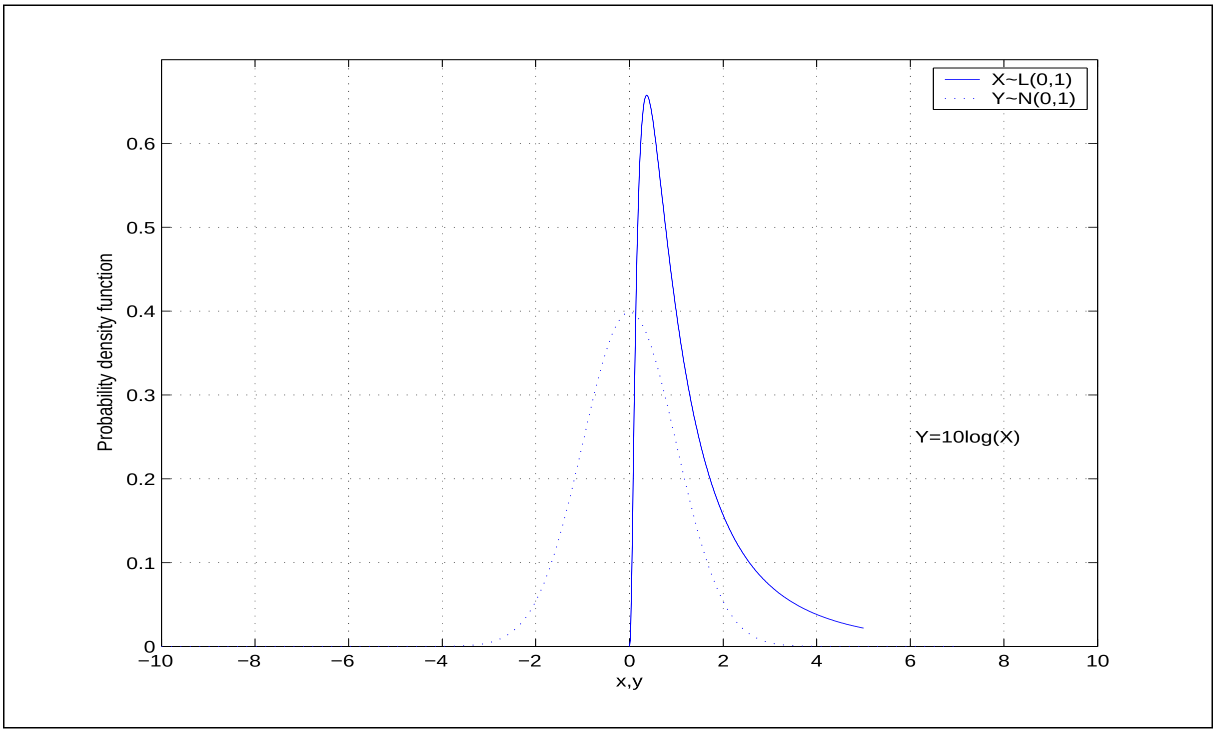

Figure 5. Lognormal (solid line) and normal (dashed line) distribution

3.2.2 Experimental data

In the calculations of the theoretical normal distribution, the mean and the standard deviation of the sample, are used as estimates for the parameters μ and σ. They are calculated as:

$$\text{estimate for } \mu = \overline{EB_{dB}} = \frac{\sum EB_{dB_i}}{N}$$
$$\text{estimate for } \sigma = \sqrt{\frac{\sum (EB_{dB_i} - \overline{EB_{dB}})^2}{(N-1)}} \qquad (8)$$

where N is the number of measurements [8].

All plots presented in this section concern the Army Radio, tp2, frequencies 3 and 7 GHz and frequency interval 1, see Section 3.1.1. There is no particular reason for choosing this grouping of data for illustration; any other one could be used as well. Corresponding plots of all other combinations of objects and probes are presented in Appendix page 68–89.

First, the data are represented with histograms, Figure 6. In this way, the shape of underlying distribution can be discerned. The histograms are graphed with superimposed estimated normal probability density function.

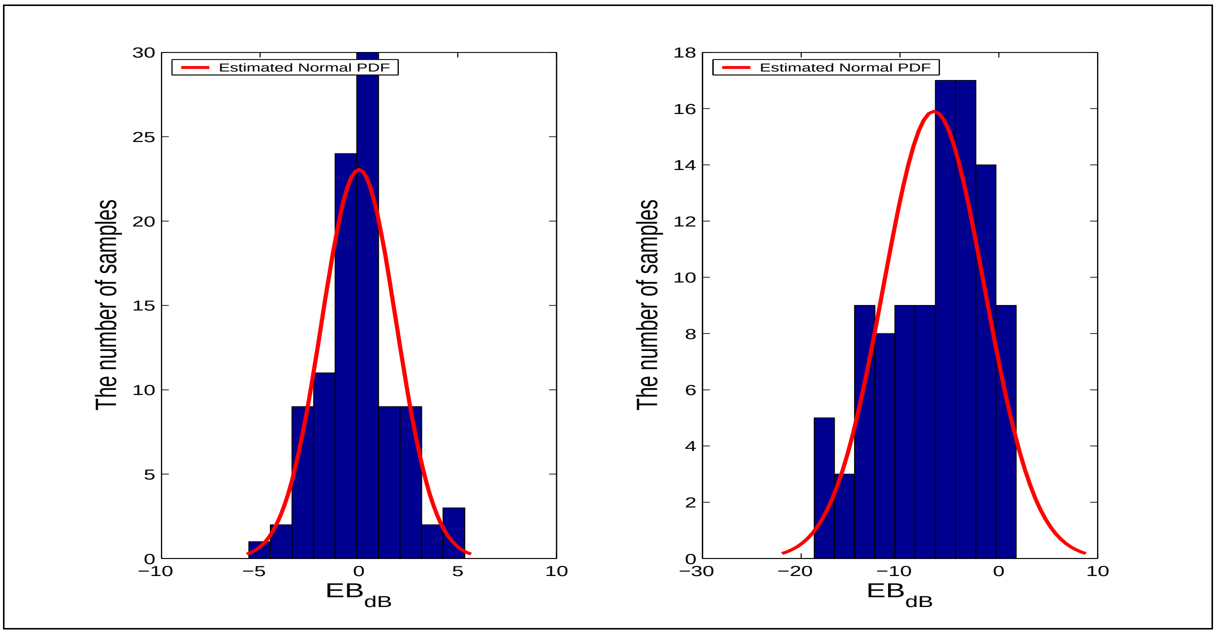

Figure 6. Histogram of EB_{dB} for the Army Radio, tp2, with superimposed normal density. Frequency 3 GHz (left) and 7 GHz (right), frequency interval 1.

The histograms in Figure 6 are not so regular and smooth. It however seems like the left histogram (3 GHz) has a normal distribution as limiting distribution. The problem is that the number of measurements is relatively small (100), so it looks like more than 100 measurements are needed to be able to draw a conclusion concerning the limiting distribution being normal distribution or not. However, the superimposed normal density does not seem to fit the right histogram (7 GHz) as well as it fits the left histogram (3 GHz) but from the practical point of view the fitting is sufficient. Furthermore, the test performed later in this section, points to that expected normal distribution is accepted at frequencies 3 and 7 GHz.

The histogram and the estimated normal probability density function (pdf), as function of both frequency and EB_{dB}, are shown in Figure 7 respectively Figure 8.

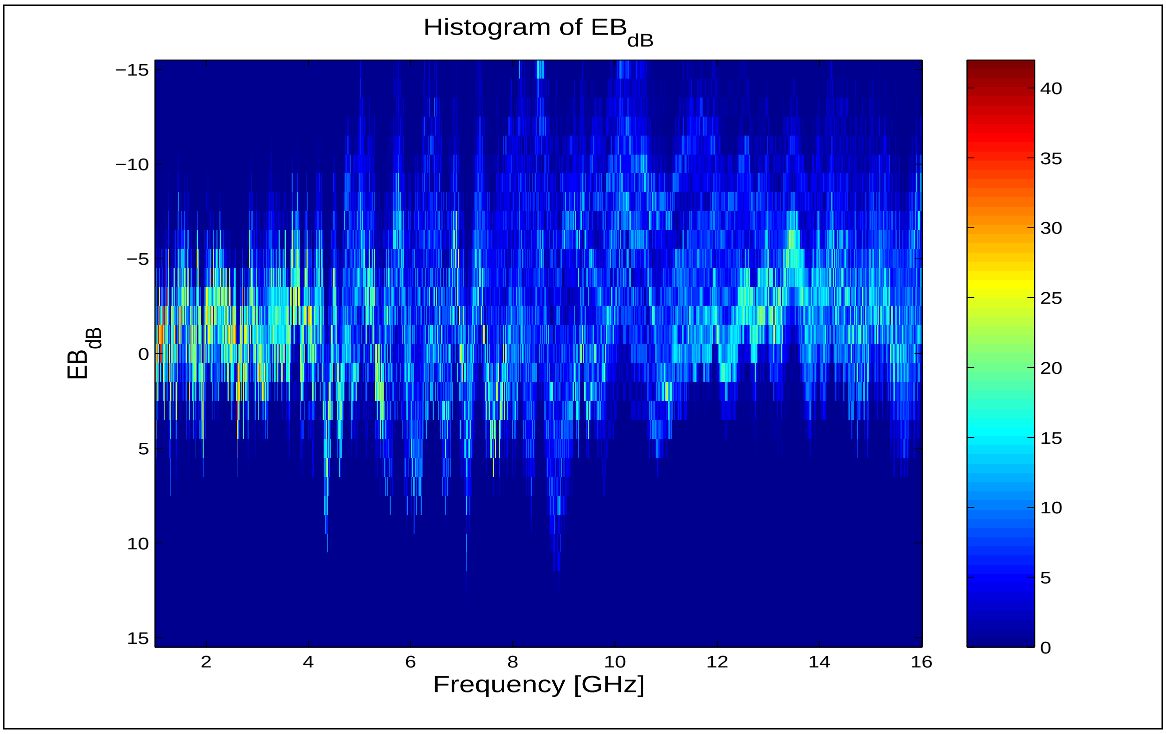

Figure 7. Histogram of EB_{dB}. Army Radio, tp2, interval 1. The colours represent the number of observations (EB_{dB}) in each interval (bin).

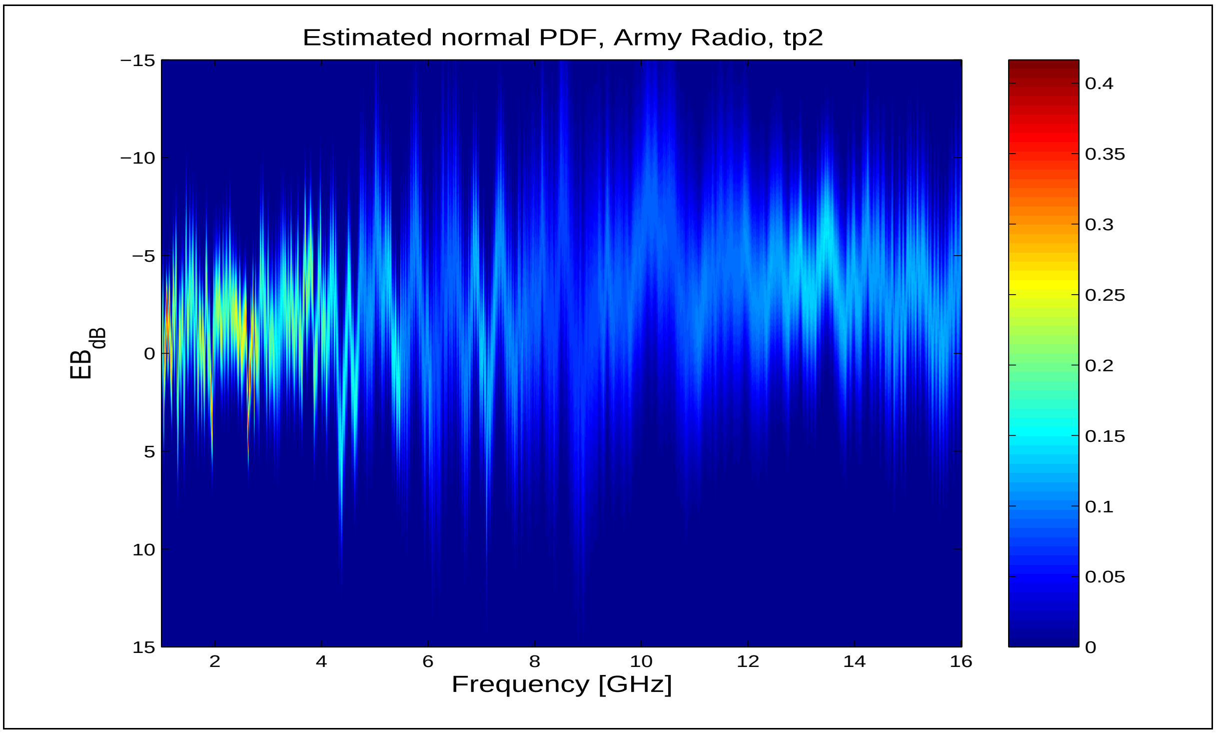

Figure 8. Estimated normal probability density function (pdf) for EB_{dB}. Army Radio, tp2, frequency interval 1. The colours represent the density of the normal pdf with parameters μ and σ calculated according to (8)**.**

Next, the data are presented with plots of empirical cumulative distribution functions, Figure 9. The measured cumulative distribution function is compared to the theoretical curve for normal distribution.

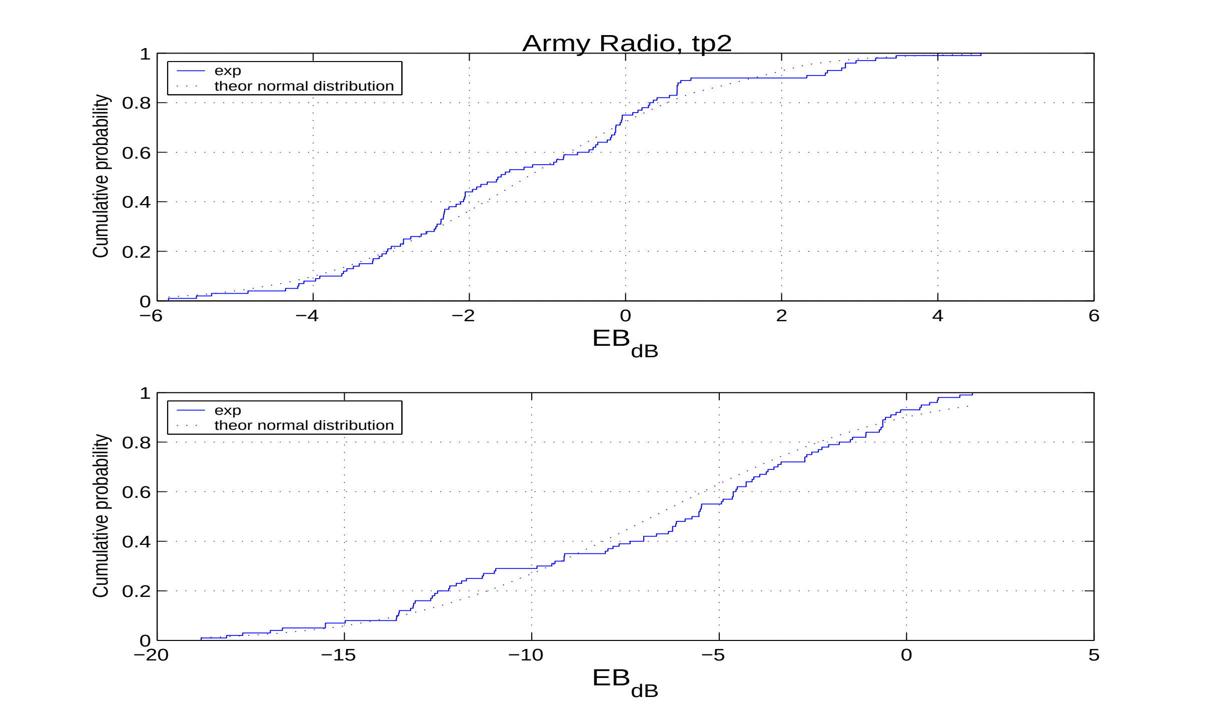

Figure 9. Measured and estimated cumulative distribution function (cdf). Frequency 3 GHz (upper) and 7 GHz (lower), frequency interval 1. Army Radio, tp2.

Figure 9 shows good agreement with the theoretical curves for the normal distribution with mean μ and standard deviation σ for both frequencies. Normal distribution seems to fit the data better then what it does on the histogram plots, despite both plots concern the same data. A reason for this is that a cdf plot is independent of the number of observations and it does not involve grouping difficulties, the problems that arise in using a histogram [11, p. 9]. Further on, the probability density function is the derivative of the distribution function and the derivatives of two similar functions do not need to be similar themselves.

A way to determine discrepancy between the measured and estimated distribution function is to use the Kolmogorov-Smirnov test [15]. This test is performed for frequencies 3 and 7 GHz. The test results indicate that we can not reject the hypothesis, that the values of EB_{dB} are normally distributed, at significance level 5% (the rejection significance level is probability that one rejects assumed distribution even if it is correct). The test results are similar for other two test object, with the exception for the Test Missile tp4 where the hypothesis is rejected at 5% significance level.

Another graph for assessing whether the data comes from a normal distribution is shown in Figure 10. Intervals, containing 95% and 99% respectively of the normally distributed sample with calculated parameters μ and σ, are drawn. The two red lines are the 95% and the two green lines are the 99% statistical control limits. If the data is normally distributed then by chance, five and one measurement respectively out of 100 should fall outside these lines.

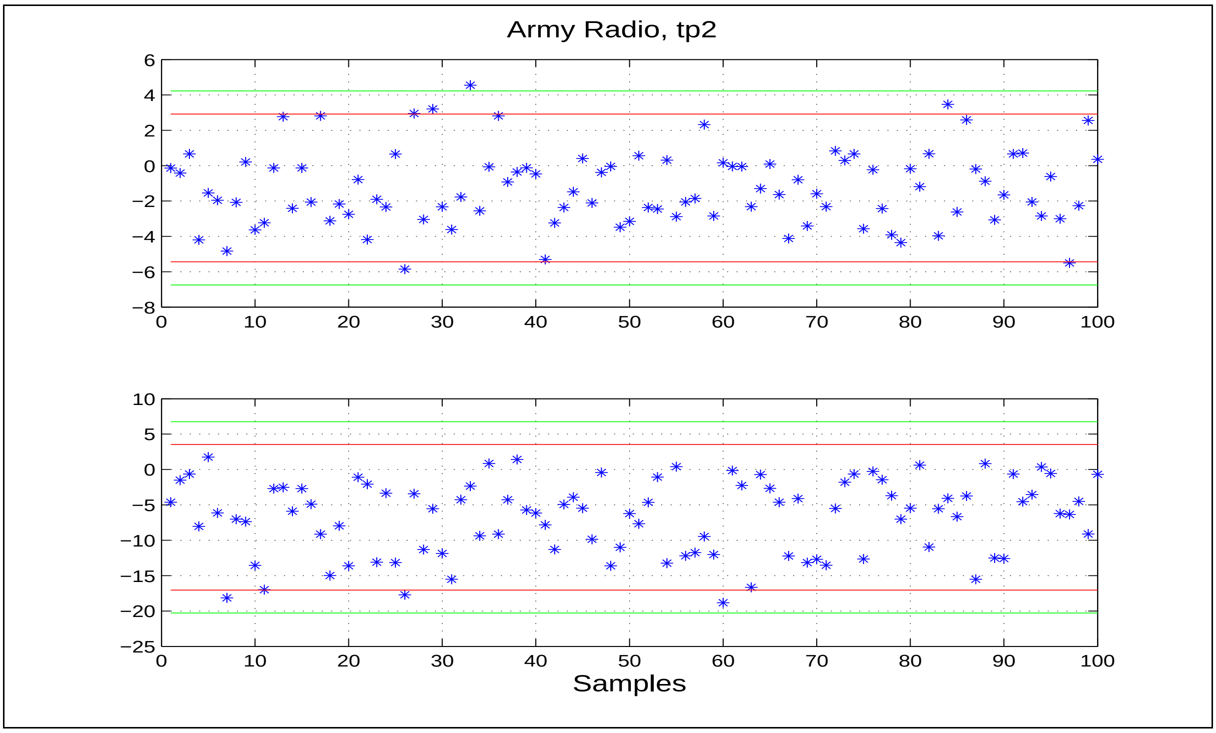

Figure 10. The 95% statistical control limits (red), the 99% statistical control limits (green) and EB_{dB} (blue). Frequency 3 GHz (upper subplot) and 7 GHz (lower subplot), frequency interval 1. The Army Radio, tp2.

On the lower subplot (Figure 10) that is not completely fulfilled. Though, on the upper subplot five measurements felt outside the red lines and one measurement felt outside the green lines. That is not a proof that the data are normally distributed but an indication that the normal distribution is worth a further investigation. The Figure 11 below shows the number of outlying obtained values of EB_{dB} with the 95% and 99% statistical limits applied, for all studied frequencies. However, the Figure 11 does not tell us anything about the symmetry, i.e. even if the number of outlying values is equal to five or one, it is still not acceptable neither if all values are found over the upper limit nor if all are found under the lower limit.

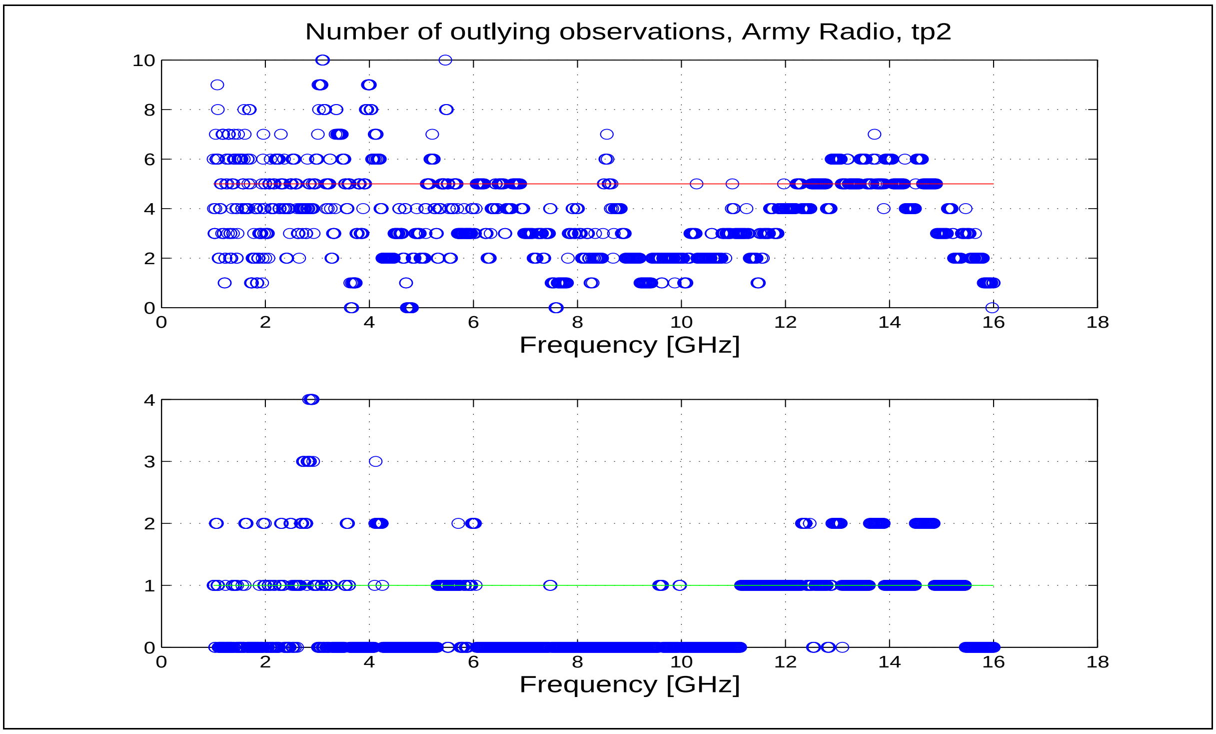

Figure 11. The number of outlying obtained values of EB_{dB} with 95% (upper subplot) and 99% statistical limits applied (lower subplot). Army Radio, tp2, frequency interval 1.

For the frequencies with five correspondingly one obtained value outside the boundaries (in a way so the symmetry is fulfilled), we can expect 95% and 99% respectively of all comparable measurements of EB_{dB}, to fall in these ranges, if the data is normally distributed. However, with the figures shown so far, we are not able to draw the conclusion that the data is normally distributed, so a more exact investigation is performed below.

3.2.3 Chi-square goodness-of-fit test

The correctness of the assumed distribution is difficult to judge visually. If one attempt to reach a decision whether the data fit a distribution function, a more objective test need to be done. The test that is used here is chi-square goodness-of-fit test [8, Chapter 12], [9, p. 269], one of the oldest and best known tests in statistics. In the χ^2-goodness of fit test, a test variable is defined:

$$Q = \sum_{k=1}^{n} \frac{(O_k - E_k)^2}{E_k} \qquad (9)$$

where n is the number of data intervals, O_k, is the number of observations in the kth interval, and E_k is the expected number of measurements in the kth interval assuming the measurements really are governed by the expected distribution. This test variable is very convenient, because the larger divergence of O_k from the expected values E_k, the larger Q. The variable Q is chi-square distributed with $n-r$ degrees of freedom, where r is the number of parameters that have to be calculated from the data to compute the expected numbers E_k. E.g., if we want to test if some data are consistent with normal distribution, to calculate the expected numbers E_k we need to use three parameters calculated from our data: the total number of the sample and the estimates for the parameters μ and σ. So in this case, r is equal to three. The calculated value of Q is compared to a value settled by chosen confidence level for the test.

In making decision whether the assumed distribution is correct or not, a significance test is used. The null hypothesis, H_0, that the measurements follow normal distribution is set up and the following statements are used:

$$\begin{array}{l}\text{Reject } H_0 \text{ if } Q > \chi_p^2(f), \text{ where } f = n - r \\ \text{Accept } H_0 \text{ otherwise.}\end{array} \tag{10}$$

The significance level (p) indicates the probability of rejecting H_0 if H_0 is true.

3.2.4 Results of the chi-square goodness-of-fit test

The goodness-of-fit test is made for all tested frequencies and intervals. The bins are chosen so that expected number of measurements (E_k) in each bin is at least five [9]. The number of bins (n) in this test, is chosen to be ten. All bins are equally spaced. The null hypothesis being tested is rejected if the calculated test variable (Q) is bigger than the value of $\chi_p^2(7)$ ($f = n - r = 10 - 3 = 7$). Normally, the significance level for rejection (p) is 5% or 1% , i.e. there are 5 respectively 1 chances in 100 that the rejected null hypothesis happens to be correct.

The outcomes of the test for the Army Radio, tp2, all tested frequencies and the interval 1 (see Section 3.1.1), with the boundaries at significance level at

5% and 1%, are shown below in Figure 12. The figures with corresponding plots for the other objects and frequency intervals are presented in Appendix, page 89–94.

According to the plots, the calculated Q values are larger then $\chi_p^2(7)$ values at some frequencies. For those frequencies at which Q values are smaller than $\chi_p^2(7)$ values, i.e. we accept H_0, the assumption about the EB_{dB} data being normally distributed is reasonable. In other words, we have not enough evidence to reject the null hypothesis.

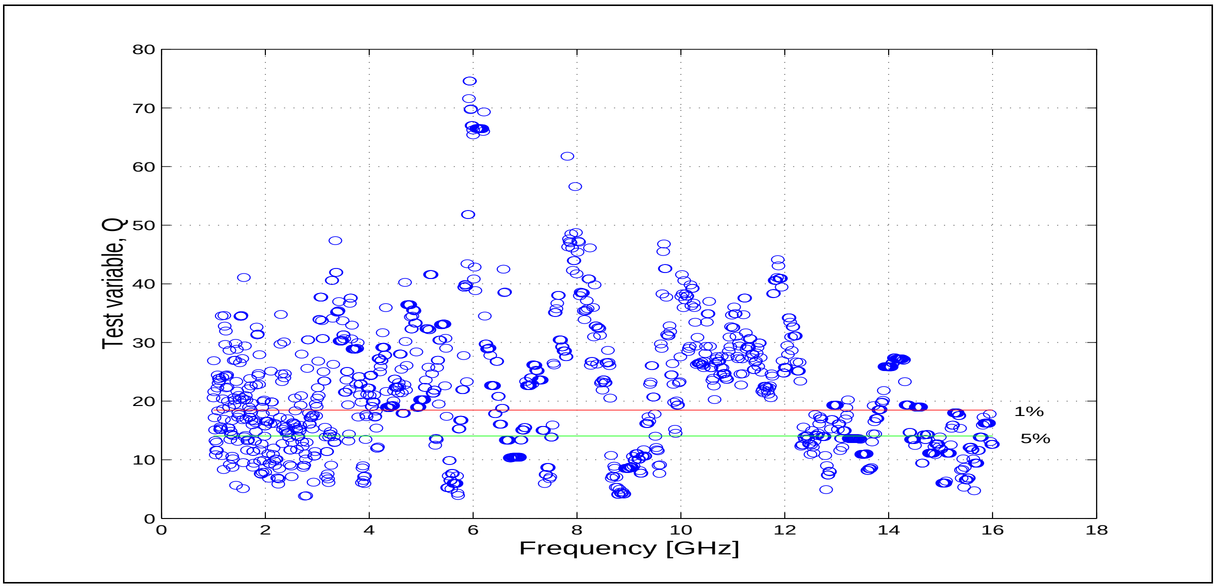

Figure 12. The test variable Q (blue) and 1% (red) respectively 5% (green) significance level for rejection for all tested frequencies, frequency interval 1. Army Radio, tp2.

As can be seen in Figure 12, H_0 is accepted at some frequencies and at some it is not. For each test point (probe position), the χ^2-test is done at many frequencies and this lead to a problem named several samples goodness of fit problem [11]. The test is expected to fail at some frequencies even if the hypothesized distribution shall not be rejected. The conclusion whether the calculated values of EB_{dB} indicate significant agreement with normal distribution, can not be made for a specific frequency, but only for the complete range of tested frequencies. We can either accept or reject the expected distribution for the complete frequency range.

A way to handle the whole range of tested frequencies is to use Fisher's method [11]. Fisher's method is based on the significance levels (p) of the component tests i.e. tests for every test frequency.

We do N independent tests of the null hypothesis, where N is the number of tested frequencies. At each test frequency i ($i = 1 : N$), the rejection significance level p_i is calculated. The following parameter is to be calculated:

$$P = -2\sum_{i=1}^{N} \ln p_i \tag{11}$$

where i - test frequency point

p_i - rejection significance level at test frequency i

N - the number of tested frequencies

If we assume that, at every test frequency EB_{dB} is normally distributed, then each p_i is uniformly distributed. This yields that the parameter P is χ^2-distributed with 2N degrees of freedom.

For each of the ten frequency intervals (Section 3.1.1) the rejection significance level p_P[3] for the total range of tested frequencies is calculated. In our case the calculated values of p_P are so small that MATLAB represents them as zeros, i.e. the probability that we reject the assumed distribution even if it is correct, is extremely low. Thus, we reject the null hypothesis for the complete test frequency range. This is common for all tested objects.

This result is not unexpected; a graphical analysis of Figure 12 points to that there is much more then 5% of the Q values over the green line, and much more then 1% of Q values over the red line, which implies that we reject the null hypothesis at 5% and 1% respectively significance level.

3.2.5 Mean and standard deviation

The average and the standard deviation of the error bias are used as estimates of the parameters μ and σ for the normal distribution (8). The plots of these two parameters as function of the frequency for the frequency intervals 1 – 5 are presented in Figure 13 and Figure 14 below.

[3] p_P is calculated outgoing from P, see [11].

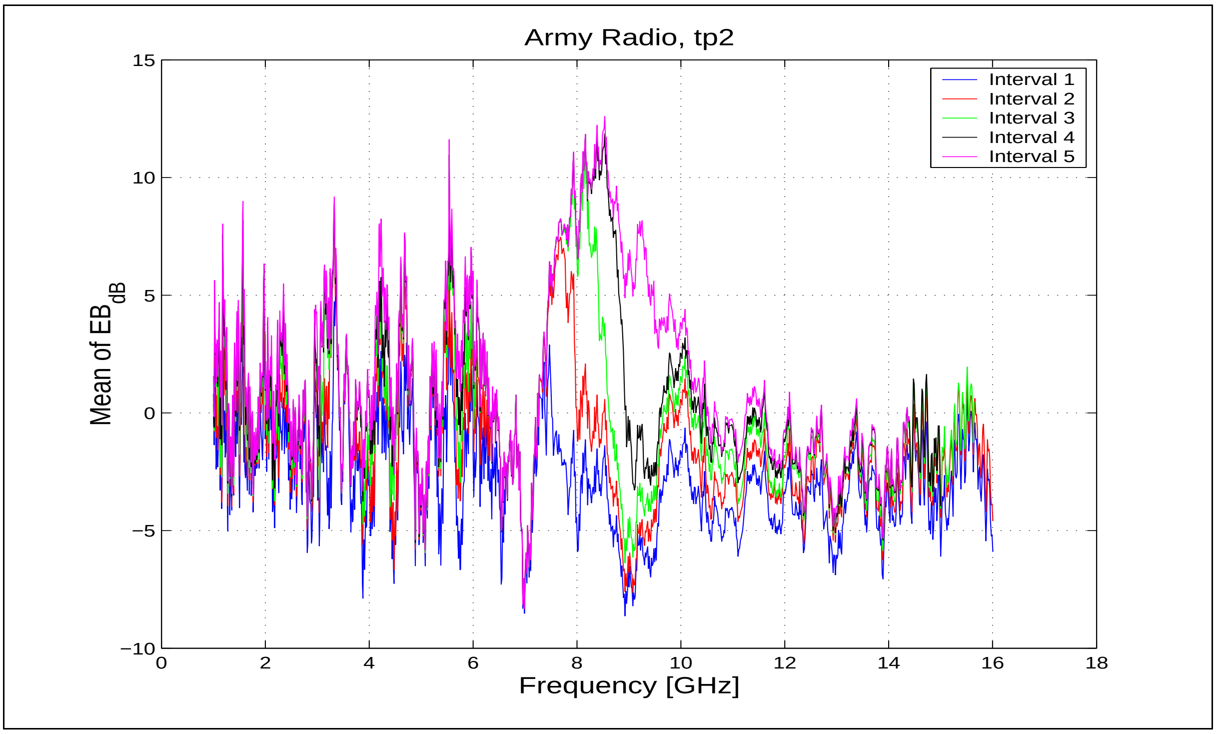

Figure 13. The mean of EB_{dB}, Army Radio, tp2, frequency intervals 1 – 5.

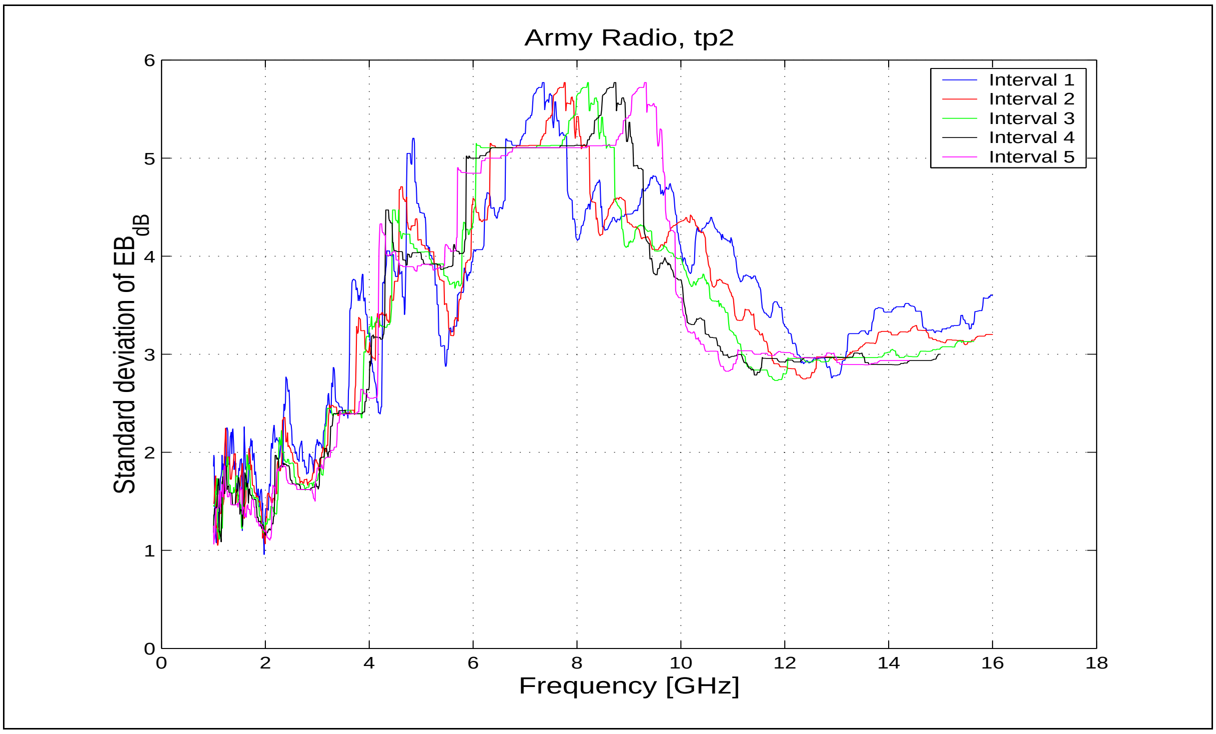

Figure 14. The standard deviation of EB_{dB}, Army Radio, tp2, frequency intervals 1 – 5.

The purpose of these figures is to investigate if there is any general trend of the frequency variation of the sample mean and standard deviation. As expected, the larger frequency interval gives the larger mean of EB_{dB} with the exception for the frequencies around the frequency 7 GHz, where we can see that all five curves follow each other, Figure 13. Irrespective of how much we vary the frequency we do not get any improvement. This implies that our method is not of use in this range of frequency. The quantity σ_{true} seems to be so high here that it is impossible to achieve that value with σ_f no matter how big frequency interval we take. The tested object Army Radio seems to have a resonance frequency at approximately 7 GHz and the Figure 4 confirms this; there is a peak in the cross section at 7 GHz. Hence, our model does not succeed at the resonance frequency of the tested object Army Radio.

As we increase the frequency interval, the mean of EB_{dB} is larger, and therefore also the risk for overtesting, (see Section 3.2.6 for more details about overtesting and undertesting). For some frequencies we achieve the positive value of EB_{dB} even with a small frequency interval, so it is unnecessary to take a larger frequency interval at those frequencies. However, this is far from to be typical for all frequencies; for the most of the frequencies it takes a larger interval to achieve a positive value of EB_{dB} and in that way reduce or avoid the risk for undertesting, particularly for the higher frequencies, Figure 13.

The standard deviation is a measure of the variability of the data. The plot in Figure 14 indicates that the values of EB_{dB} are more scattered as we increase the frequency, in the frequency range 1-6 GHz (approximately). The frequency interval, however, do not seem to make any difference since all five curves follow each other. For the frequencies larger than approximately 6 GHz, the standard deviation seems to be constant for all intervals as function of the frequency and then decrease as we increase the frequency.

For each test frequency we calculate 100 values (for 100 different angle combinations) of EB_{dB}. For some frequencies, σ_f will have the same value as σ_f of the previous frequency. Hence it is only the difference in σ_{true} for these two frequencies, which changes the values of EB_{dB}. As an example, Figure 15 presents, EB_{dB} for the two adjacent frequencies, 7.24 and 7.26 GHz. As can be seen, there is only an offset between the blue and the red line. This offset corresponds to difference between $\sigma_{true,7.24GHz}$ and $\sigma_{true,7.26GHz}$. Hence, the standard deviations of EB_{dB} for these two frequencies have the same values. This explains why the standard deviation of EB_{dB} is constant within some frequency intervals in Figure 14.

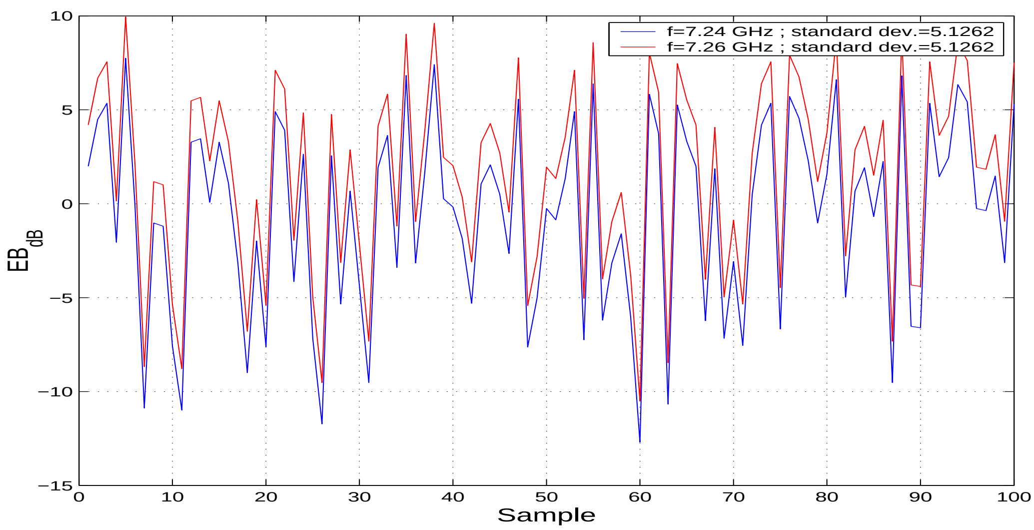

Figure 15. EB_{dB} **for two adjacent frequencies. Army Radio, tp2, frequency interval 3.**

3.2.6 Overtesting and undertesting

As expected, the results of the method with only a few angles of incidence (σ_f) differ from the true value (σ_{true}). The deviation is in some cases as big as 15 dB (see Figure 10), which implies exposing the internal parts of equipment to much lower or much higher stress levels than what is appropriate to perform a radiated susceptibility test. For that reason, it is important to have this in mind when a frequency interval is to be chosen. Problems with overtesting are not as serious as problems with undertesting. Overtesting may make one believe that the tested equipment endures less than what it really does and may result in being more cautious than necessary. This may lead to redesign or unnecessary restrictions. Overtesting may also cause a testing to be more expensive than what is necessary. It is however much more serious to underestimate the immunity properties of the tested equipment, i.e. to believe that the tested equipment endures more than it actually does, which may be a consequence of the undertesting.

4 Statistical analysis of the receiving cross-section

Some attempts to find a statistical model for coupling measurements has been performed before. The major objective for those statistical analyses was to investigate if a test in an AC could be simulated by using an RC (Reverberation Chamber), where the number of stirrer positions in the RC would correspond to the number of angles in the AC [3], [4]. The distribution that was tested on the coupling data was a χ^2-distribution with two degrees of freedom, which the RC data support. The conclusion was that the coupling data are not $\chi^2(2)$-distributed.

An attempt to find a statistical distribution that fits the coupling data for some frequencies and angles of incidence is presented below. Earlier research results showed that σ_q in the RC is equal to the average σ_q in the AC, measured for both all angles of incidence as well as all polarisations. Given this knowledge, there is an (obvious) advantage with the derivation of the probability density function for $\sigma_{q,AC}$, for various frequencies. Testing in a Reverberation Chamber gives the mean of $\sigma_{q,AC}$, so knowing the pdf would enable one to calculate the probability of obtaining the maximum value of $\sigma_{q,AC}$ within some specific boundaries, where the average value from the coupling measurements in the Anechoic Chamber is found from measurements using many different angles of incidence as well as many different polarisations.

4.1 Statistical model for σ_q

Figure 3 (Section 2) shows the angular dependence of the coupling at the frequencies 0.5, 1, 2, 4, 8 and 18 GHz. The coupling data in the statistical analysis below are expressed in terms of the normalized received power, i.e. the ratio between the power received to the load connected to the probe, P_{rec}, and the average received power, $P_{rec,average}$, taken over all angles of incidence and polarizations. This can be written as:

$$\text{Received power normalized to mean} = \frac{P_{rec}\left(p,\theta,\varphi\right)}{P_{rec,average}} \qquad (12)$$

The figures presented below are for the Army Radio, tp2. Corresponding figures for the other probe, tp4, and the other two objects show similar results and are presented in Appendix, page 97–102.

Earlier estimates indicated that σ_q was not χ^2- distributed with two degrees of freedom. An analogous investigation, but for χ^2- distribution with one degree of freedom, started by showing a very good fit between the experimental data and the assumed distribution. Consequently, this is investigated further and the results are presented below.

The measured cumulative distribution function is compared to the theoretical curves for χ^2-distribution with one respectively two degrees of freedom in Figure 16. As it can be seen, there is a rather good fit with the theoretical χ^2-distribution with one degree of freedom with the exception for 0.5 and 8 GHz. A more exact evaluation of the hypothesis that the data are described by the χ^2-distribution with one degree of freedom is done below. The receiving cross section is proportional to the received power which is proportional to the square of the E-field. So, if we show that we have insufficient evidence to reject the hypothesized χ^2-distribution with one degree of freedom, it would indicate that the absolute value of a component of the E-field inside the EUT is normally distributed [9, p. 227].

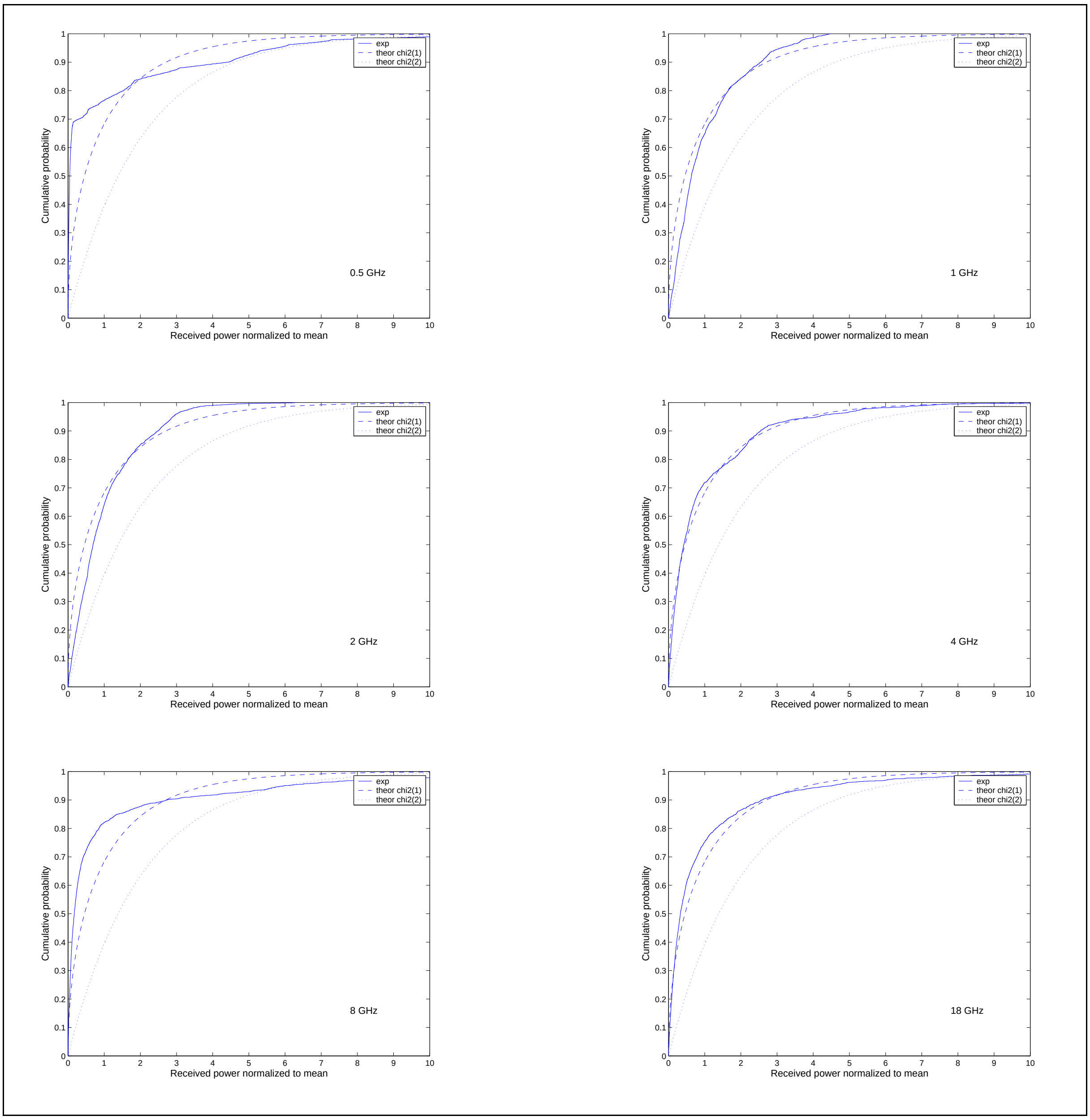

Figure 16. Measured cumulative (solid) and calculated cumulative distribution function. Army Radio, tp2.

Figure 17 below shows as function of frequency the plots of the variance of the received power normalized to mean.

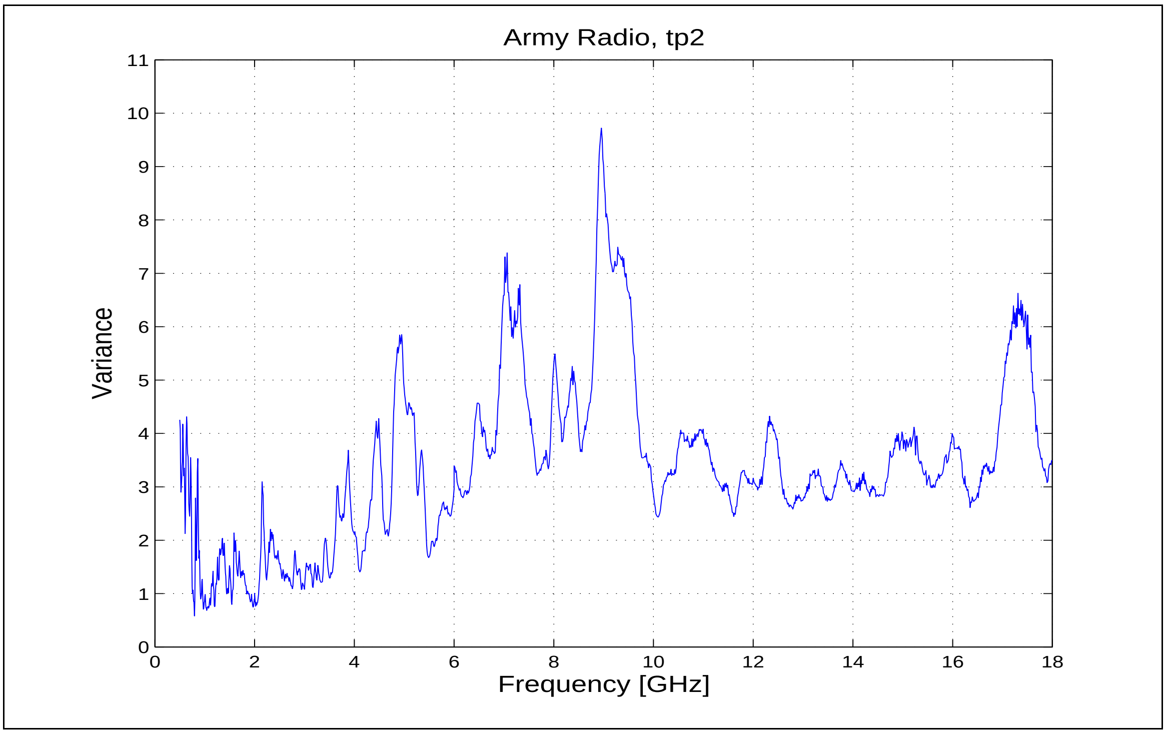

Figure 17. Variance of the received power normalized to mean, taken for all three planes. Army Radio, tp2.

The variance of the normalized χ^2-distribution with one degree of freedom is equal to two [13]. According to the plot above, there is a large deviation from two. An evident variation of the variance with frequency can also be noticed. The similar variation can be observed even in Figure 18 below, where the variation is plotted for each plane individually.

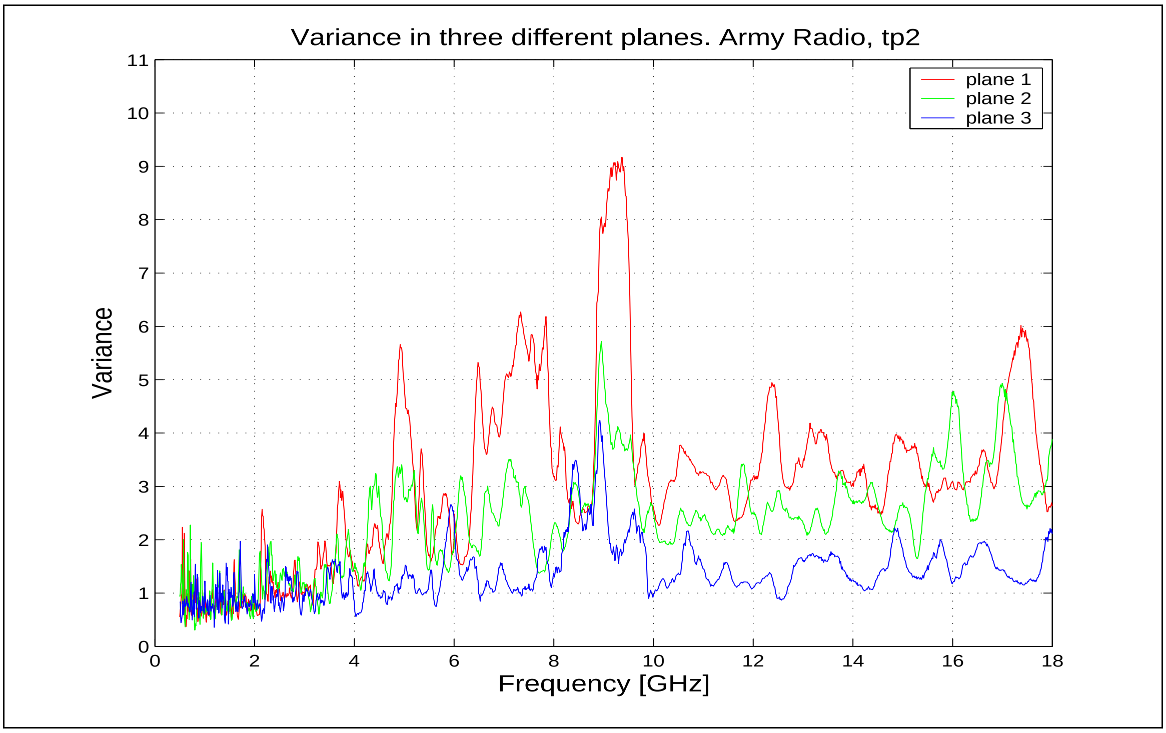

Figure 18. Variance of the received power normalized to mean taken for each plane individually. Army Radio, tp2.

According to the variance plots, it is apparent that the data does not follow a χ^2-distribution with one degree of freedom. The results of the chi-square goodness-of-fit test (Section 3.2.3), rejection significance level (p) are plotted for each frequency in Figure 19. As expected from the variance plots, the significance level for rejection p is extremely low for all frequencies. Obviously, the data are not $\chi^2(1)$-distributed. This is characteristic for tp4 and the two other objects as well. Significance level for rejection for the Avionics Box, tp4 and Test Missile, tp4 are presented in Appendix, page 93. Other test object – test point combinations are not given in Appendix because all the values of the significance level for rejection are so low that MATLAB represents them as zeros.

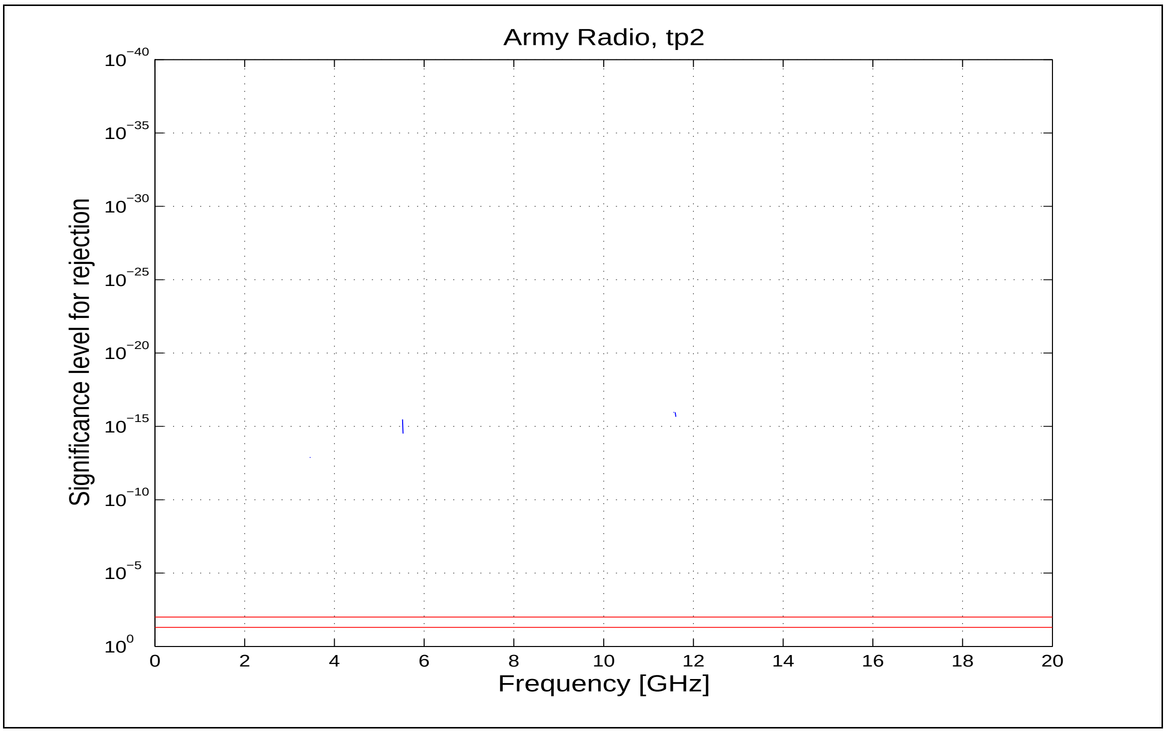

Figure 19. Significance level of rejection for received power normalized to mean. Army Radio, tp2. Only a few values of p can be seen; all other values are so small that MATLAB represents them as zeros.

However, the plots in Figure 16 indicate that the $\chi^2(1)$-distribution could be used as a rough estimate since there is a decent agreement with the measurement data. In order to measure the difference between measured and calculated cumulative distribution function the Kolmogorov-Smirnov test [15] is performed. The hypothesized $\chi^2(1)$-distribution is rejected at 5% significance level.

5 Conclusions

The investigated method, which uses only a few angles of incidence and polarisations and a frequency interval consisting of frequencies that are adjacent to the frequency of interest, seems to work for all frequencies with the exception for the frequency interval where the EUT has a major aperture resonance. Accordingly, taking this exception into account, the method can potentially be used as one part in more precise requirements regarding the angular resolution in radiated susceptibility (RS) testing of electronic equipment for microwave frequencies. In view of the fact that in practice one can often only afford to perform a testing for a few polarizations and angles of incidence, this method could be of great practical and economical interest.

The calculated values of EB_{dB} seem to be consistent with the expected normal distribution. This agreement is confirmed within some frequency intervals, but not all. However, an analysis, carried out for the complete range of tested frequencies, gives rejection at extremely low significance level.

The statistical analysis of the receiving cross section for several different frequencies resulted in the conclusion that the data are not χ^2- distributed with one degree of freedom. However, a decent fit between measured cumulative – and calculated cumulative distribution functions indicate that the $\chi^2(1)$ – distribution can be used as a rough estimate. This knowledge can enable one to, after that a test is performed in the Reverberation Chamber, calculate rough estimate of the probability of obtaining the maximum value of the measurement data within some specific boundaries (where the average value from the coupling measurements in the Anechoic Chamber is found from measurements using many different angles of incidence and many different polarisations).

6 Acknowledgments

I would like to express my appreciation to Magnus Höijer at the Swedish Defence Research Agency, FOI, for bringing me in to the problem and for the help all the way through this work. I would also like to thank Mats Bäckström at FOI for valuable discussions and Pontus Andersson at the Institute of Mathematics at Linköping University for mathematical and editorial assist. Furthermore, I wish to express gratitude to my boyfriend Adin Hadziselimovic for all support and to whom I could turn for help in all hours throughout this work.

7 References

[1] P. F. Wilson, D. A. Hill and C. L. Holloway. *On Determining the Maximum Emissions From Electrically Large Sources*. In IEEE Trans. on Electromagn. Compat., vol.44 no.1, pp. 79-86, February 2002.

[2] P. G. Landgren. *Some directivity properties of test objects in the microwave region*. In IEEE Int. Symp. on EMC, pp. 887-891, Montréal, Canada, 2001.

[3] M. Bäckström and L. Jansson. *Directivity of Equipment and Its Effect on Testing in Mode-Stirred and Anechoic Chamber*. In IEEE Int. Symp. on EMC, pp. 17-22, Seattle, WA, USA, 1999.

[4] M. Bäckström and J. Lorén. *Microwave Coupling into a Generic Object. Properties of Angular Receiving Pattern and its Significance for Testing in Anechoic and Reverberation Chambers*. Scientific Report FOI-R--0392--SE, Swedish Defence Research Agency FOI, SE-581 11 Linköping, Sweden, February 2002.

[5] M. Höijer. *Shielding Effectiveness of Apertures – Directional Pattern*. FOI Memo 03-2029, Swedish Defence Research Agency FOI, SE-581 11 Linköping, Sweden.

[6] O. Lundén. *Mätsystemet i Stora Mäthallen. Dokumentation. Version 1.1*. FOA Internal Report FOA-D--00-00508-408--SE, Swedish Defence Research Agency FOI, SE-581 11 Linköping, Sweden, December 2002.

[7] G. E. Noether. *Introduction to Statistics : The Nonparametric Way*. Springer-Verlag, New York, 1991, ISBN 0-387-97284-6.

[8] J. R. Taylor. *An Introduction to Error Analysis. The Study of Uncertainties in Physical Measurements*. Second Edition, University Science Books, Sausalito, California, USA, 1997, ISBN 0-935702-75-X.

[9] G. Blom. *Sannolikhetsteori och statistisk teori med tillämpningar*. Studentlitteratur, Lund, 1989, ISBN 91-44-03594-2.

[10] E. L. Bronaugh and J. D. M. Osburn. *Estimating EMC Measurements Uncertainty Using Logarithmic Terms (dB)*. In IEEE Int. Symp. on EMC, pp. 376-378, Seattle, WA, USA, 1999.

[11] R. B. D'Agostino and M. A. Stephens. *Goodness-of-Fit Techniques*. Marcel Dekker, Inc., New York, 1986, ISBN 0-8247-7487-6.

[12] C. A. Balanis. *Antenna Theory : Analysis and Design.* John Wiley & Sons, Inc, New York, 1997, ISBN 0-471-59268-4.

[13] M. Bäckström and O. Lundén. *Transmissions Cross Sections of Apertures Measured by Use of Nested Mode-Stirred Chambers.* Scientific Report FOA-R--96-00359-3.2--SE, Swedish Defence Research Agency FOI, SE-581 11 Linköping, Sweden, December 1996.

[14] M. Evans, N. Hastings and B. Peacock. *Statistical Distributions*. John Wiley & Sons, Inc., New York, 1993, ISBN 0-471-55951-2.

[15] http://www.itl.nist.gov/div898/handbook/eda/section3/eda35g.htm

Appendix A

General trend

As can be seen in any standard antenna textbook, e.g. [12, p. 86], the impedance matched receiving cross section, σ_q, is given by:

$$\sigma_q = \frac{\lambda^2}{4\pi q} G_{R,p}\left(f, p, \theta, \varphi\right) = \frac{c^2}{4\pi f^2 q} G_{R,p}\left(f, p, \theta, \varphi\right) \qquad (13)$$

The partial realized gain, $G_{R,p}$, depends on the angle of incidence, $\Omega = (\theta, \varphi)$, the polarisation p, and the frequency, f. This frequency dependence is used in the method investigated in this paper. But, as seen in (13), there is one more factor in the expression that depends on the frequency, the general trend one over frequency squared. So, when we vary the frequency in our method and calculate the value of σ_f, it is not a priori obvious if the frequency variation originate from the general trend or from the frequency dependence of $G_{R,p}$. In practice it is perhaps not so important to know the origin of the frequency variation[4], but from an interpretation point of view it is interesting to e.g. deduct the general trend from the frequency variation in order to see the isolated contribution from the frequency dependence of $G_{R,p}$ on the frequency variation. Thus, it is of interest for the investigated method to consider the general trend. One possible way to do that is to introduce a quantity that represents the general trend for each tested frequency and interval.

[4] That since the sum of the two contributions is used in our method.

The general trend can be determined by studying the general trend of the average receiving cross section, $\sigma_{q,average}$, taken over all angles of incidence and polarizations, which tentatively can be written as:

$$\sigma_{q,average} = \frac{c^2}{4\pi f^2 q} G_{R,p,average} = \frac{c^2}{8\pi f^2} \qquad \text{(tentative)} \qquad (14)$$

where $G_{R,p,average}$ is the average of the partial realized gain taken over all directions (angles of incidence) and all polarizations. If we assume that the partial realized gain can be approximated as the ratio of the received intensity in the direction $\Omega = (\theta, \varphi)$ for the polarisation p, and the average received intensity taken over all directions (angles of incidence) and polarisations of the incident field, it follows directly that $G_{R,p,average}$ is equal to $q/2$.

The following quantities can be used for the evaluation of the general trend:

$$gt = \frac{\sigma_{q,average}\left(f_0 - \Delta f\right)}{\sigma_{q,average}\left(f_0\right)}$$
$$gt' = \frac{\sigma_{q,average}\left(f_0 + \Delta f\right)}{\sigma_{q,average}\left(f_0\right)} \qquad (15)$$

where f_0 is the test frequency, $f_0 - \Delta f$ and $f_0 + \Delta f$ is the first respectively the last frequency of the frequency interval in use.

In this way we can compensate for the general trend. However, it does not work in reality, since $\sigma_{q,average}$ does not look like it should do according to (14). This can be seen in Figure 4, where experimental values of $\sigma_{q,average}$ are plotted (expressed in decibel relative to a square meter, dBsm). $\sigma_{q,average}$ does apparently not decrease with the factor $\frac{1}{f^2}$. This means that the average partial realized gain is not equal to $q/2$. This can be explained using the following expression:

$$G_{R,p}(f,p,\theta,\varphi) = \eta(f) \cdot D_{R,p}(f,p,\theta,\varphi) \quad (16)$$

where η is the radiation efficiency and $D_{R,p}$ is the realised partial directivity. As can be concluded, the radiation efficiency obviously depends on the frequency (and we use this frequency variation in our investigated method). But, there is also a general frequency dependence in η[5]. This general frequency dependence is the reason why $\sigma_{q,average}$ does not as a trend decrease with the factor $\frac{1}{f^2}$. Since we do not know this general trend in η, we do not do the compensation for the general trend. We hope to be able to return to this problem in the future.

[5] To be correct, the general frequency dependence in $D_{R,p}$ should be included, but that dependence is insignificant [1].

Appendix B

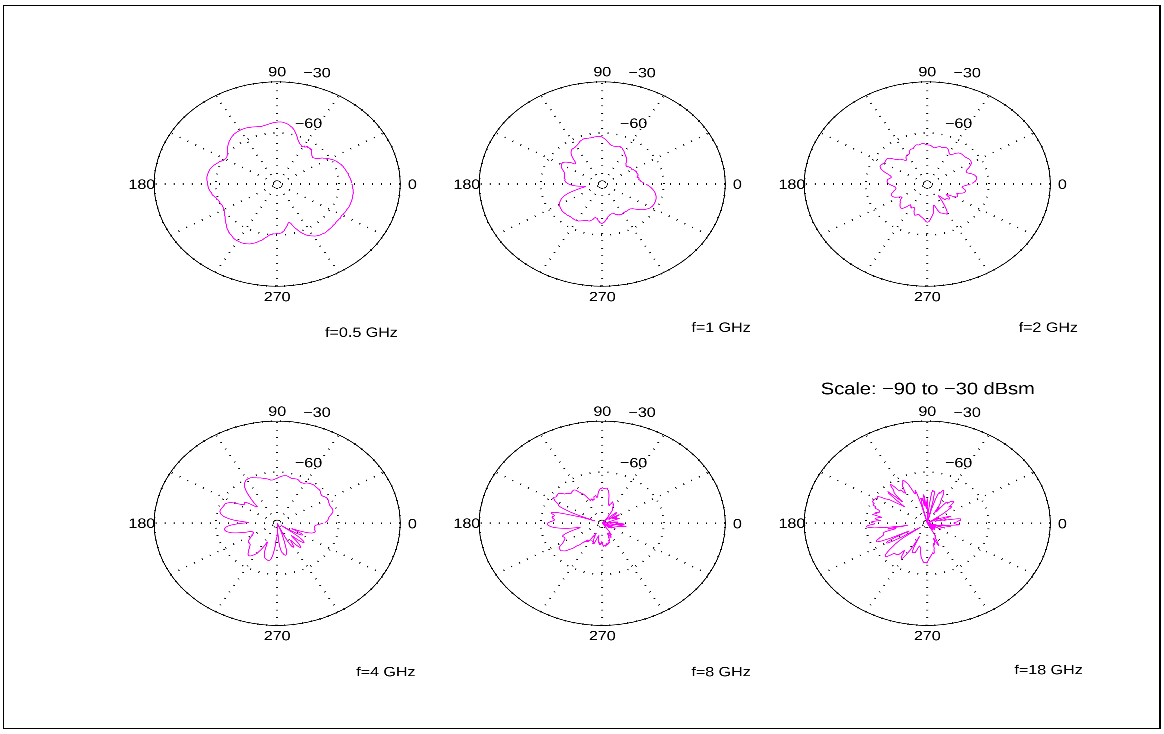

Angular dependence of σ_q. The Army Radio, plane 1, horizontal polarisation, tp2.

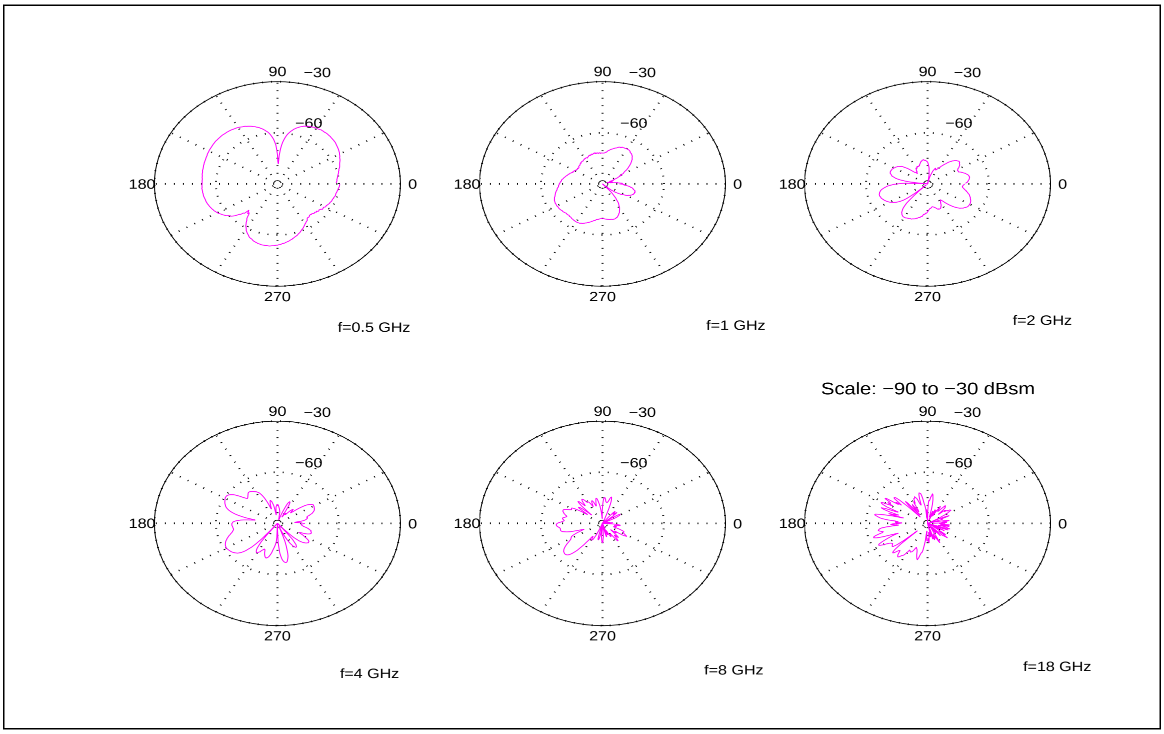

Angular dependence of σ_q. The Army Radio, plane 1, vertical polarisation, tp2.

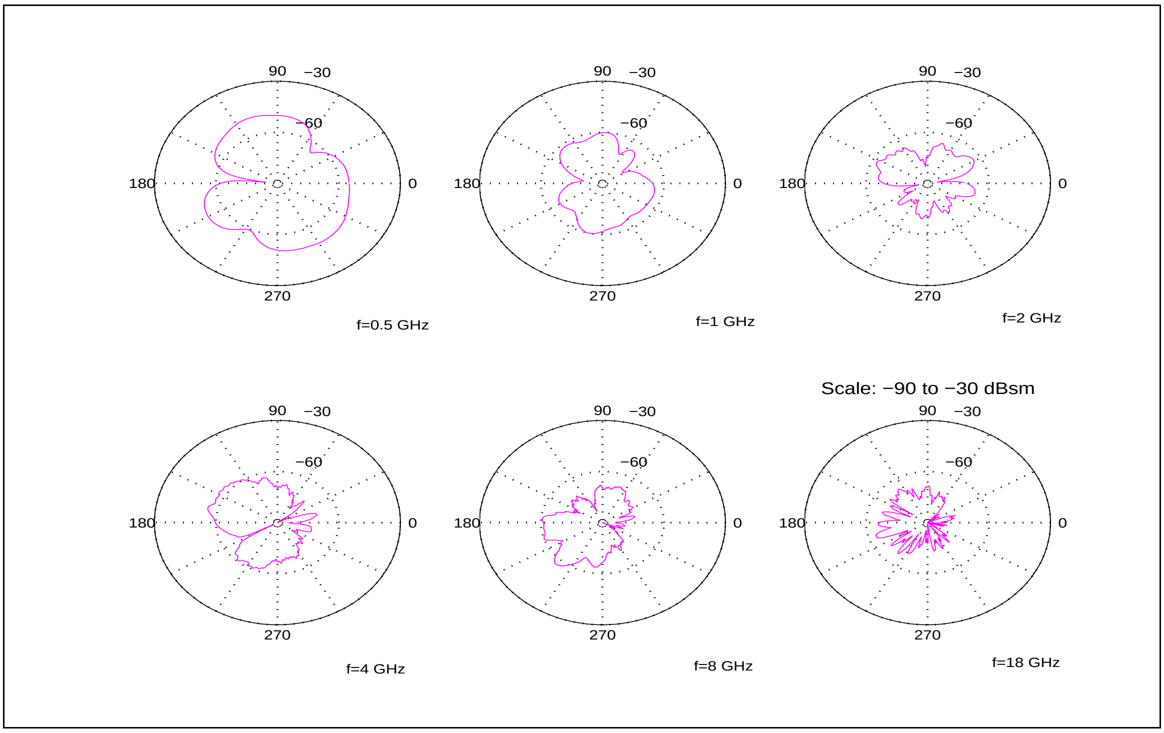

Angular dependence of σ_q. The Army Radio, plane 2, horizontal polarisation, tp2.

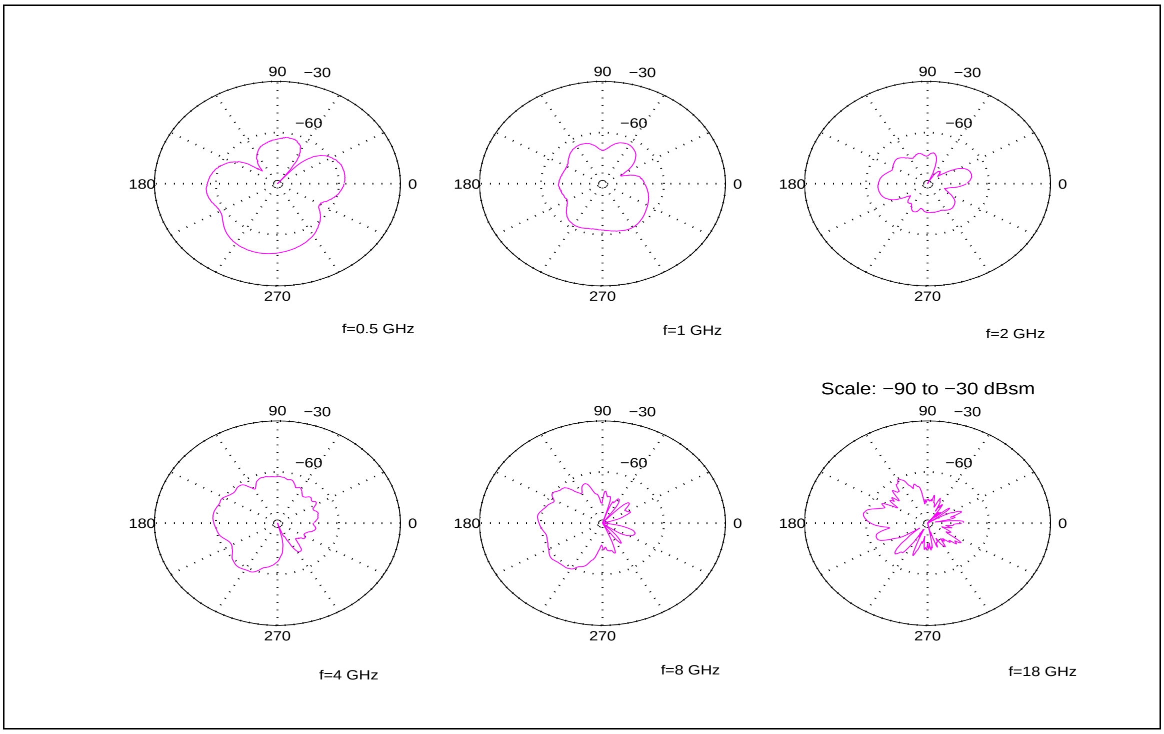

Angular dependence of σ_q. The Army Radio, plane 2, vertical polarisation, tp2.

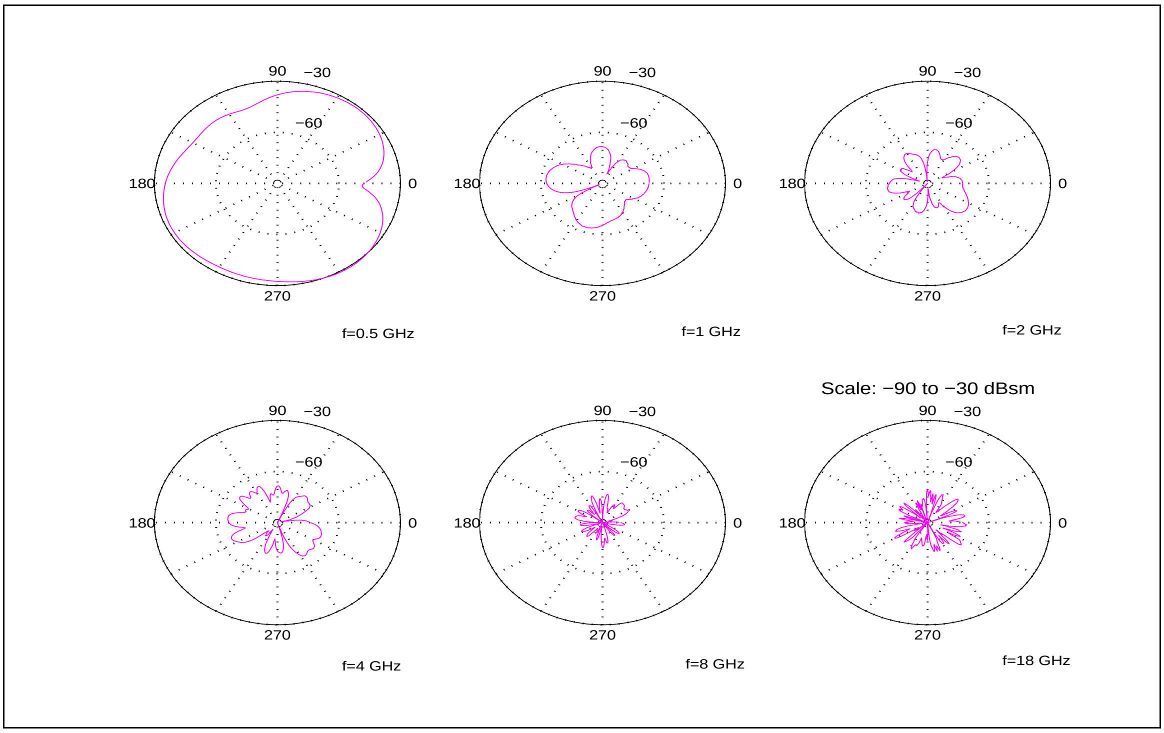

Angular dependence of σ_q. The Army Radio, plane 3, horizontal polarisation, tp2.

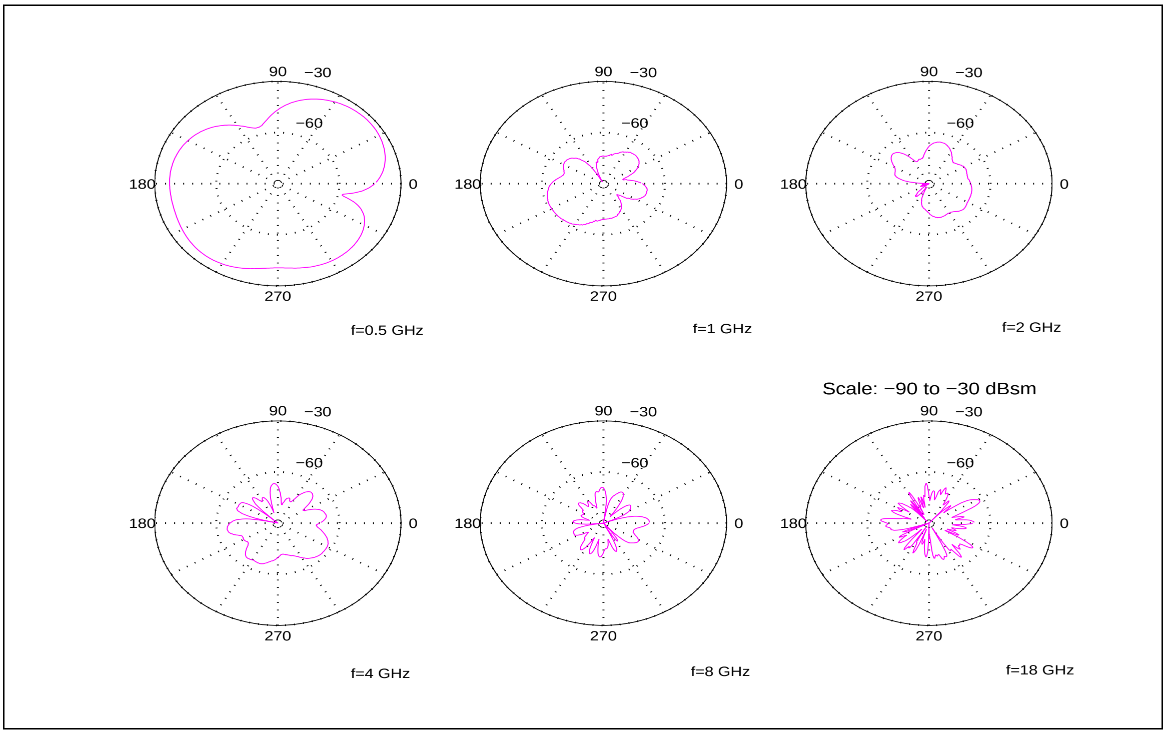

Angular dependence of σ_q. The Army Radio, plane 3, vertical polarisation, tp2.

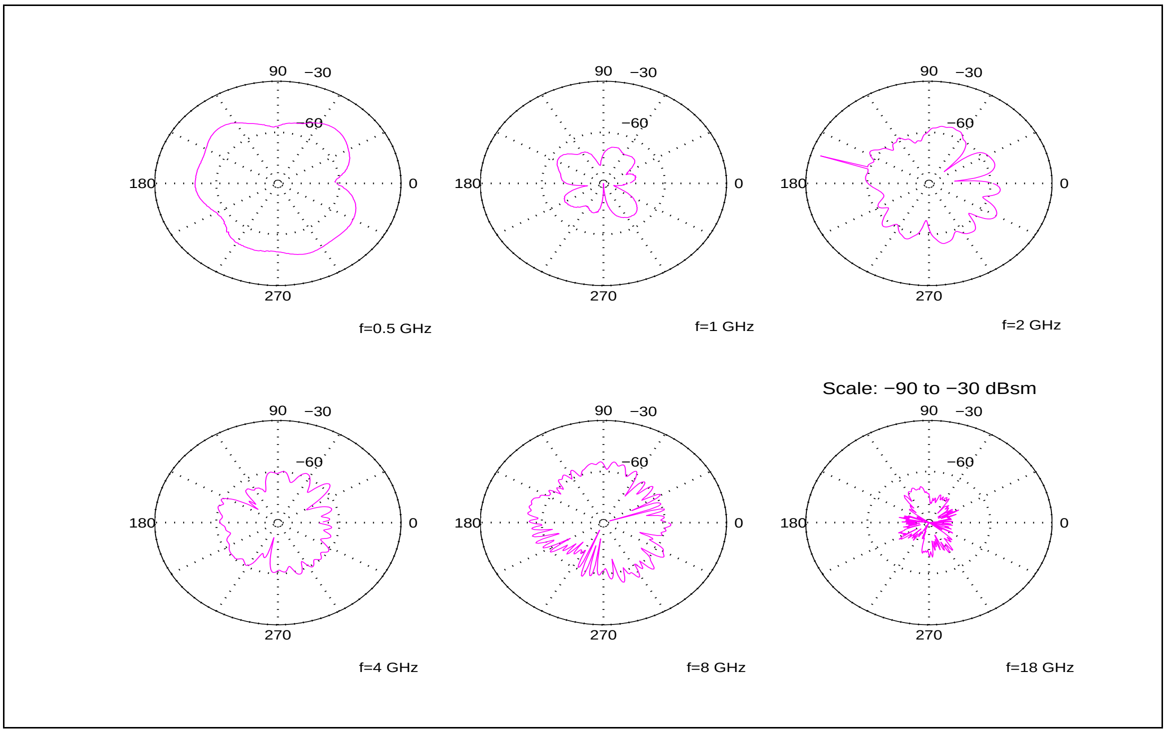

Angular dependence of σ_q. The Army Radio, plane 1, horizontal polarisation, tp4.

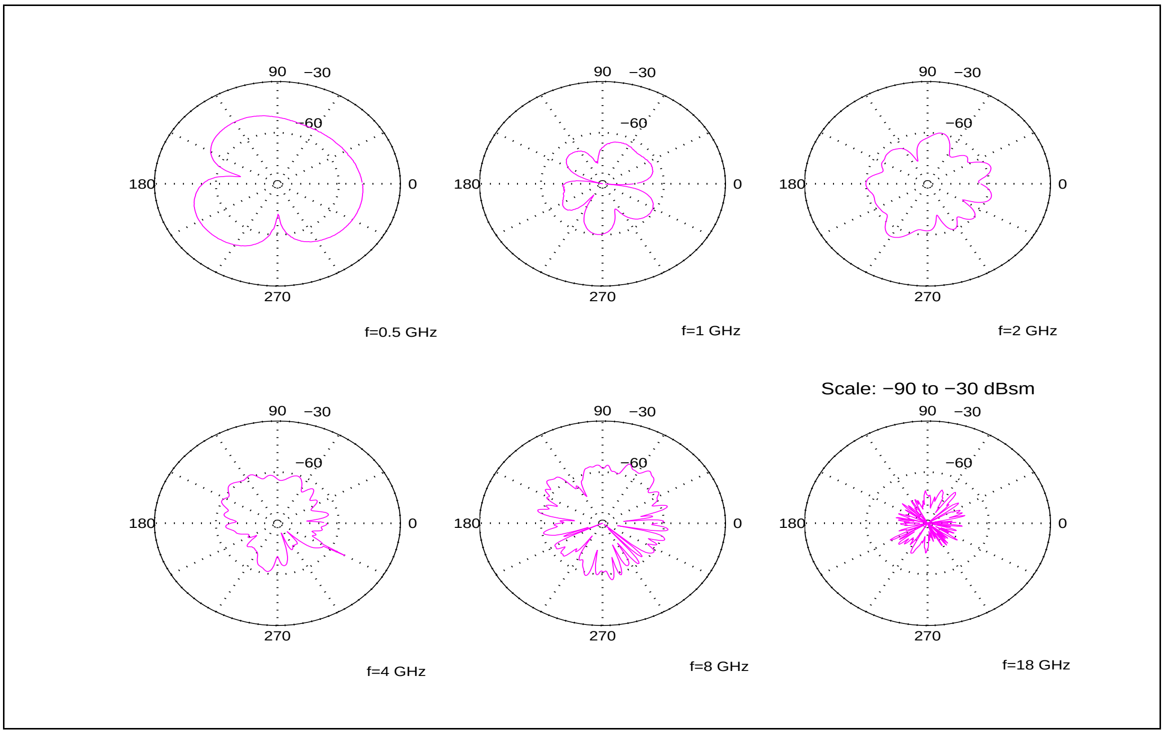

Angular dependence of σ_q. The Army Radio, plane 1, vertical polarisation, tp4.

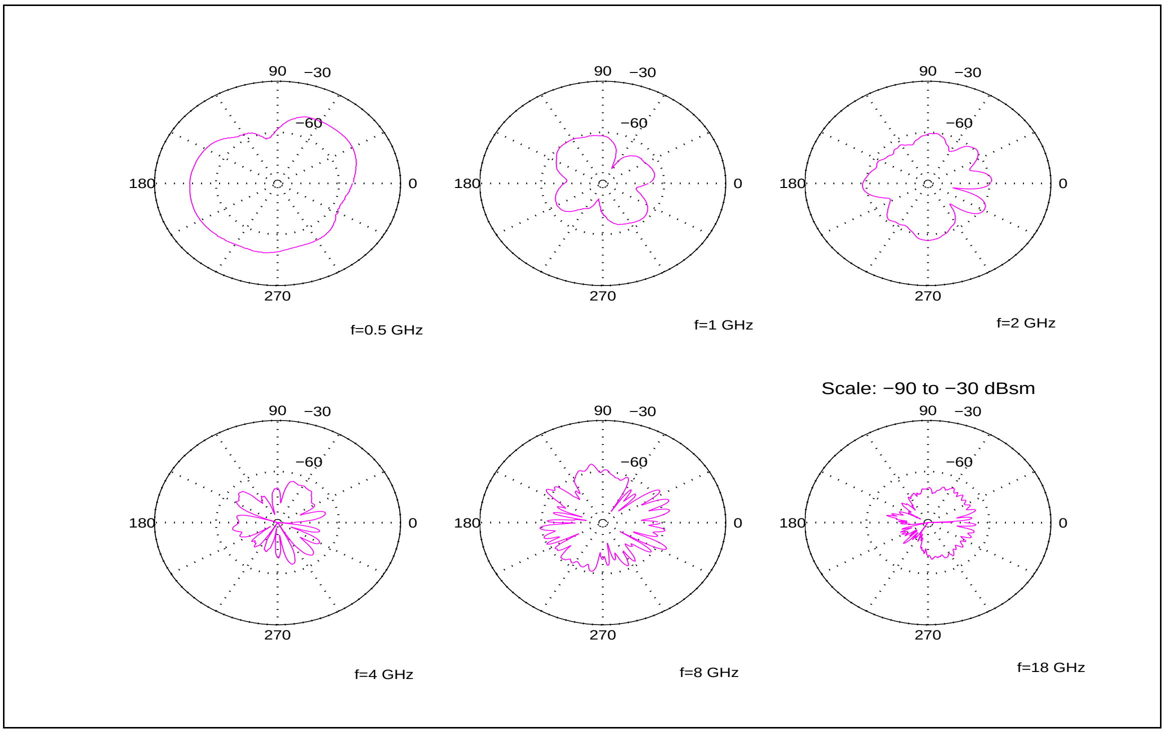

Angular dependence of σ_q. The Army Radio, plane 2, horizontal polarisation, tp4.

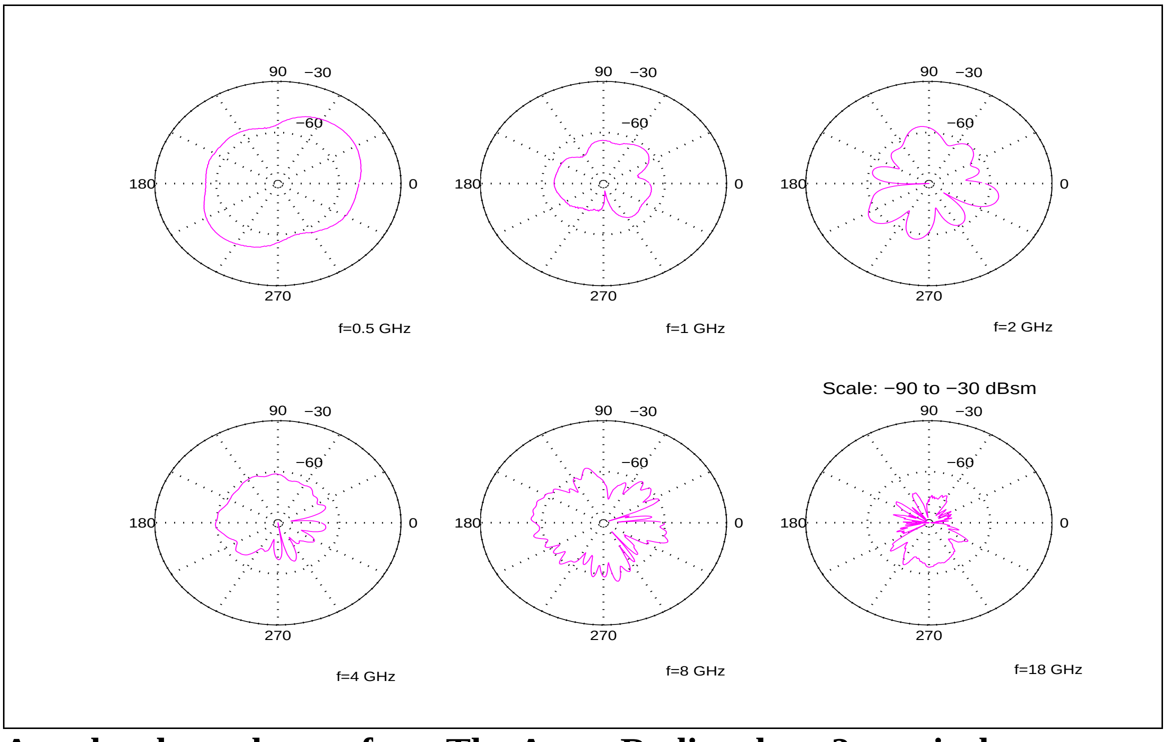

Angular dependence of σ_q. The Army Radio, plane 2, vertical polarisation, tp4.

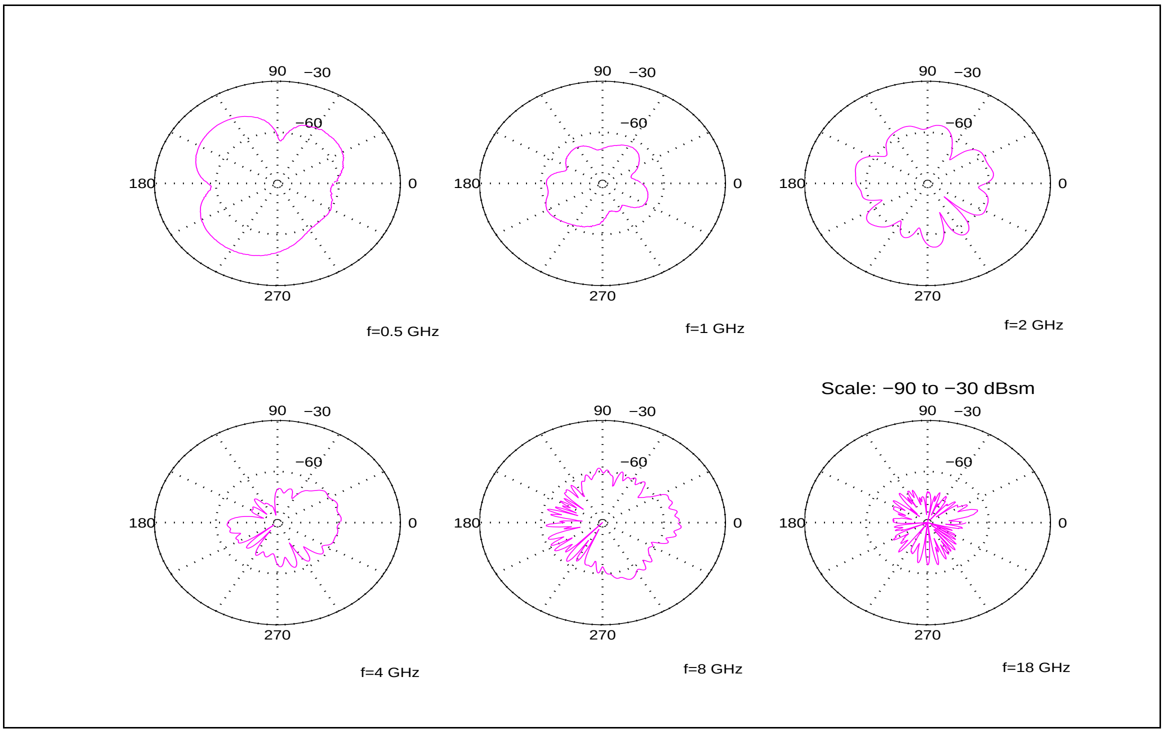

Angular dependence of σ_q. The Army Radio, plane 3, horizontal polarisation, tp4.

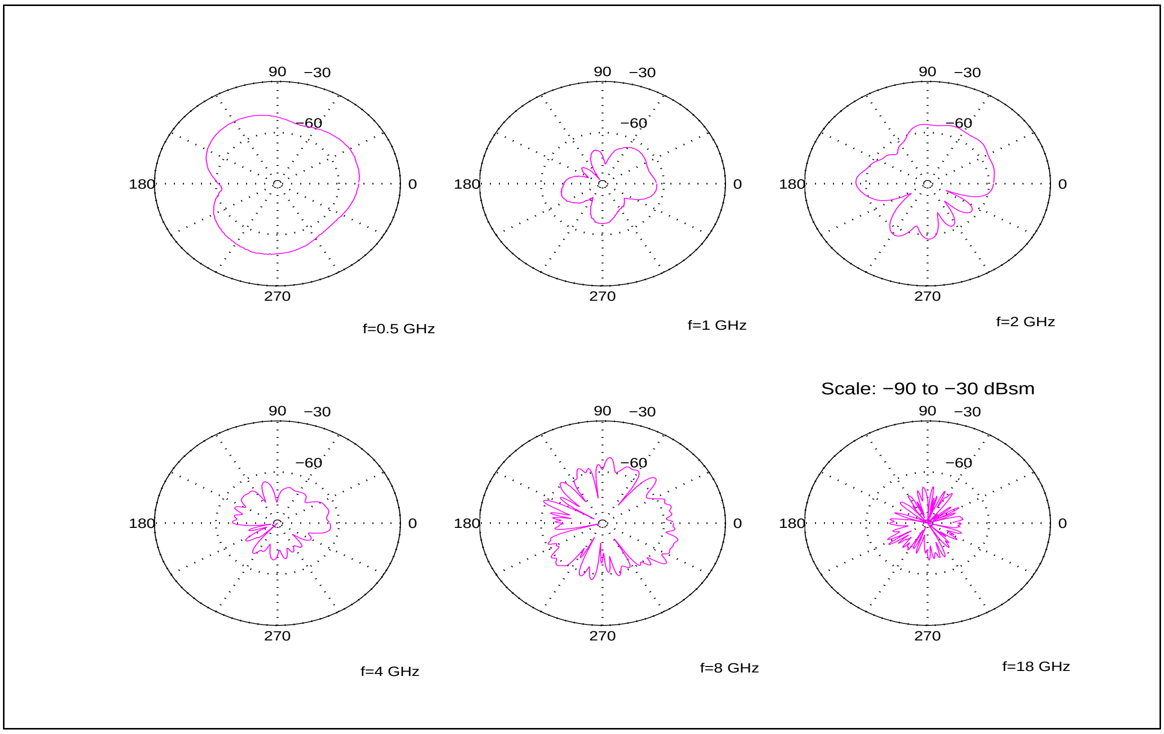

Angular dependence of σ_q. The Army Radio, plane 3, vertical polarisation, tp4.

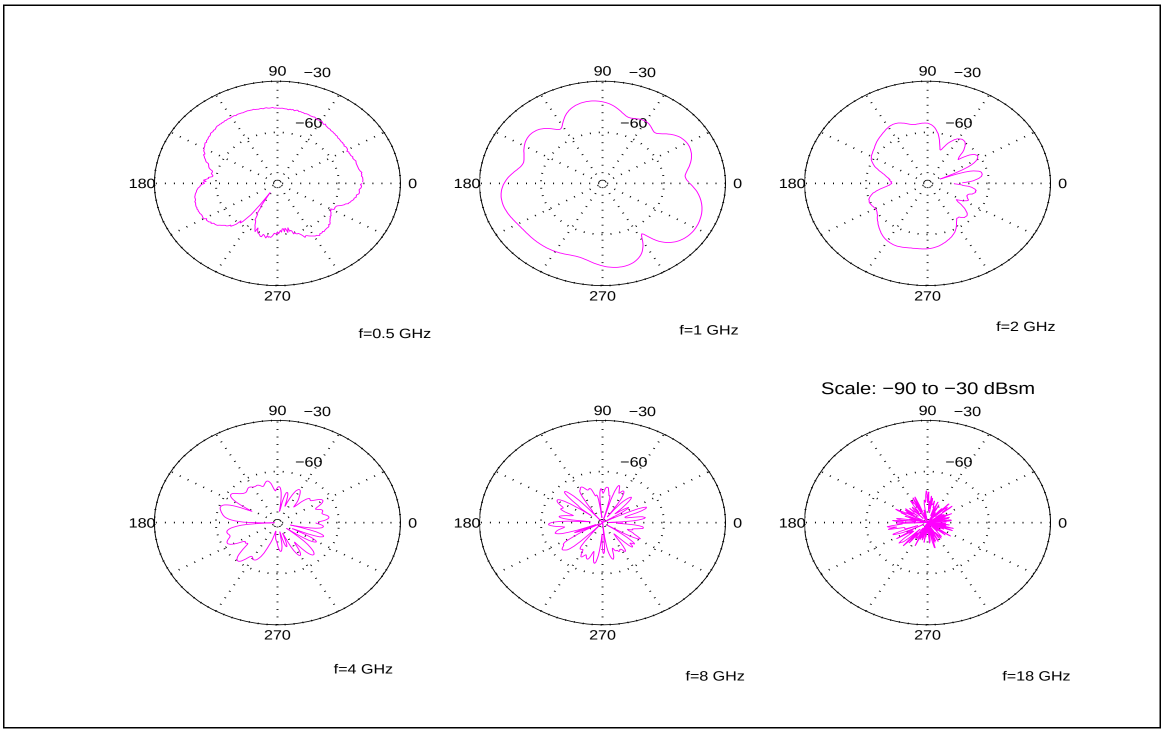

Angular dependence of σ_q. The Avionics Box, plane 1, horizontal polarisation, tp2.

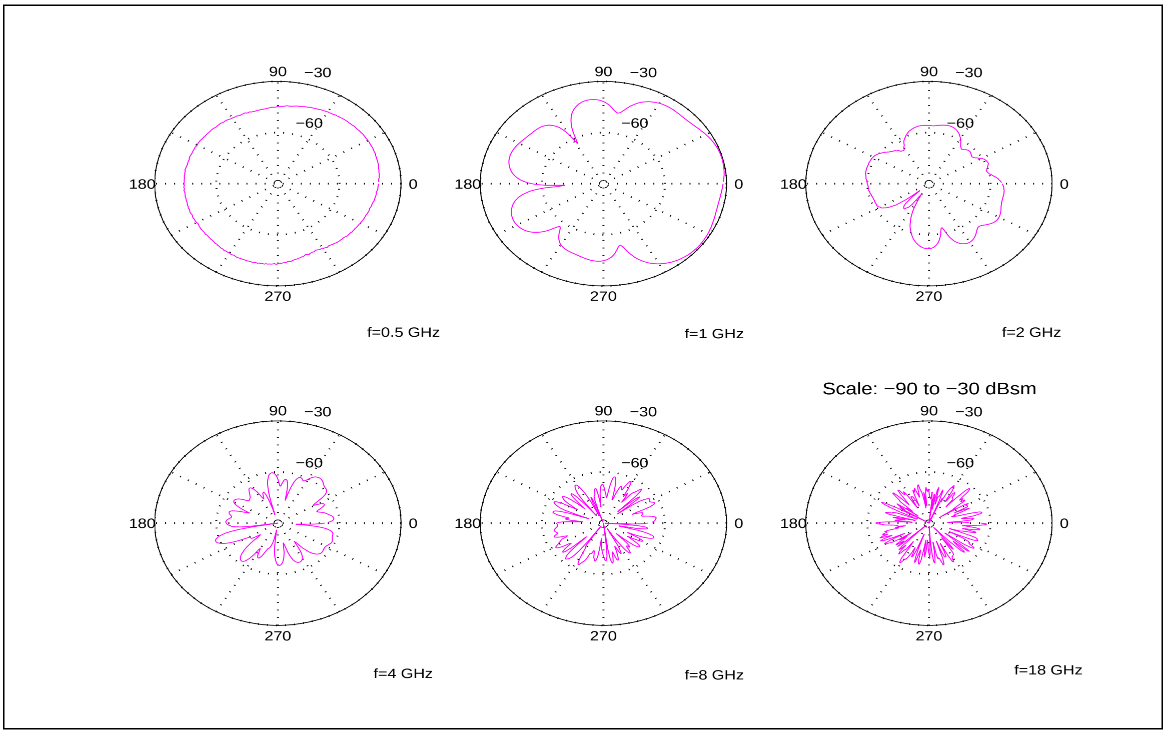

Angular dependence of σ_q. The Avionics Box, plane 1, vertical polarisation, tp2.

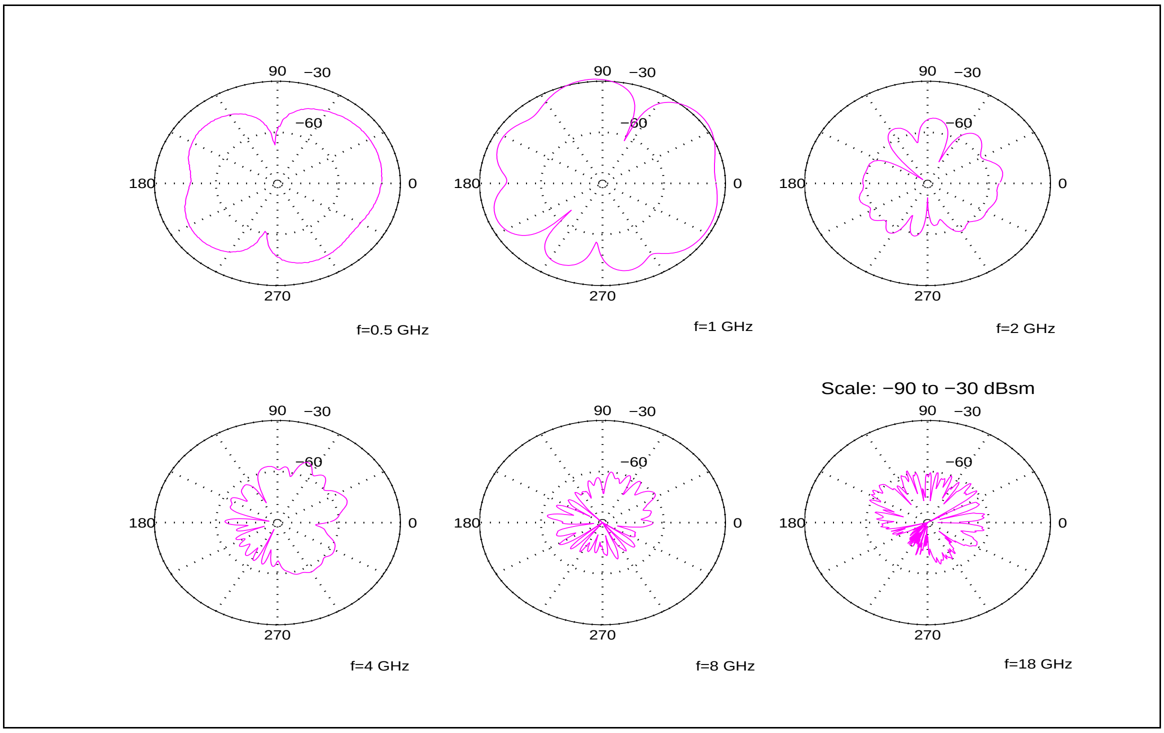

Angular dependence of σ_q. The Avionics Box, plane 2, horizontal polarisation, tp2.

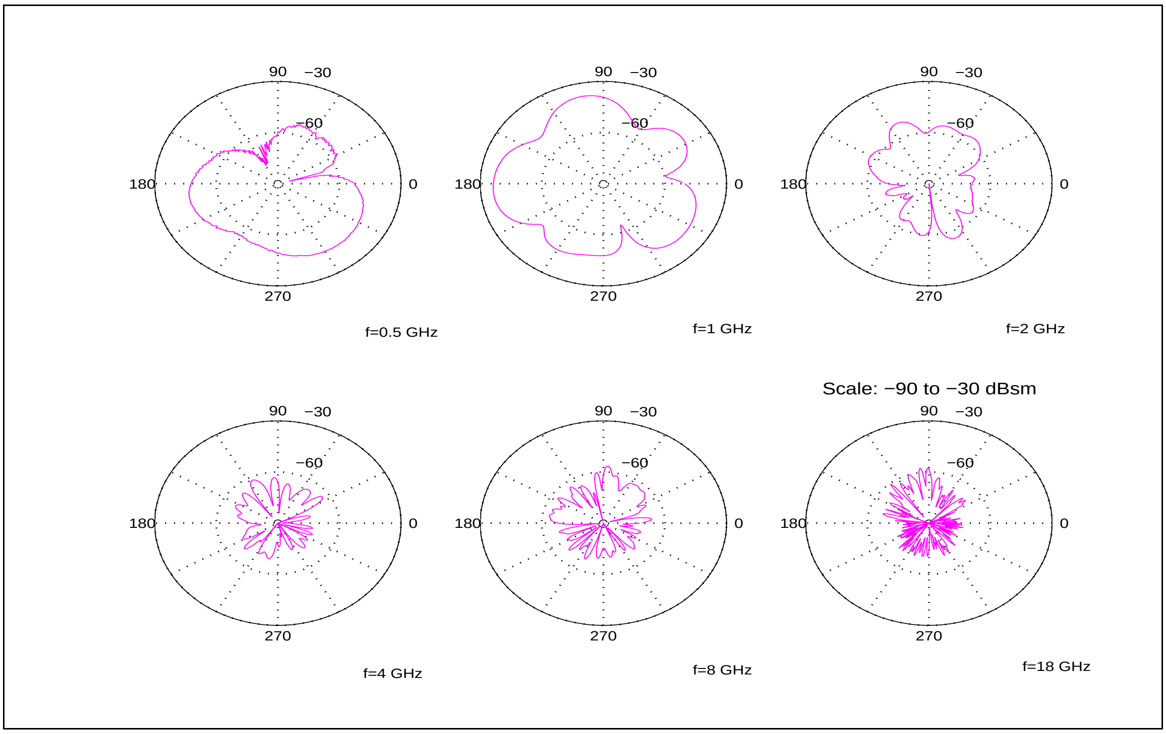

Angular dependence of σ_q. The Avionics Box, plane 2, vertical polarisation, tp2.

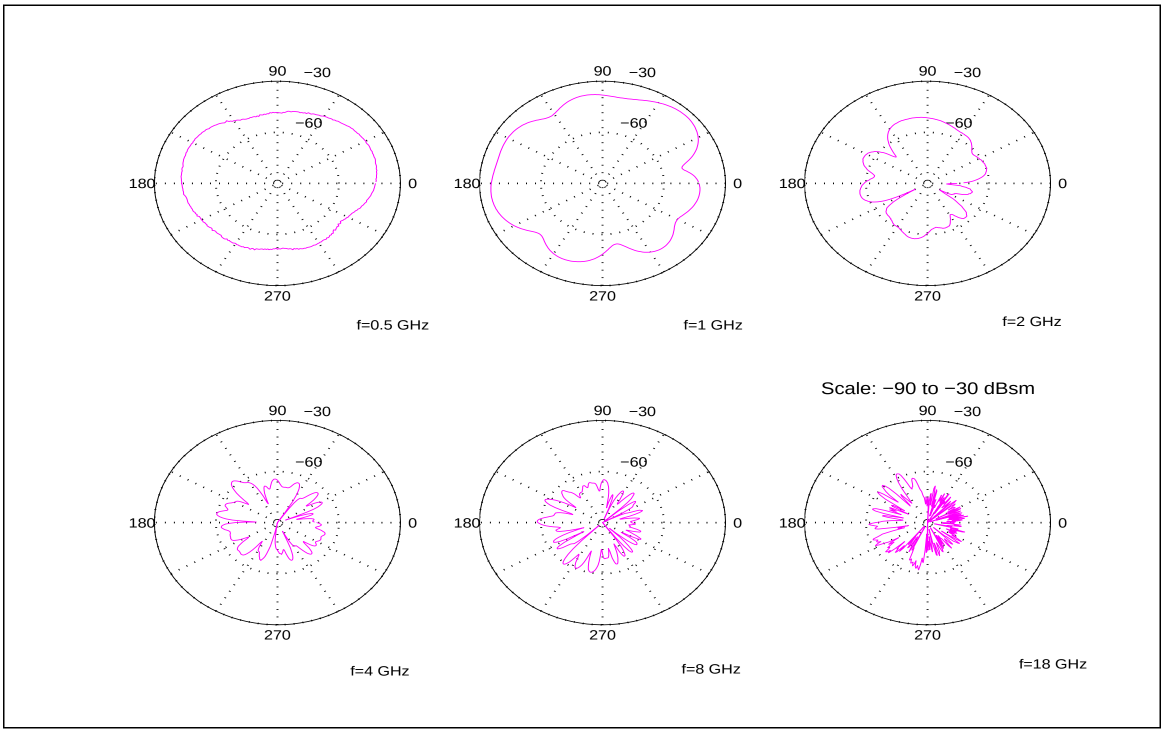

Angular dependence of σ_q. The Avionics Box, plane 3, horizontal polarisation, tp2.

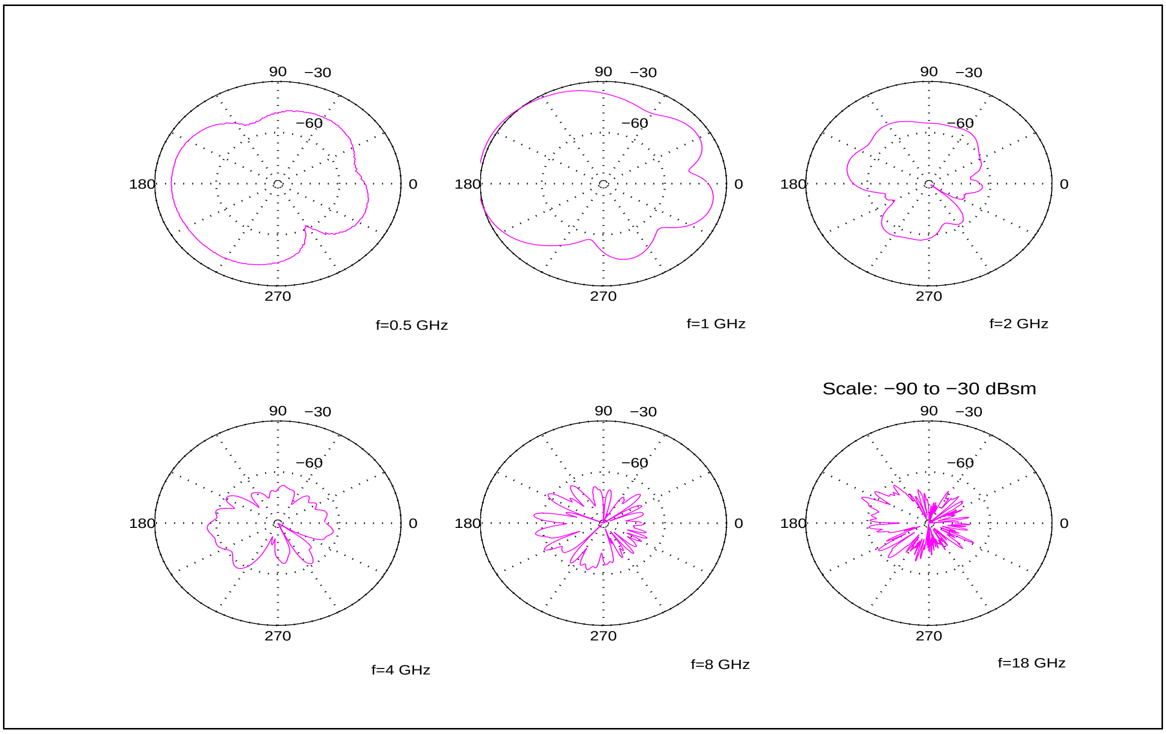

Angular dependence of σ_q. The Avionics Box, plane 3, vertical polarisation, tp2.

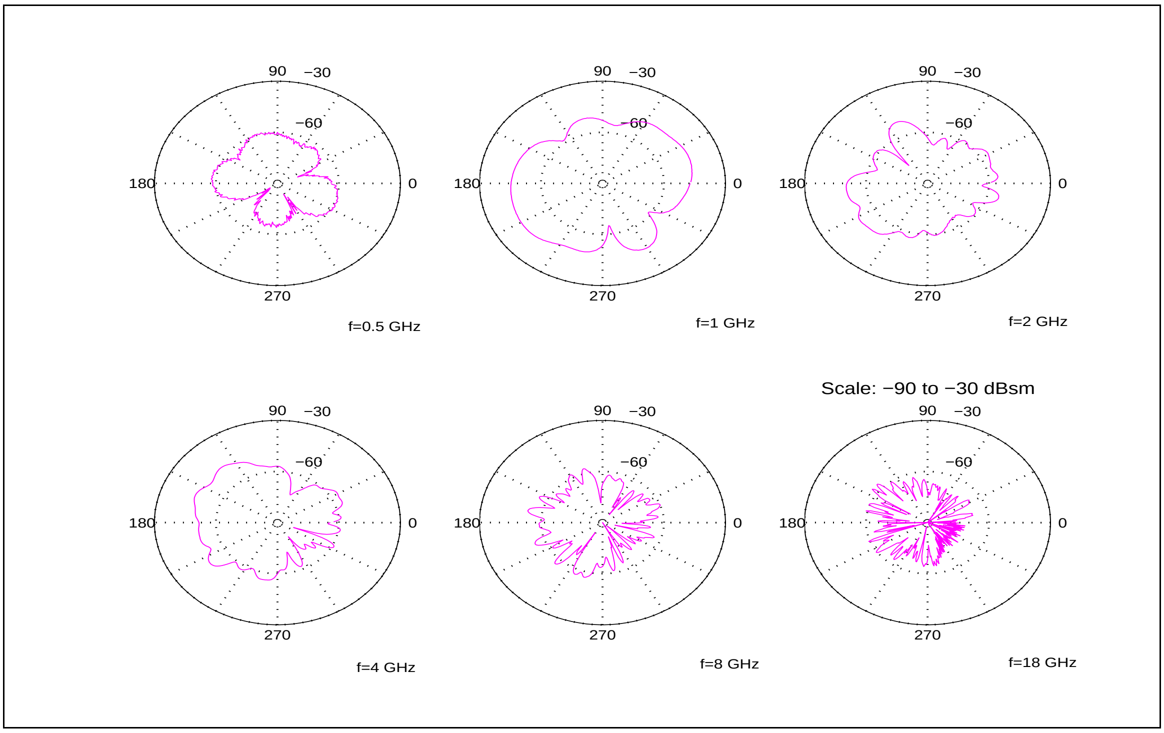

Angular dependence of σ_q. The Avionics Box, plane 1, horizontal polarisation, tp4.

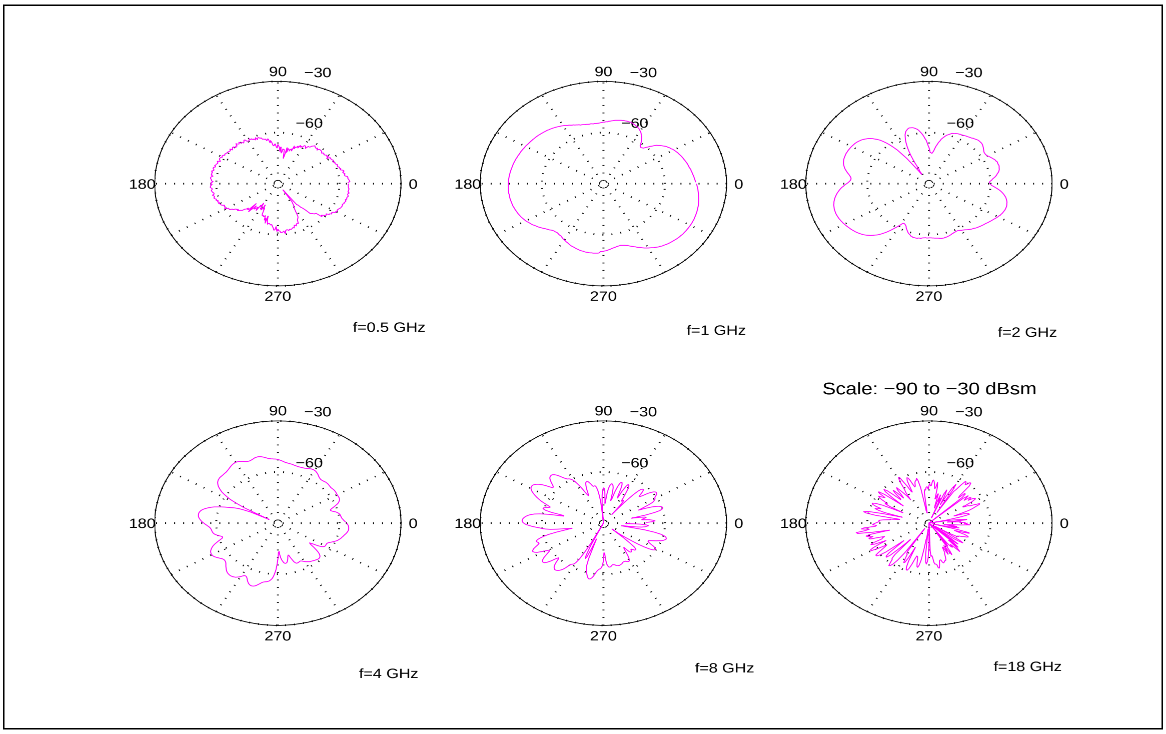

Angular dependence of σ_q. The Avionics Box, plane 1, vertical polarisation, tp4.

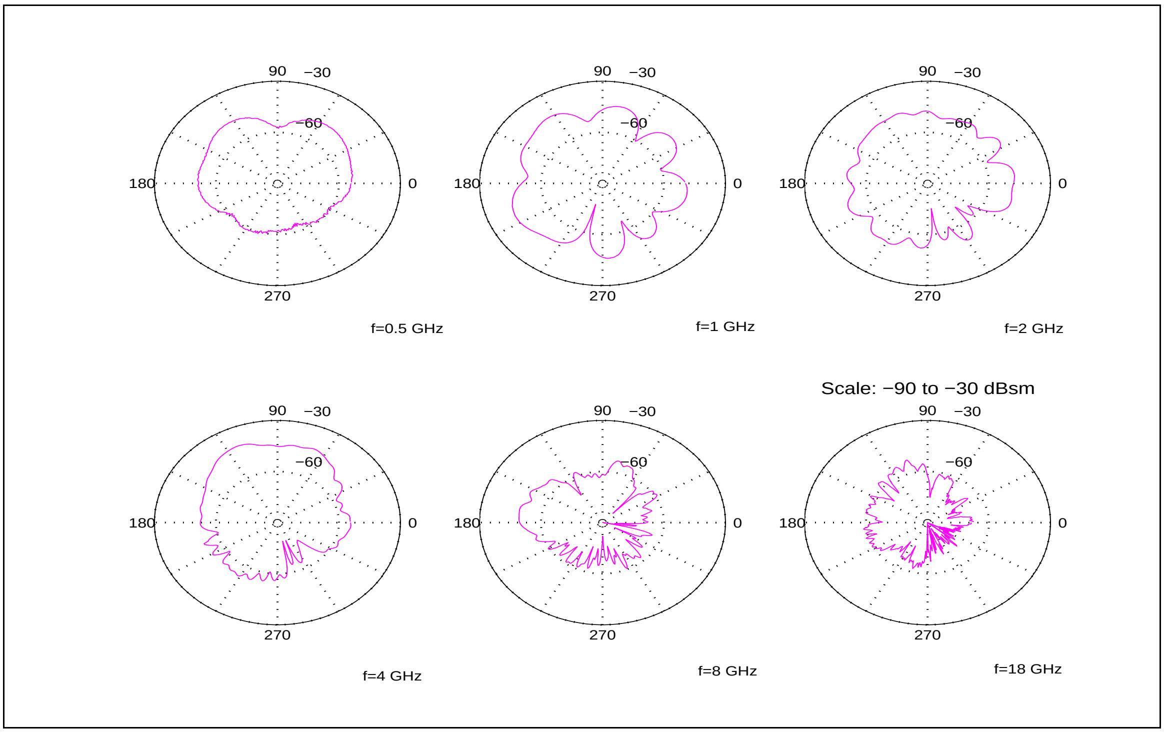

Angular dependence of σ_q. The Avionics Box, plane 2, horizontal polarisation, tp4.

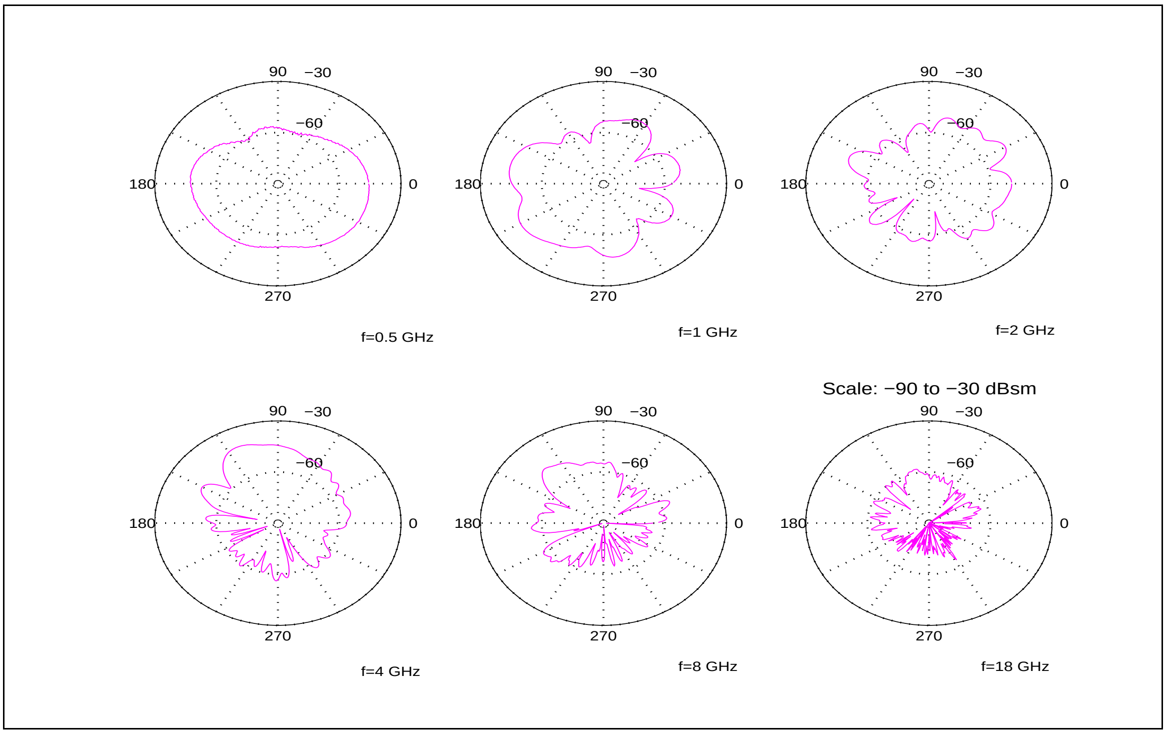

Angular dependence of σ_q. The Avionics Box, plane 2, vertical polarisation, tp4.

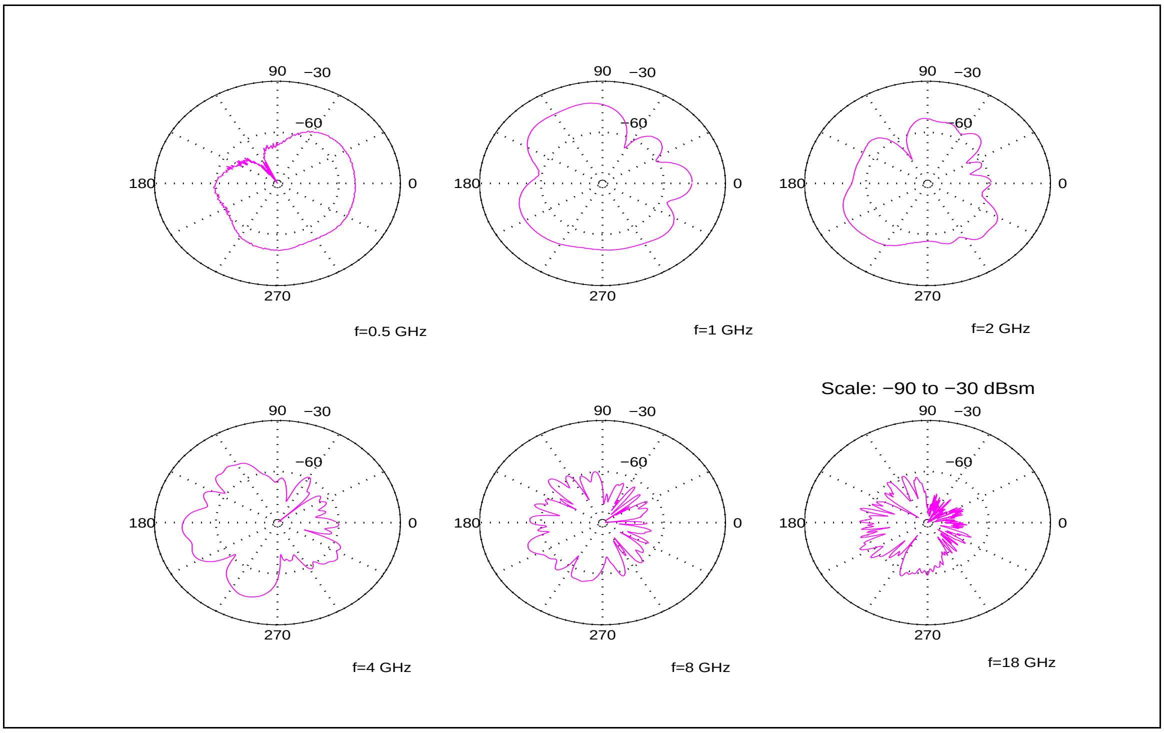

Angular dependence of σ_q. The Avionics Box, plane 3, horizontal polarisation, tp4.

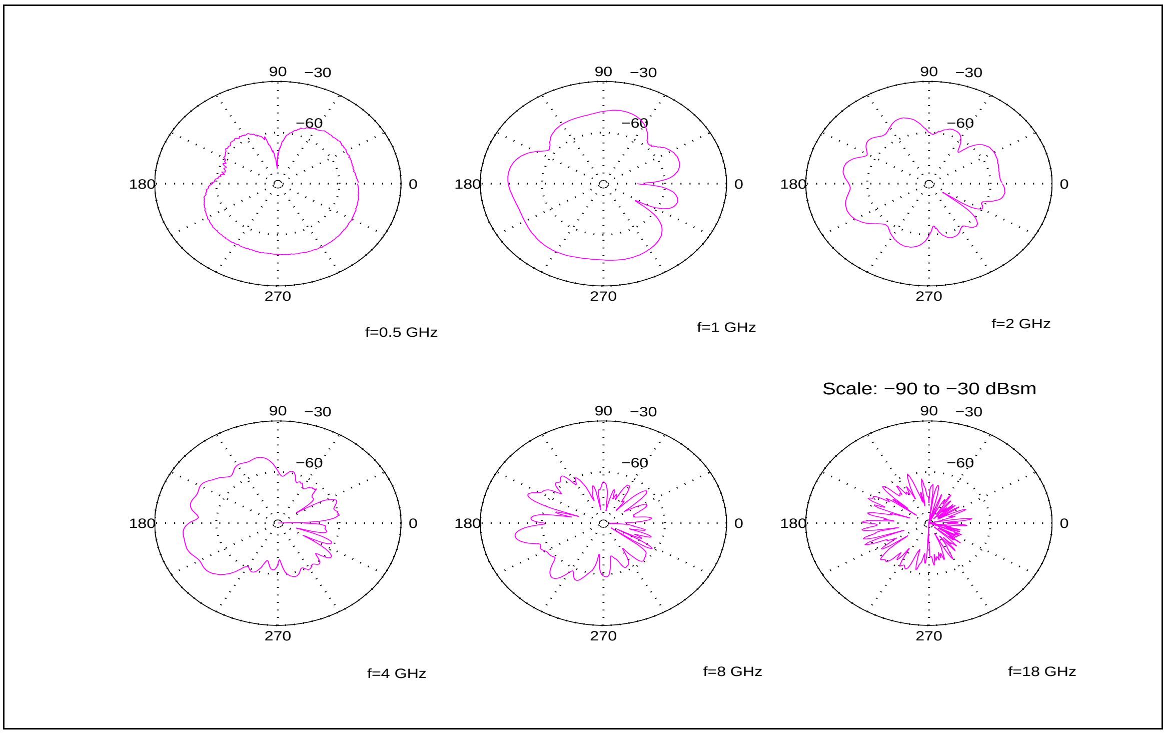

Angular dependence of σ_q. The Avionics Box, plane 3, vertical polarisation, tp4.

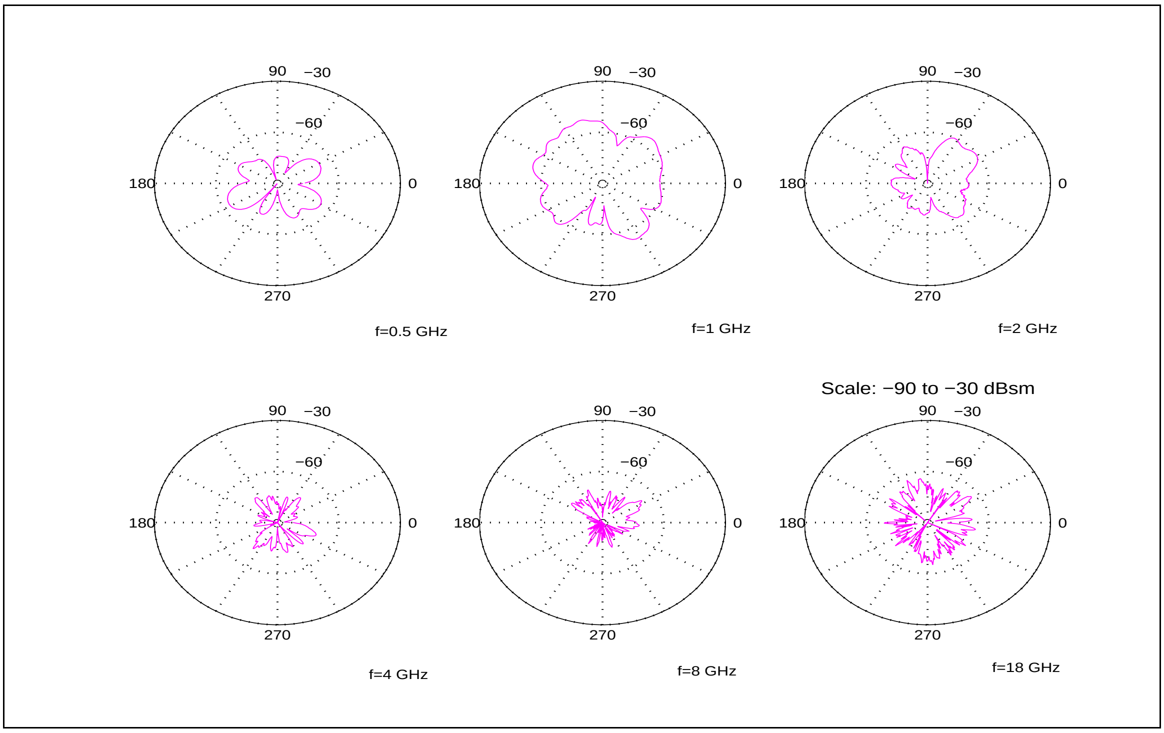

Angular dependence of σ_q. The Test Missile, plane 1, horizontal polarisation, tp2.

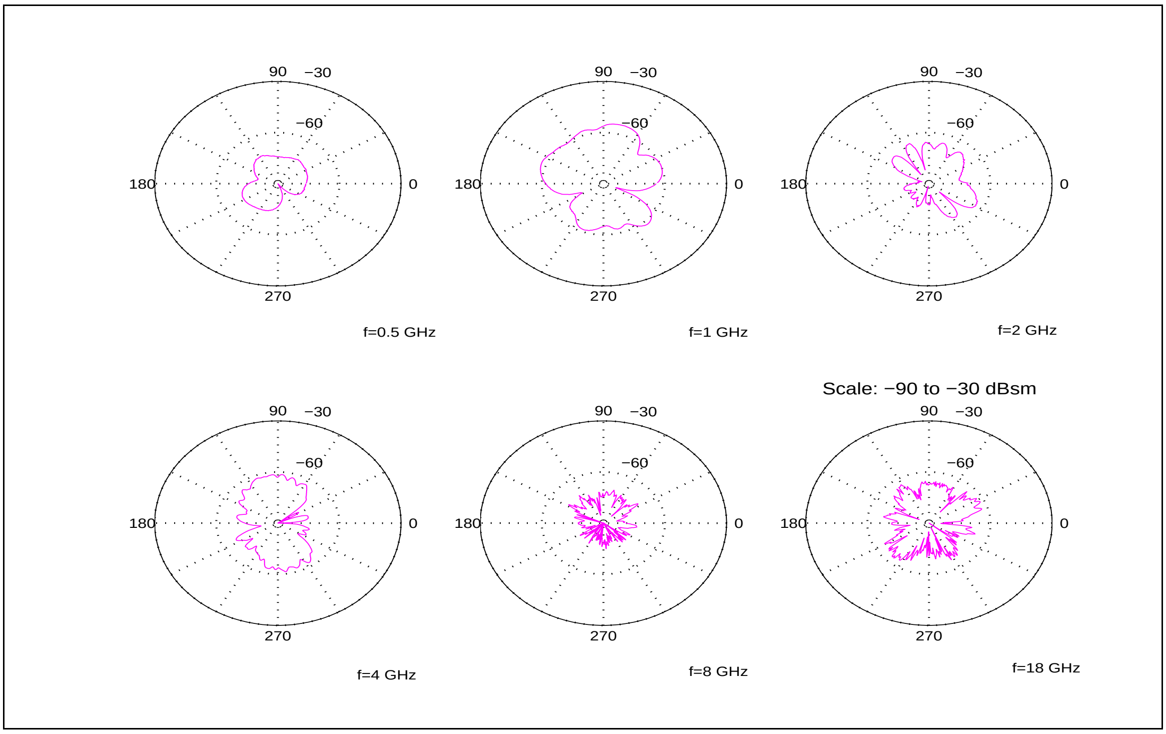

Angular dependence of σ_q. The Test Missile, plane 1, vertical polarisation, tp2.

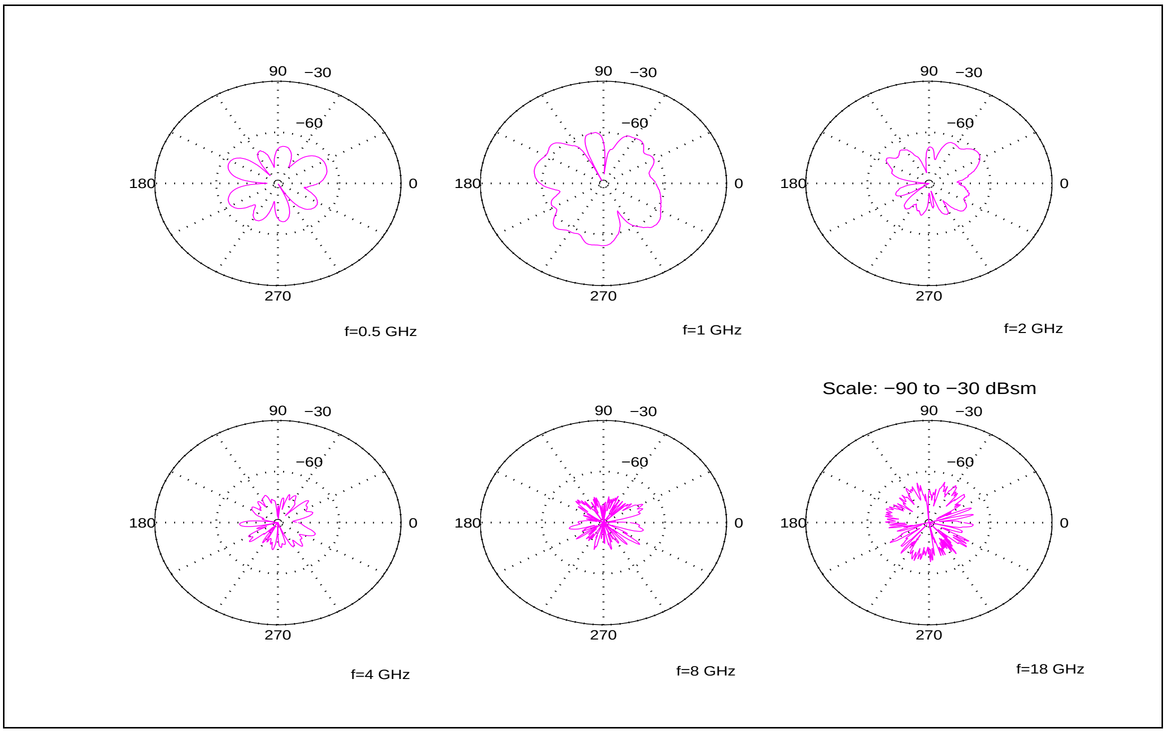

Angular dependence of σ_q. The Test Missile, plane 2, horizontal polarisation, tp2.

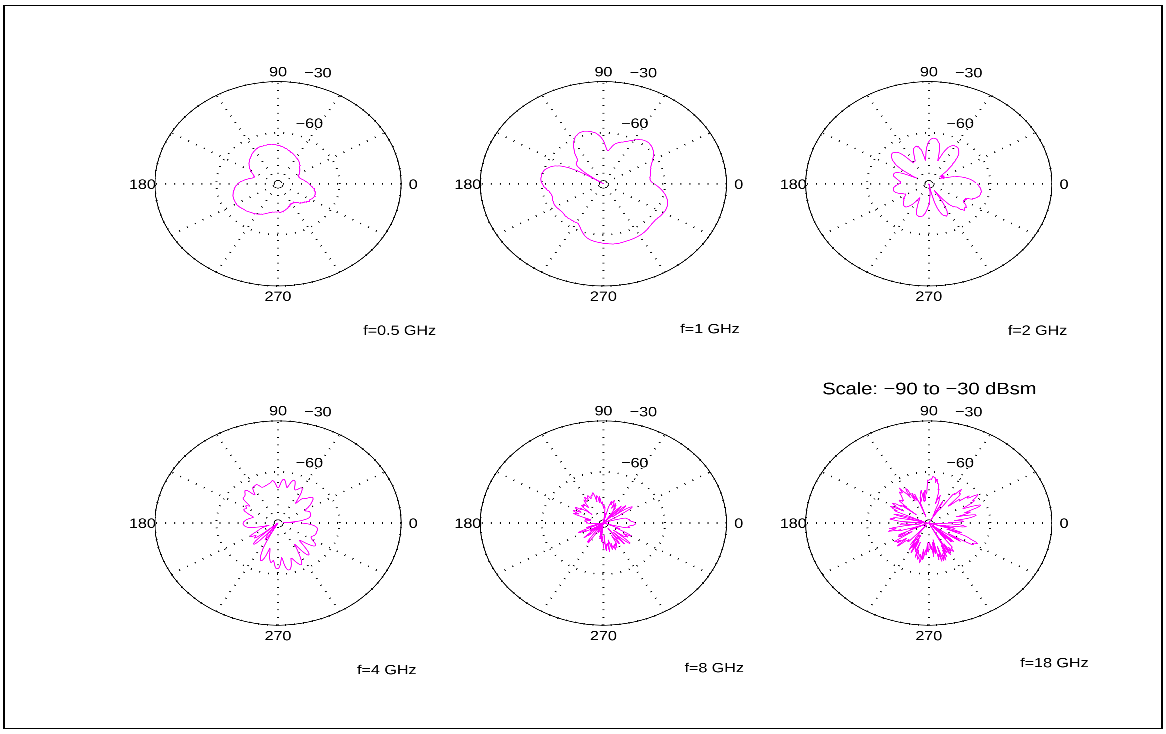

Angular dependence of σ_q. The Test Missile, plane 2, vertical polarisation, tp2.

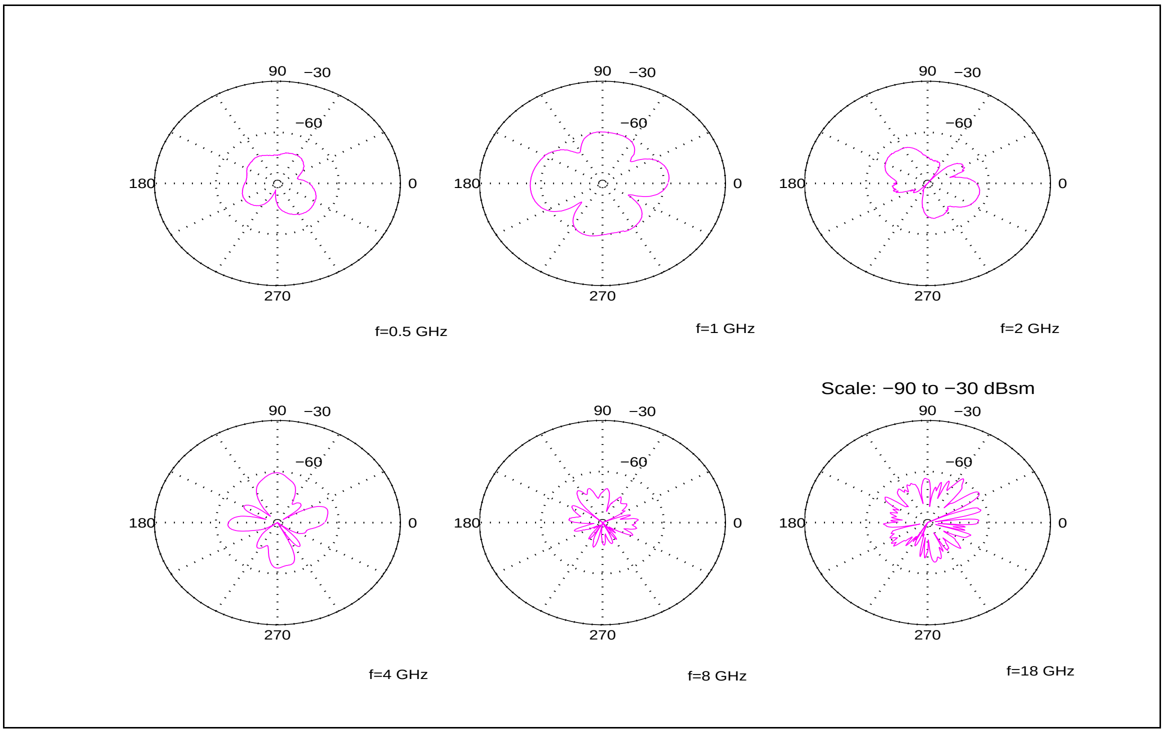

Angular dependence of σ_q. The Test Missile, plane 3, horizontal polarisation, tp2.

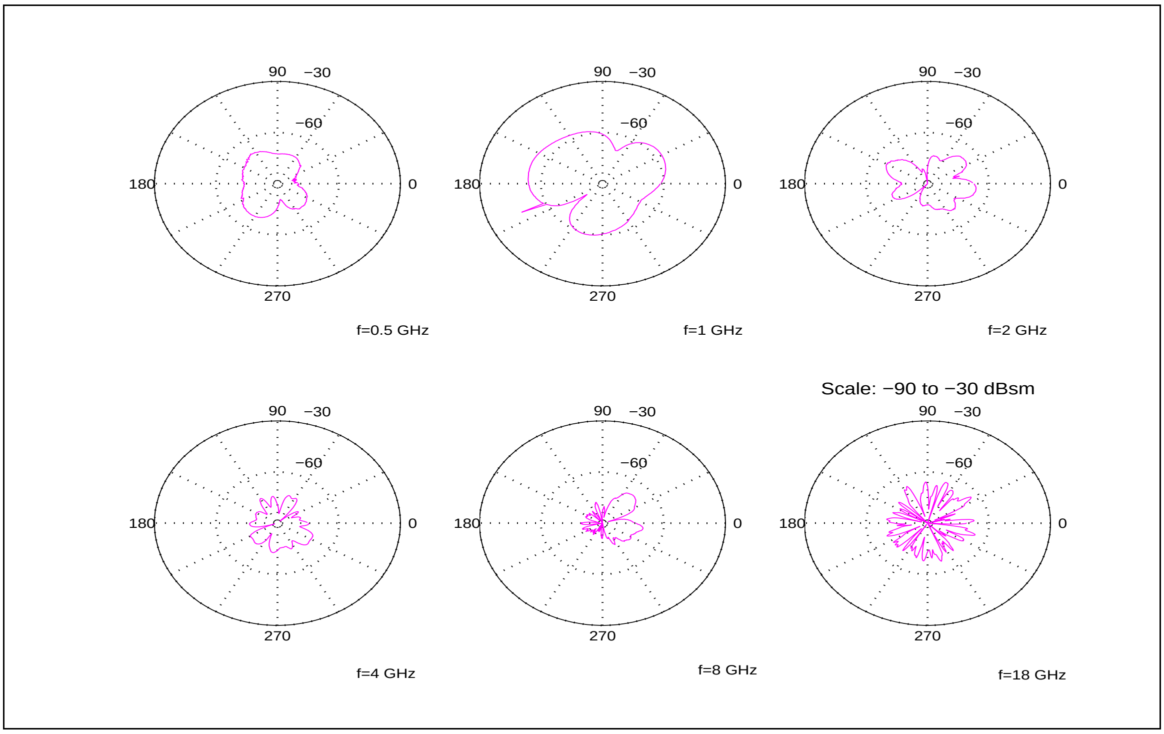

Angular dependence of σ_q. The Test Missile, plane 3, vertical polarisation, tp2.

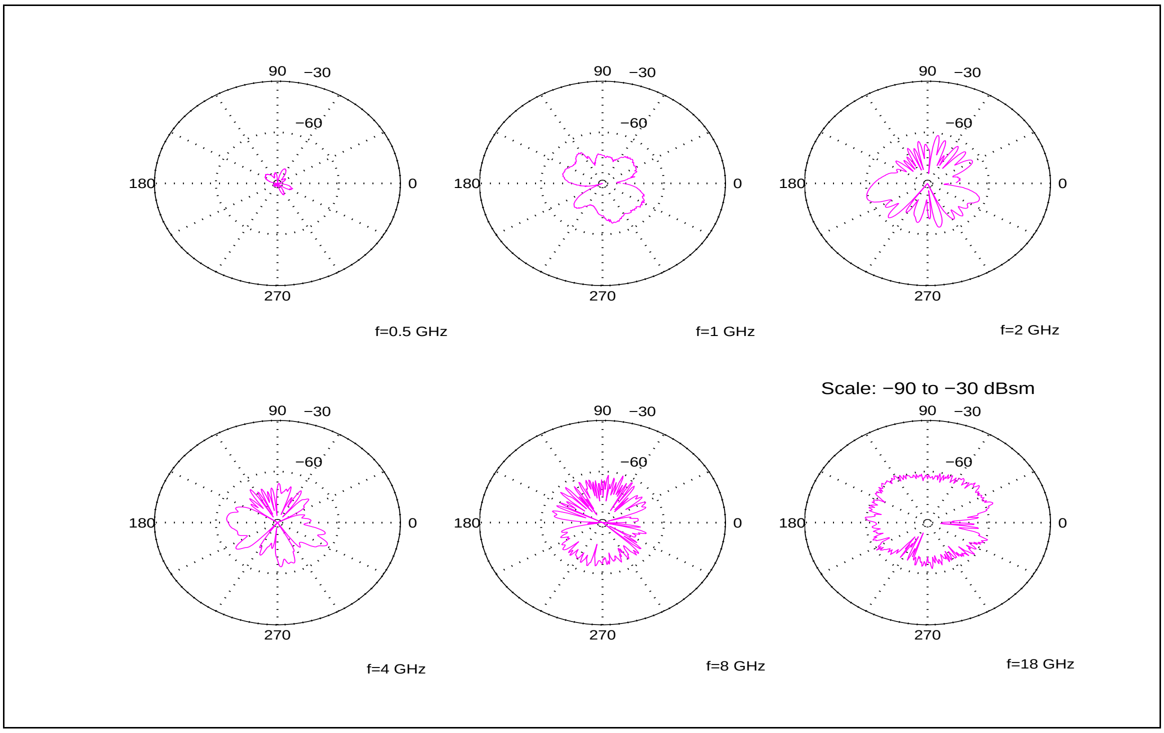

Angular dependence of σ_q. The Test Missile, plane 1, horizontal polarisation, tp4.

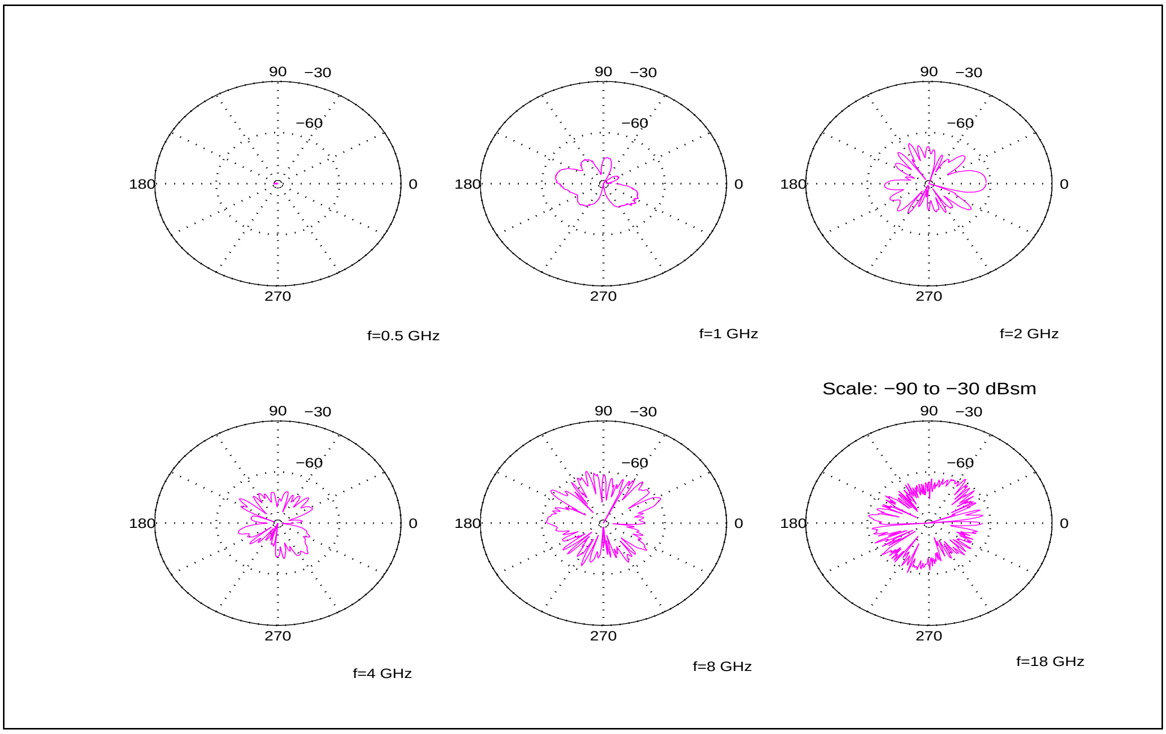

Angular dependence of σ_q. The Test Missile, plane 1, vertical polarisation, tp4.

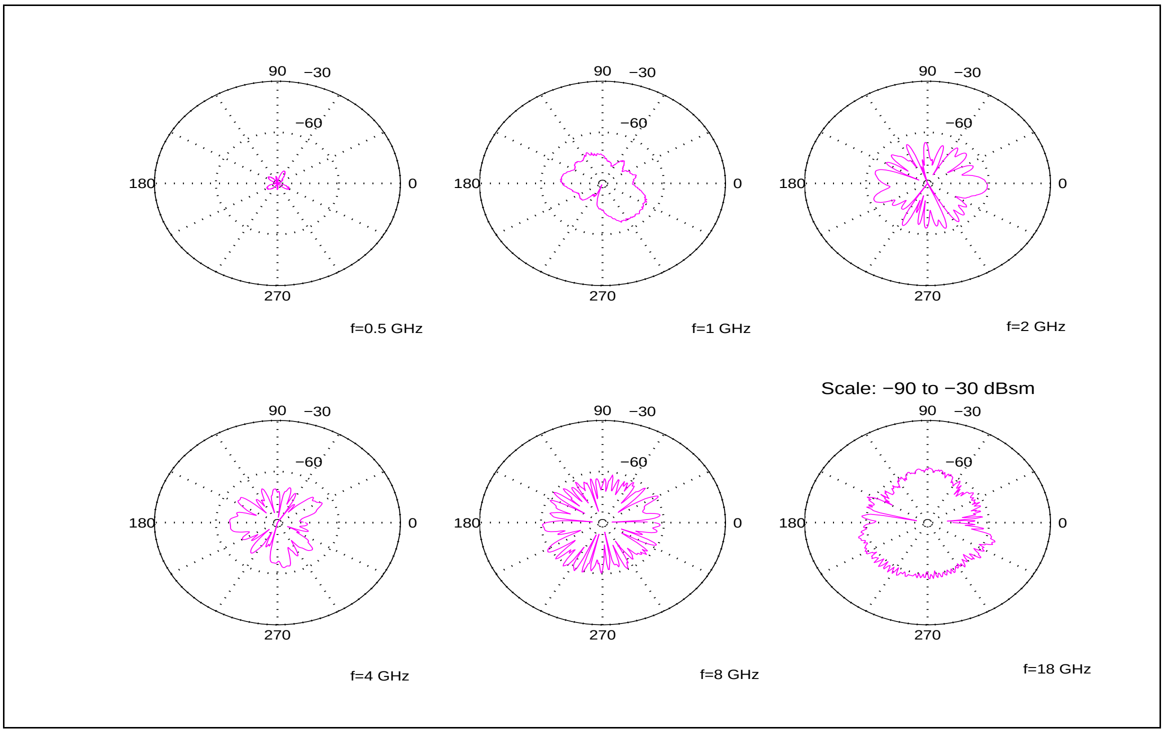

Angular dependence of σ_q. The Test Missile, plane 2, horizontal polarisation, tp4.

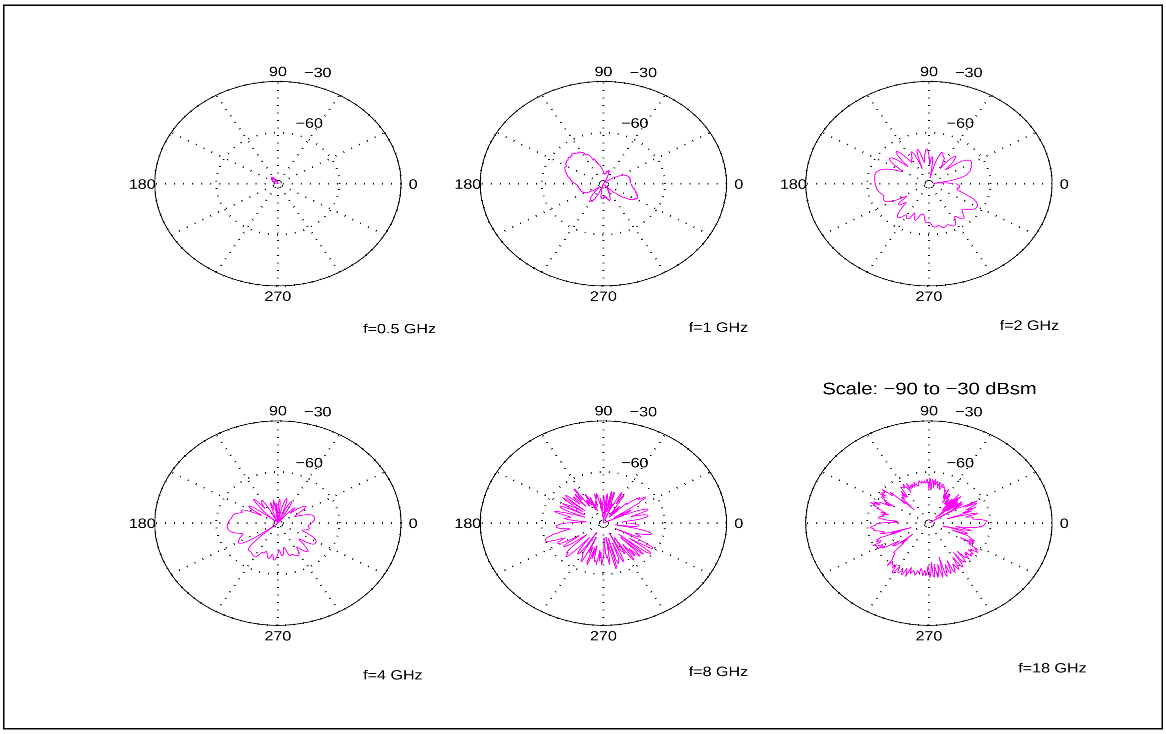

Angular dependence of σ_q. The Test Missile, plane 2, vertical polarisation, tp4.

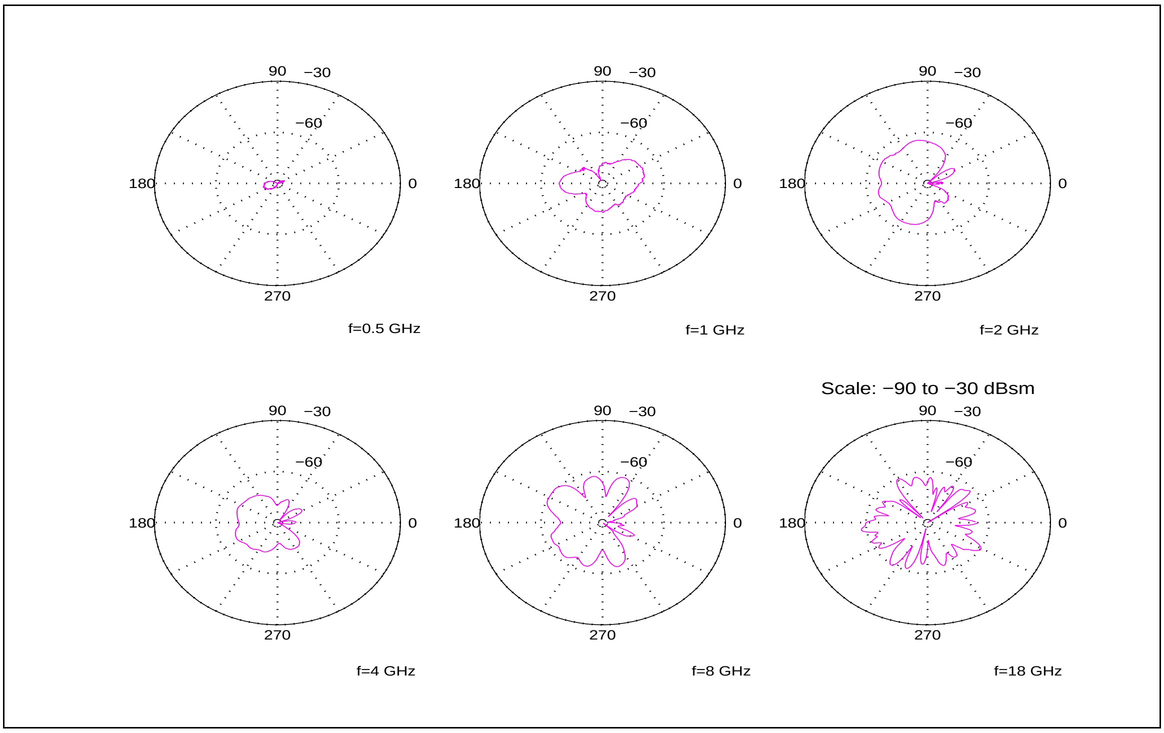

Angular dependence of σ_q. The Test Missile, plane 3, horizontal polarisation, tp4.

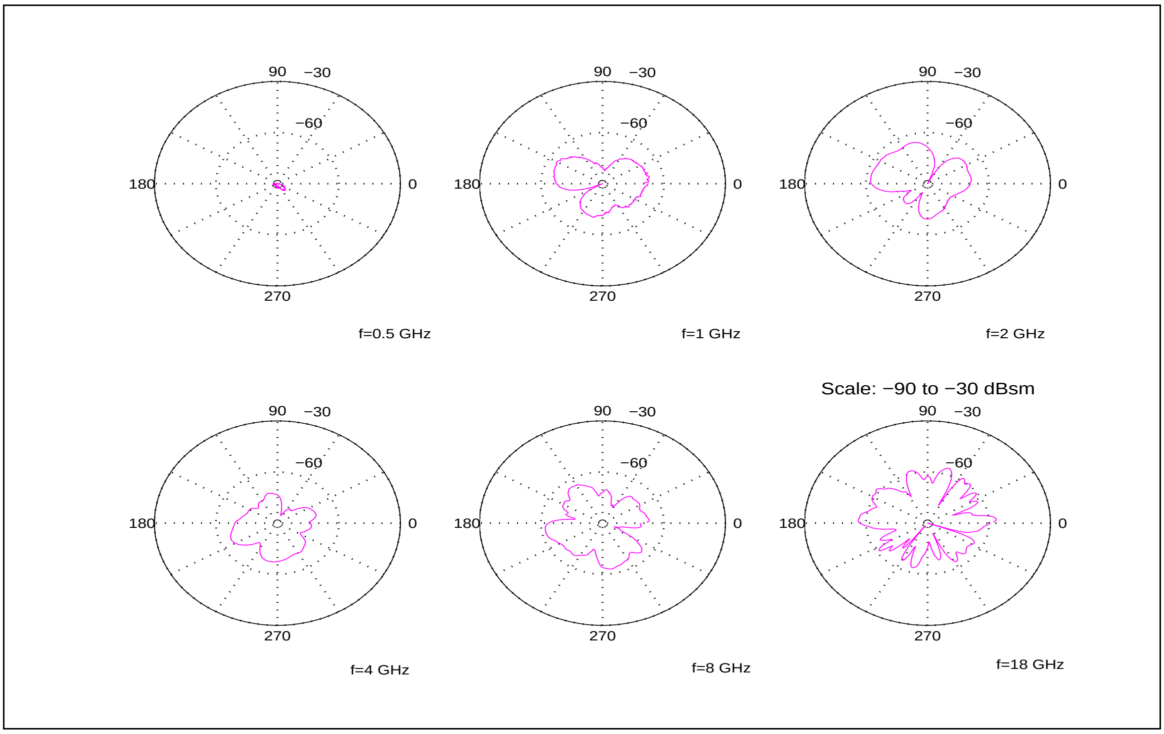

Angular dependence of σ_q. The Test Missile, plane 3, vertical polarisation, tp4.

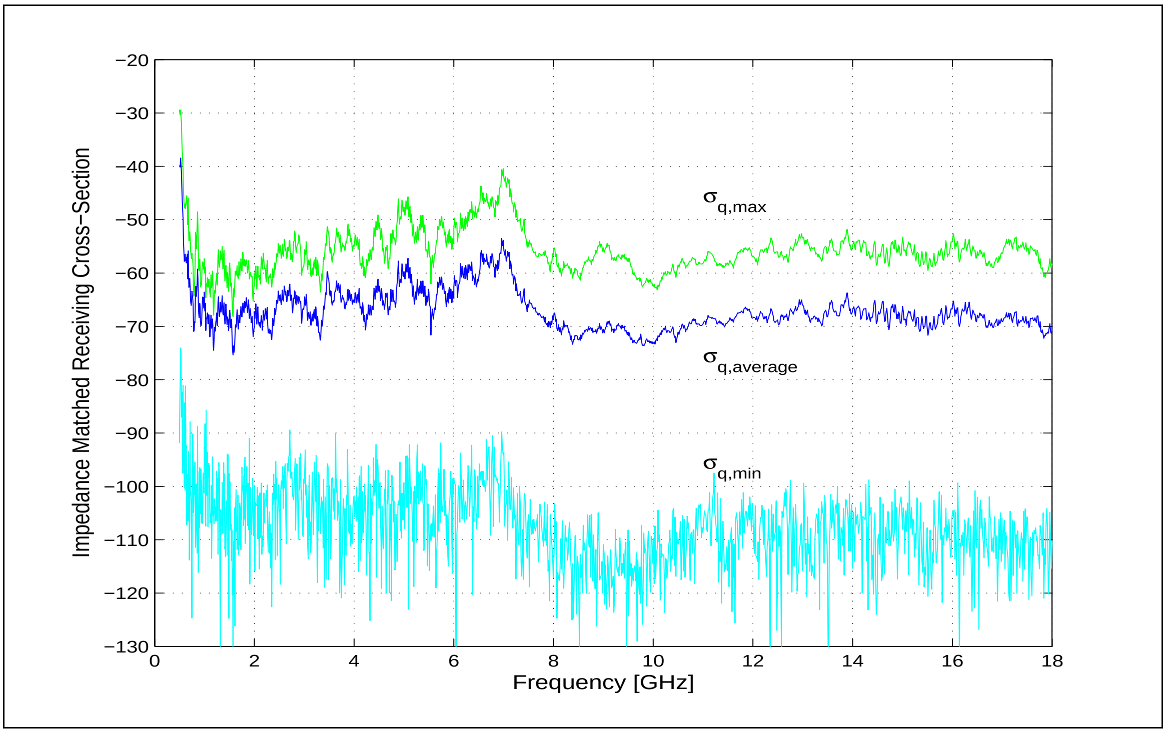

Impedance matched receiving cross-section σ_q for the Army Radio, tp2.

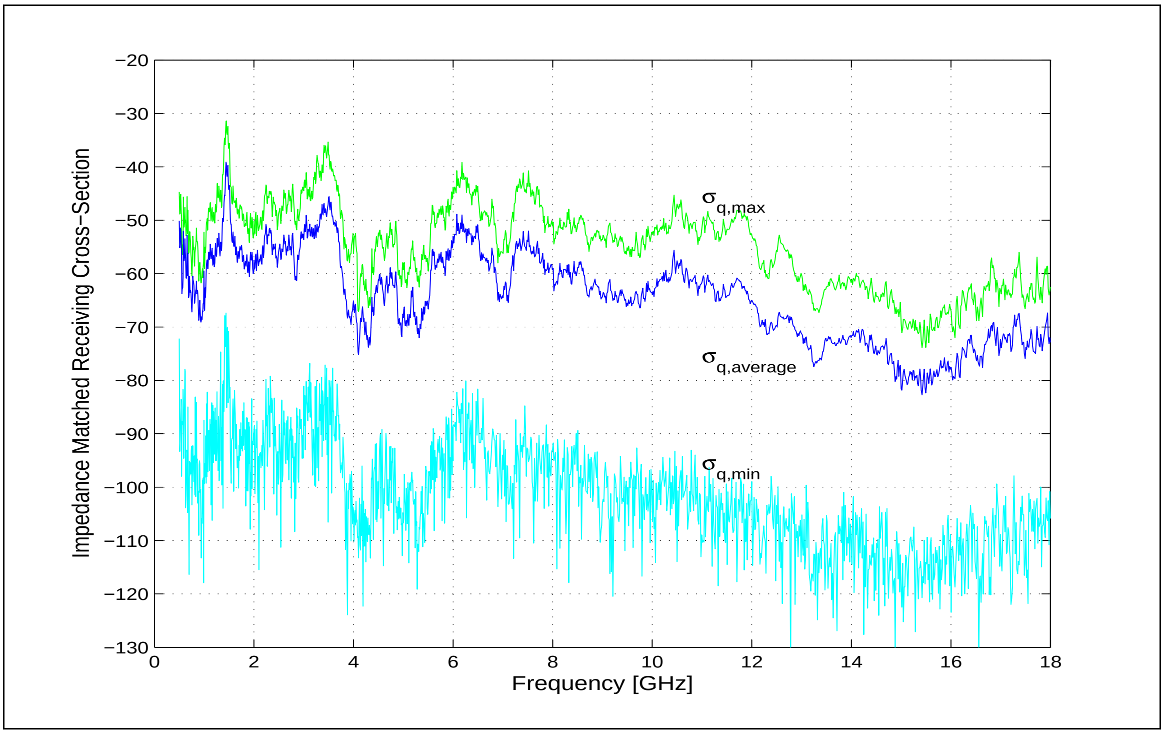

Impedance matched receiving cross-section σ_q for the Army Radio, tp4.

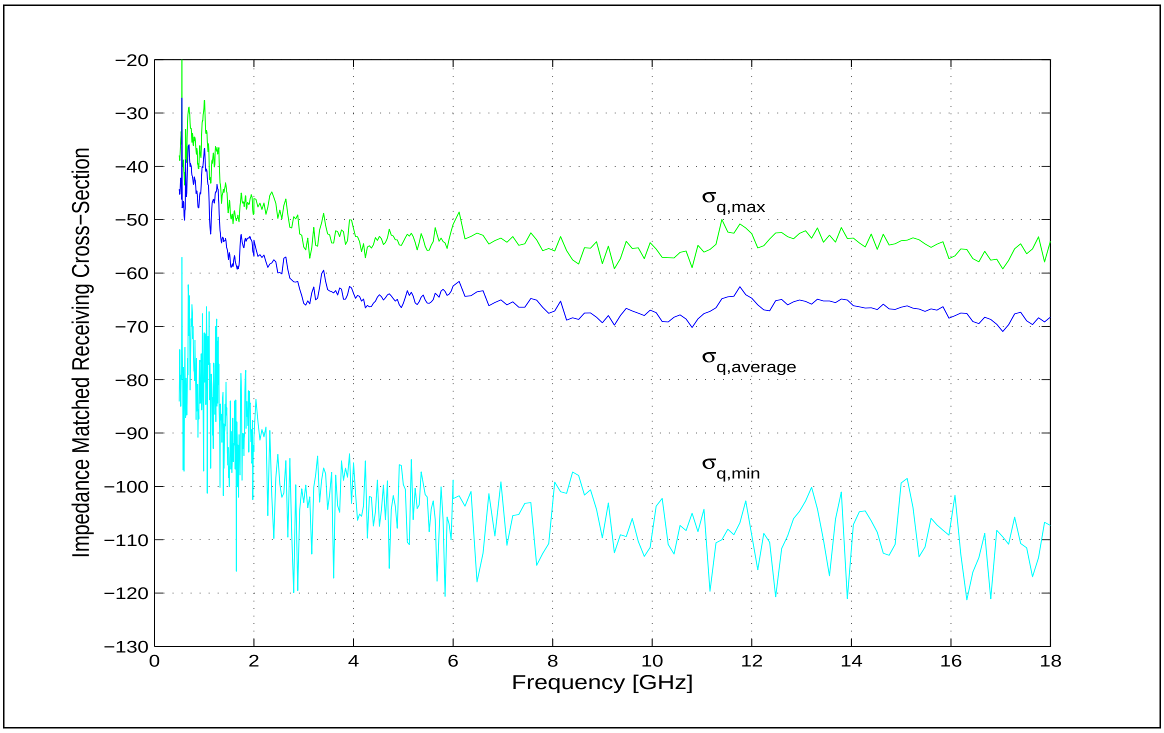

Impedance matched receiving cross-section σ_q for the Avionics Box, tp2.

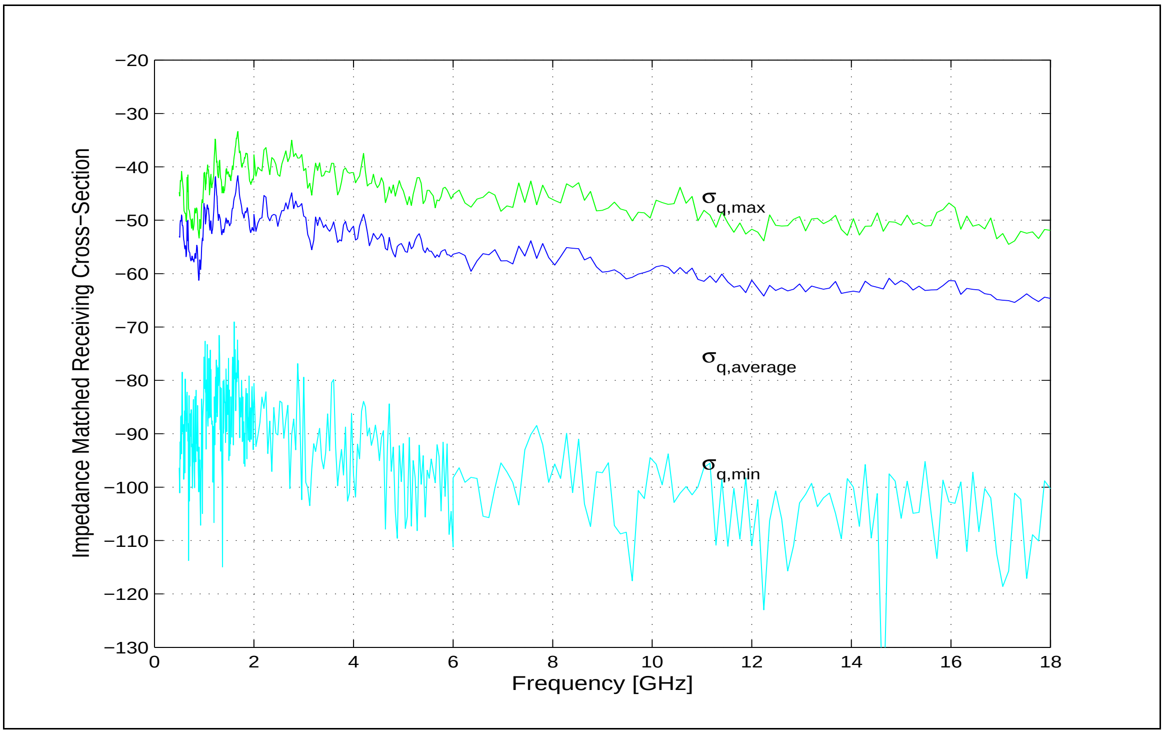

Impedance matched receiving cross-section σ_q for the Avionics Box, tp4.

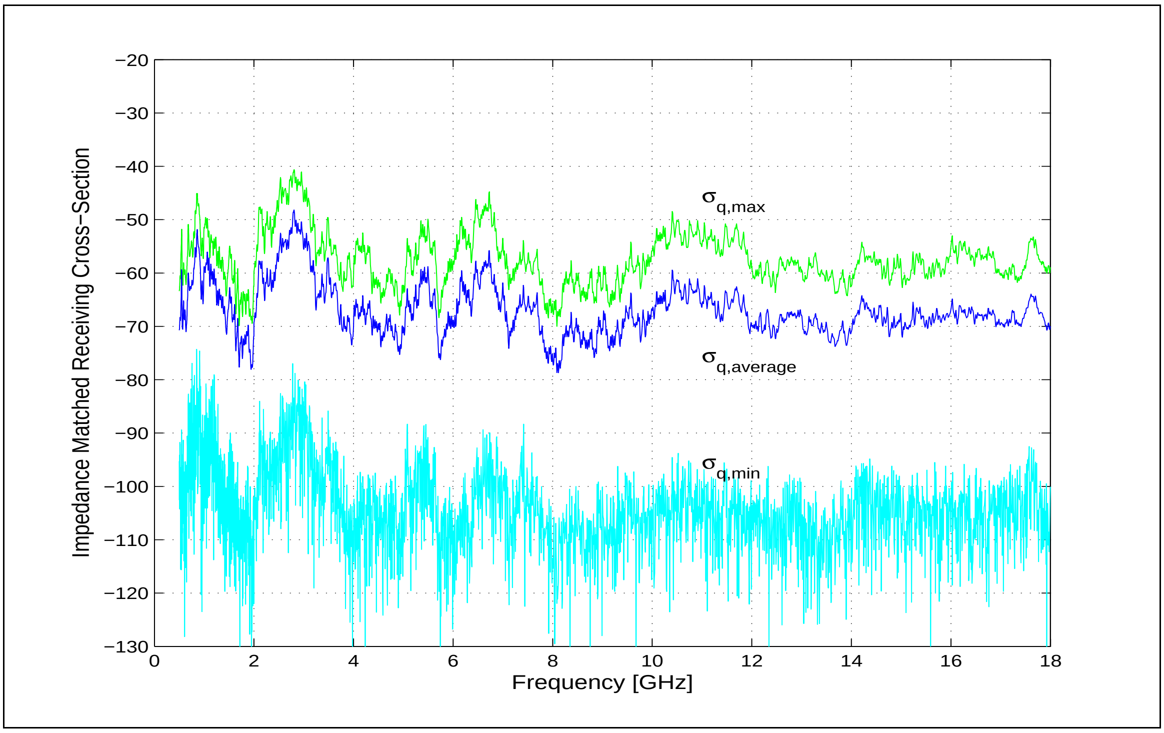

Impedance matched receiving cross-section σ_q for the Test Missile, tp2.

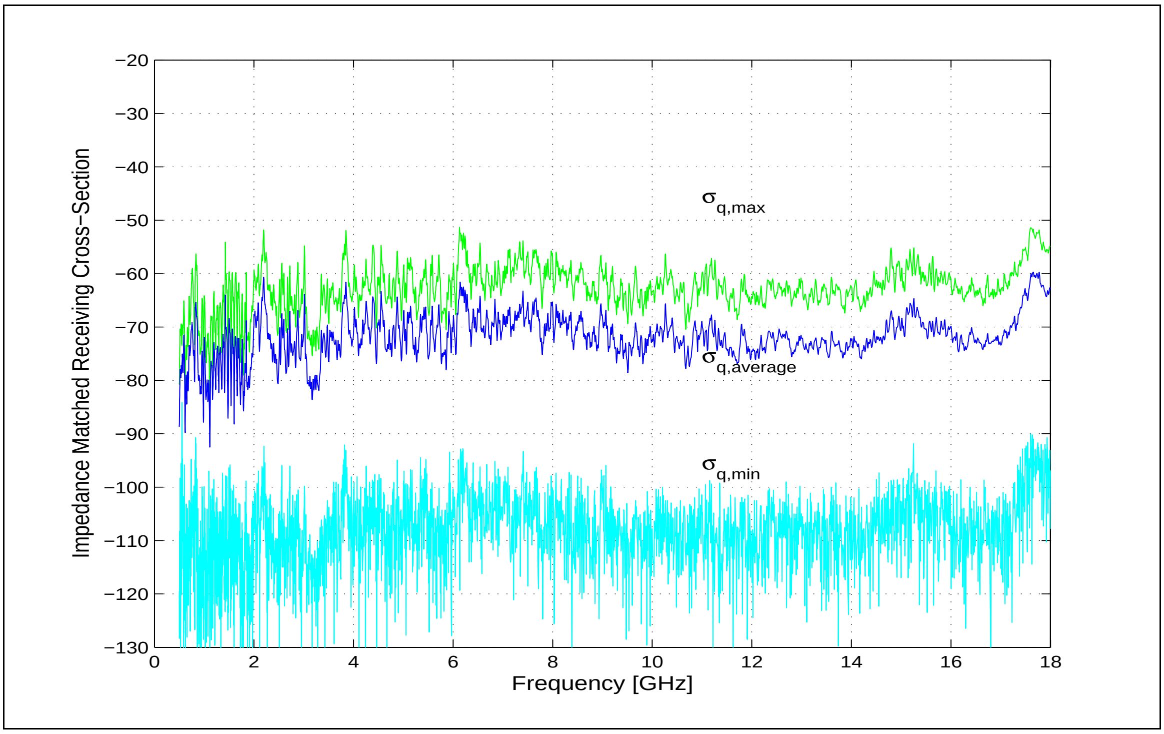

Impedance matched receiving cross-section σ_q for the Test Missile, tp4.

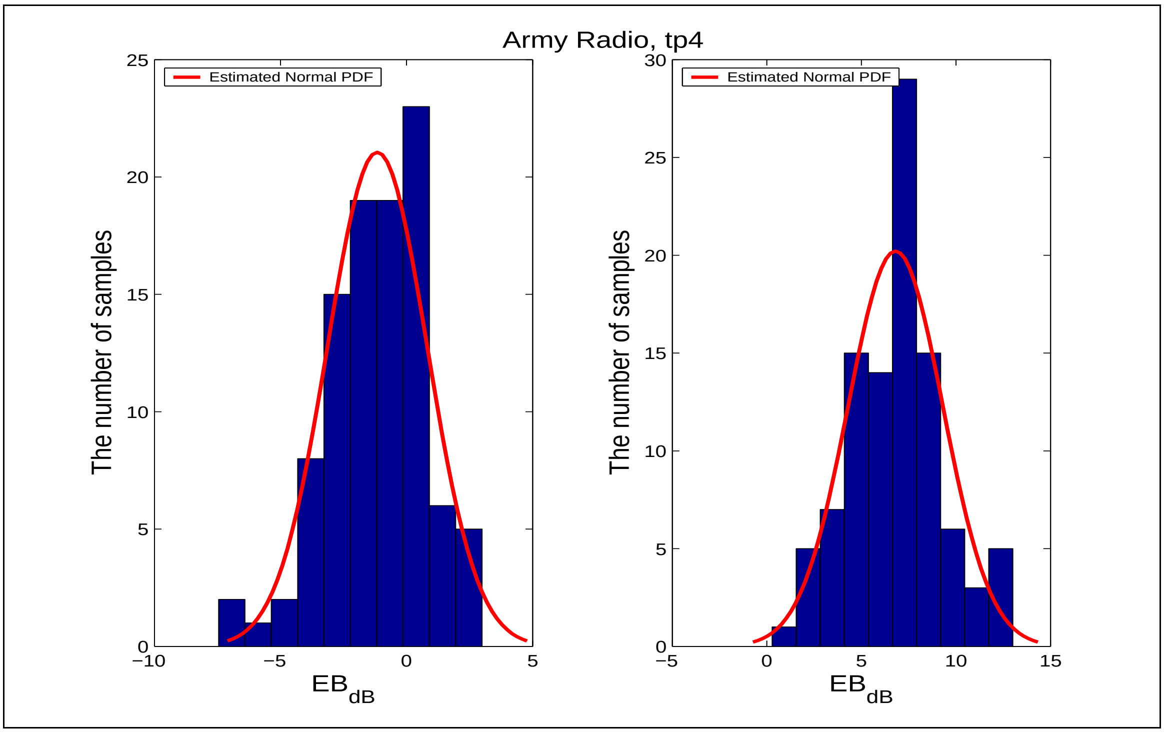

Histogram of EB_{dB} with superimposed normal density. Frequency 3 GHz (left) and 7 GHz (right), frequency interval 1. The Army Radio, tp4.

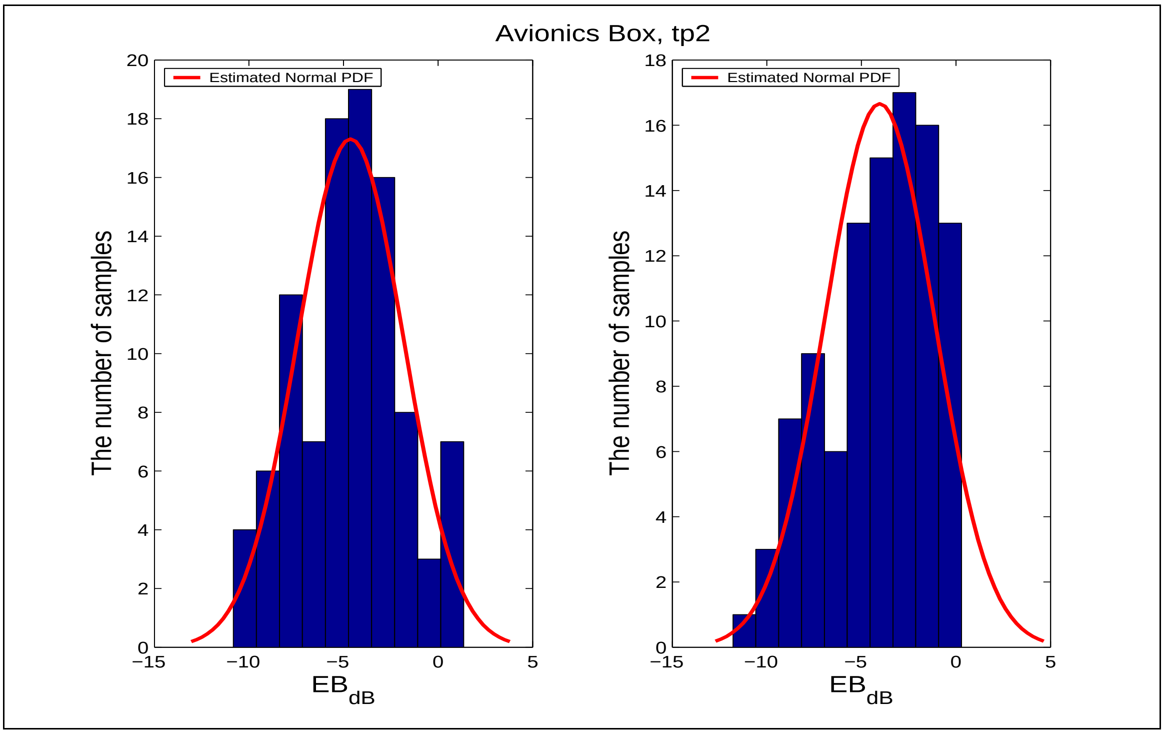

Histogram of EB_{dB} with superimposed normal density. Frequency 3 GHz (left) and 7 GHz (right), frequency interval 1. The Avionics Box, tp2.

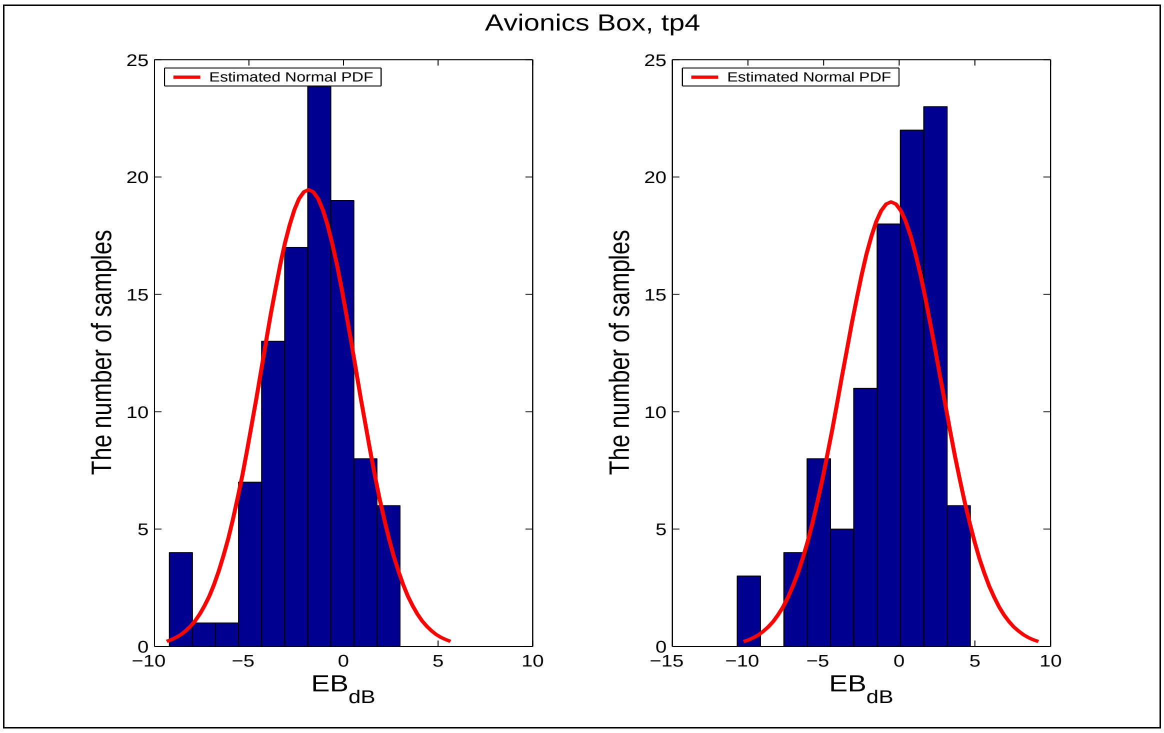

Histogram of EB_{dB} with superimposed normal density. Frequency 3 GHz (left) and 7 GHz (right), frequency interval 1. The Avionics Box, tp4.

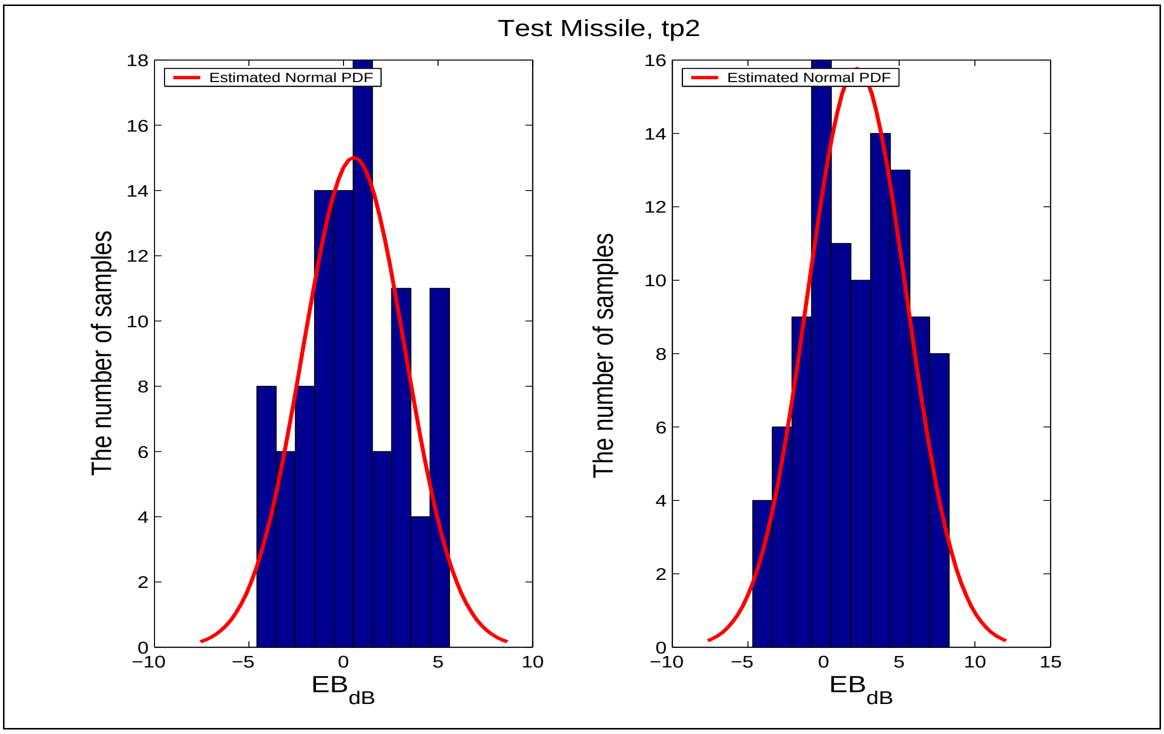

Histogram of EB_{dB} with superimposed normal density. Frequency 3 GHz (left) and 7 GHz (right), frequency interval 1. The Test Missile, tp2.

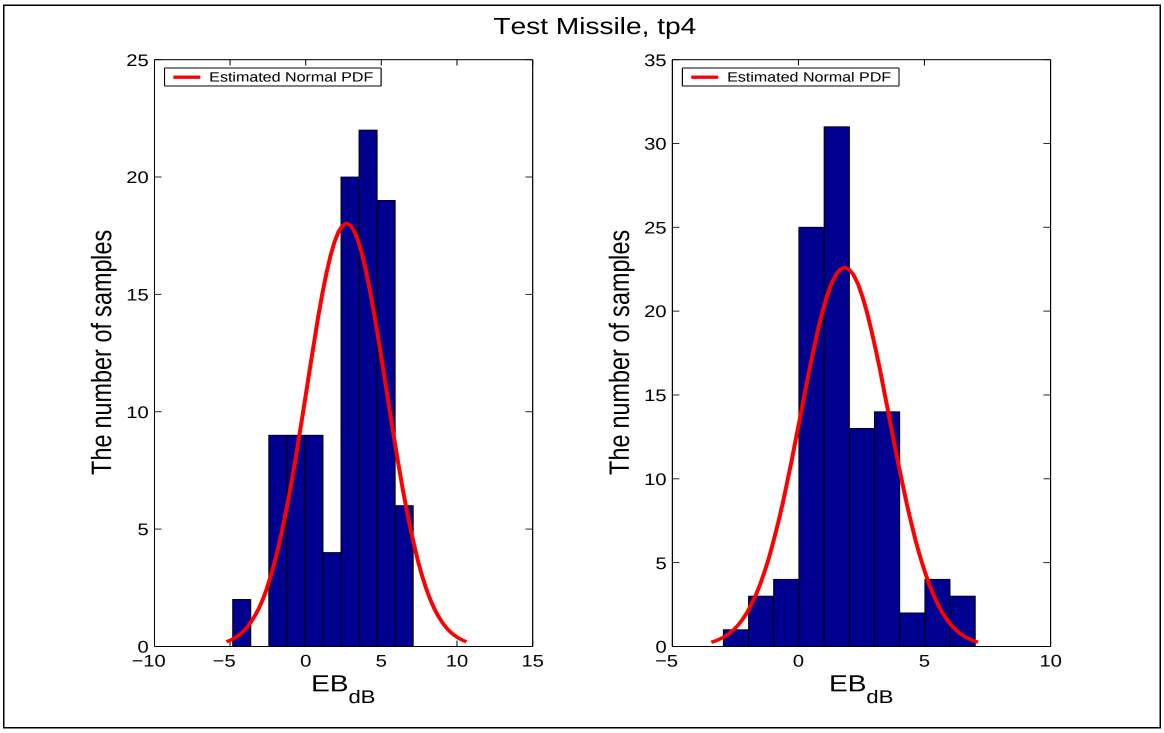

Histogram of EB_{dB} with superimposed normal density. Frequency 3 GHz (left) and 7 GHz (right), frequency interval 1. The Test Missile, tp4.

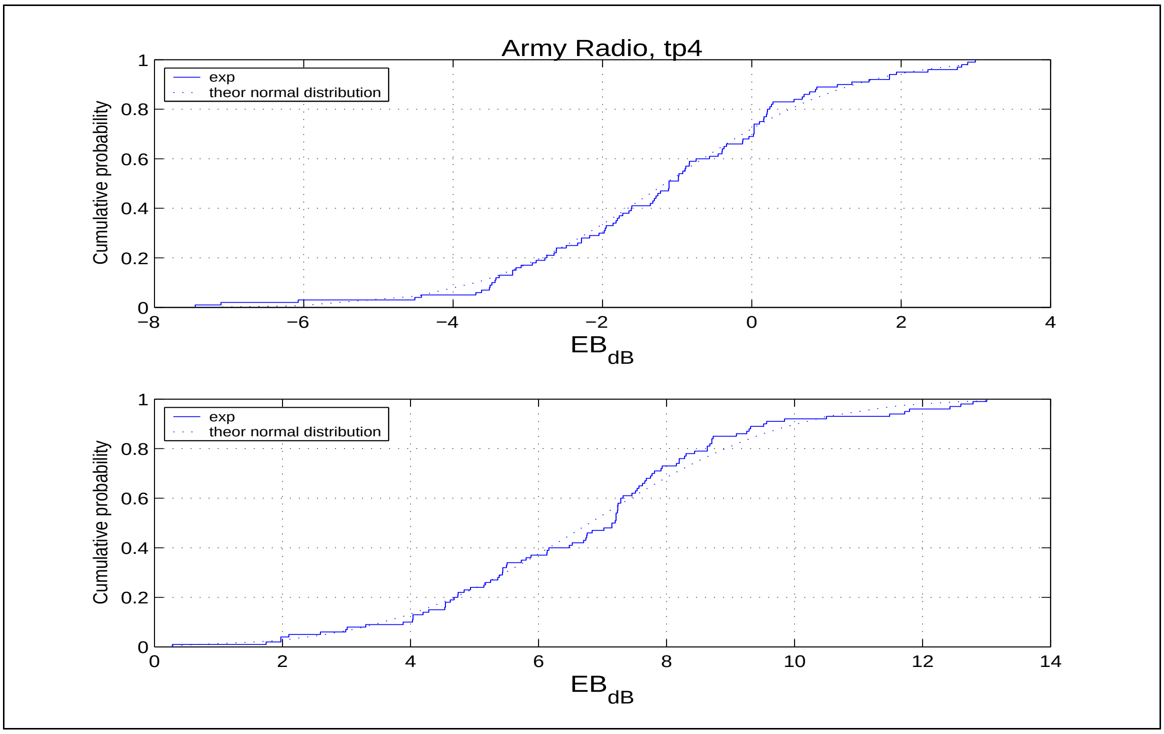

Measured and estimated cumulative distribution function. Frequency 3 GHz (upper subplot) and 7 GHz (lower subplot), frequency interval 1. The Army Radio, tp4.

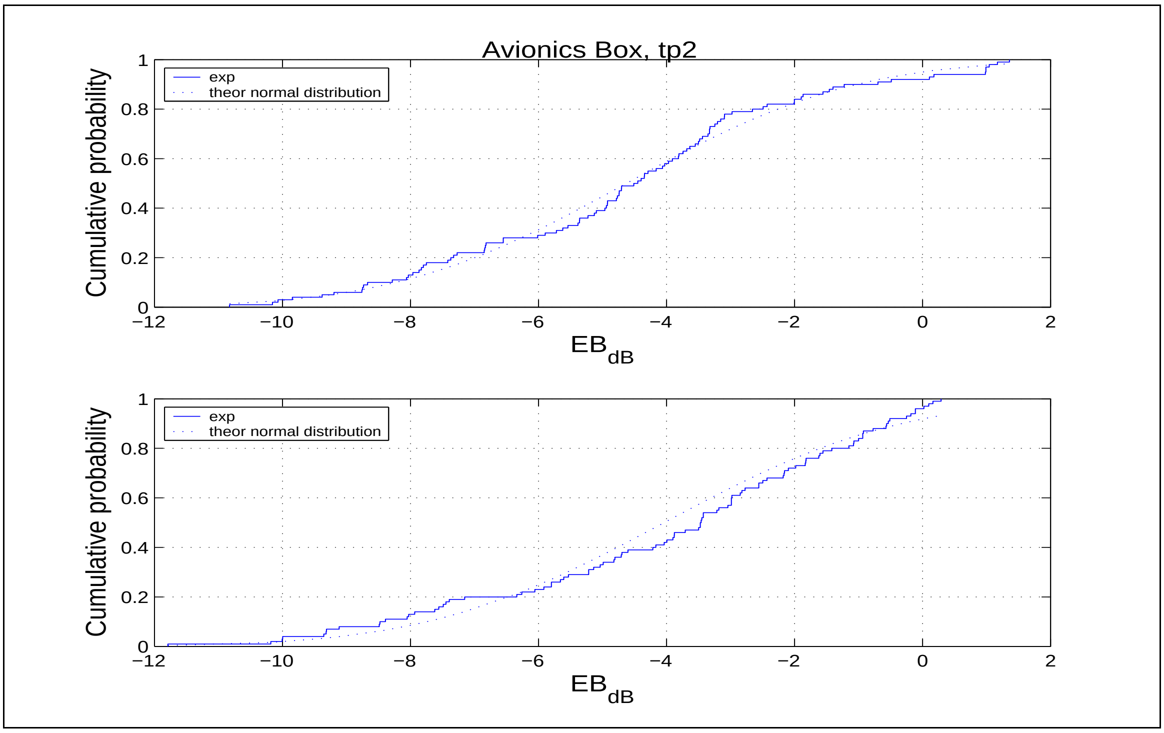

Measured and estimated cumulative distribution function. Frequency 3 GHz (upper subplot) and 7 GHz (lower subplot), frequency interval 1. The Avionics Box, tp2.

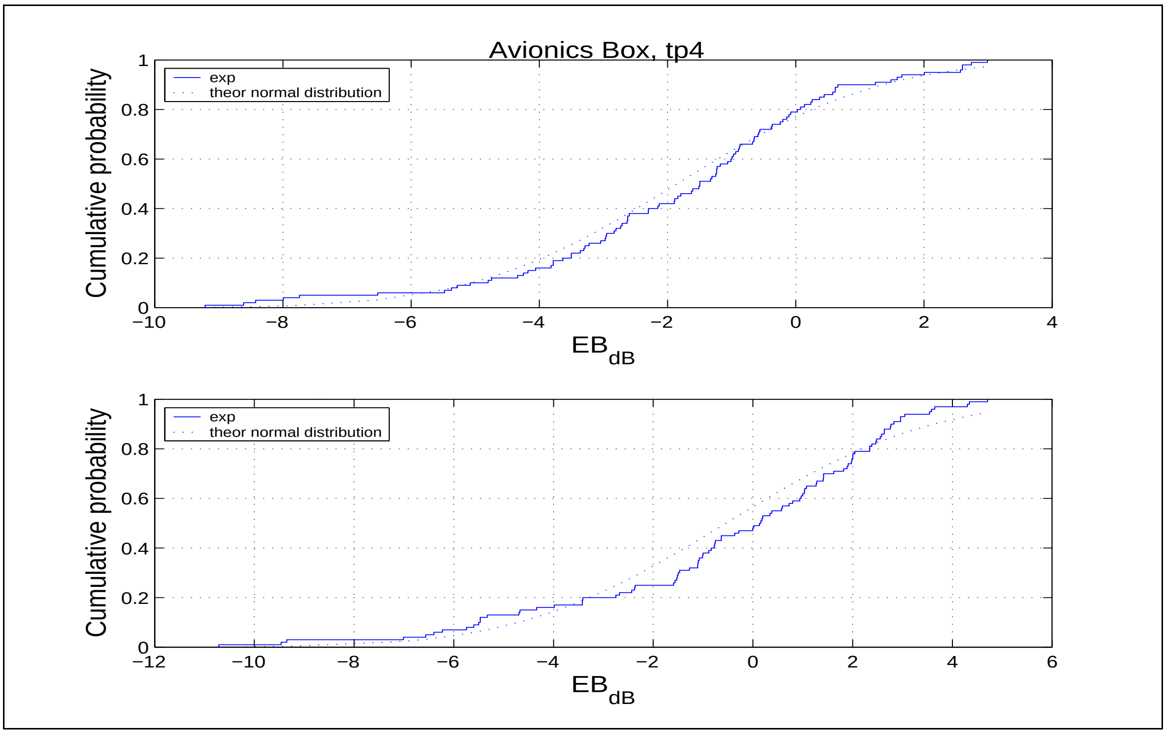

Measured and estimated cumulative distribution function. Frequency 3 GHz (upper subplot) and 7 GHz (lower subplot), frequency interval 1. The Avionics Box, tp4.

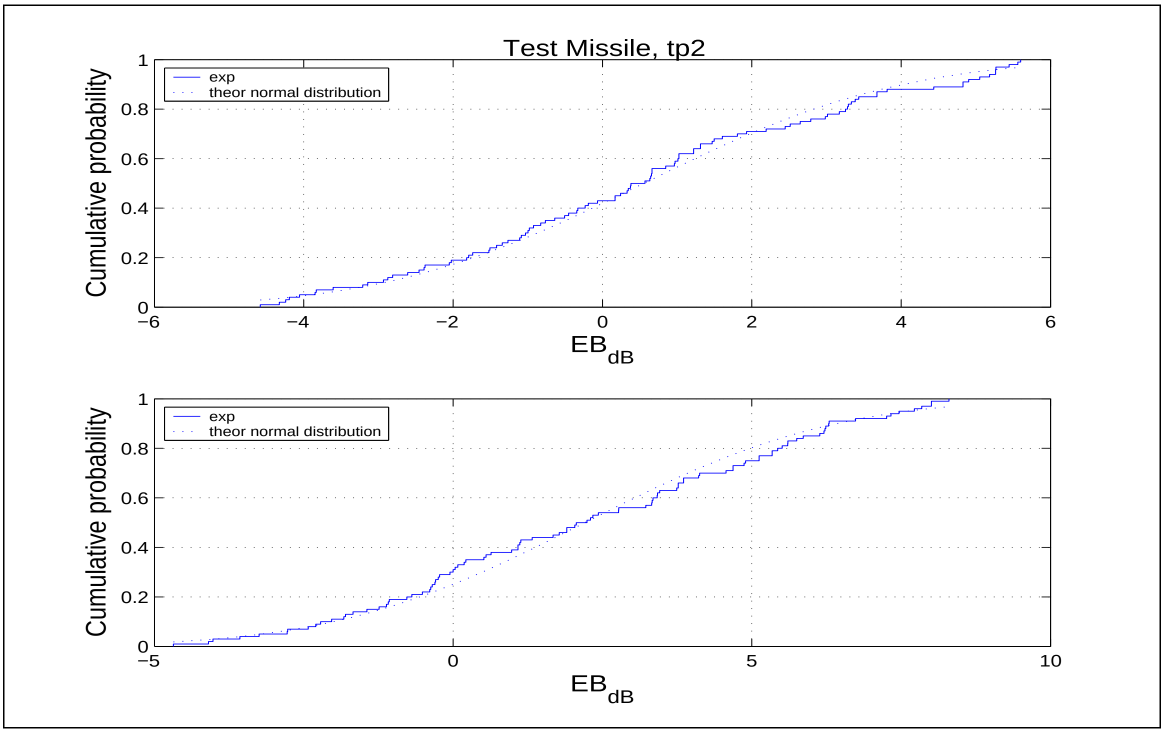

Measured and estimated cumulative distribution function. Frequency 3 GHz (upper subplot) and 7 GHz (lower subplot), frequency interval 1. Test Missile, tp 2.

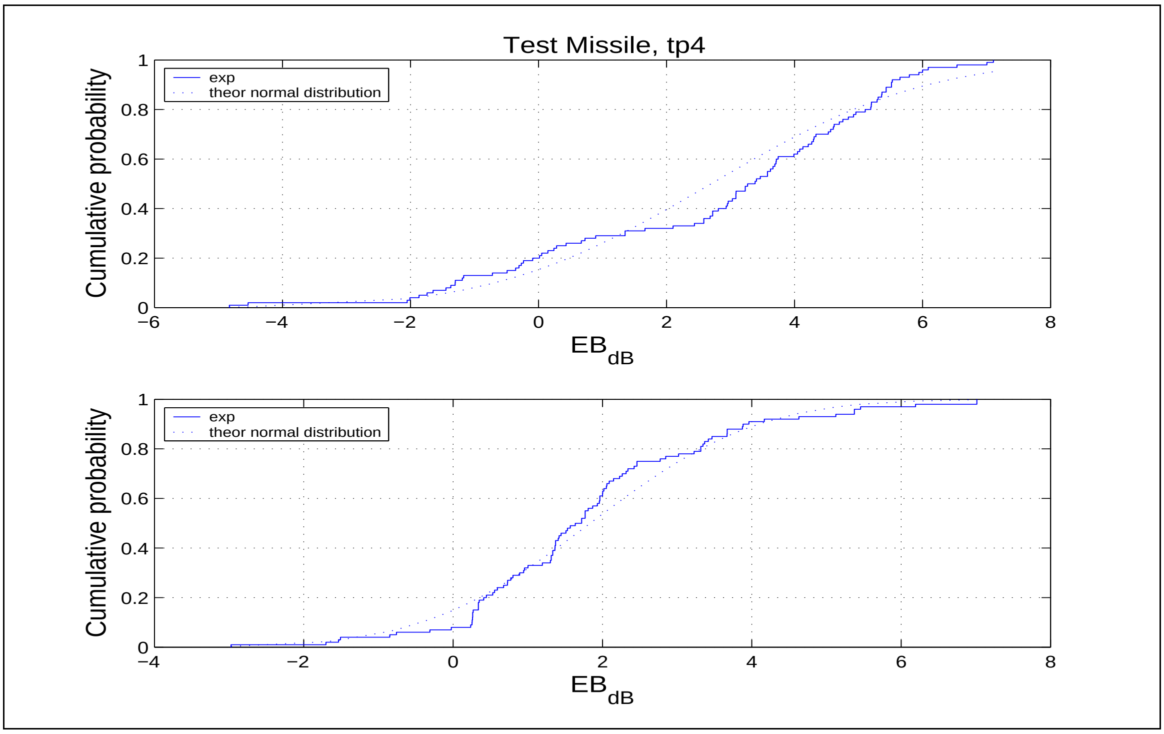

Measured and estimated cumulative distribution function. Frequency 3 GHz (upper subplot) and 7 GHz (lower subplot), frequency interval 1. Test Missile, tp4.

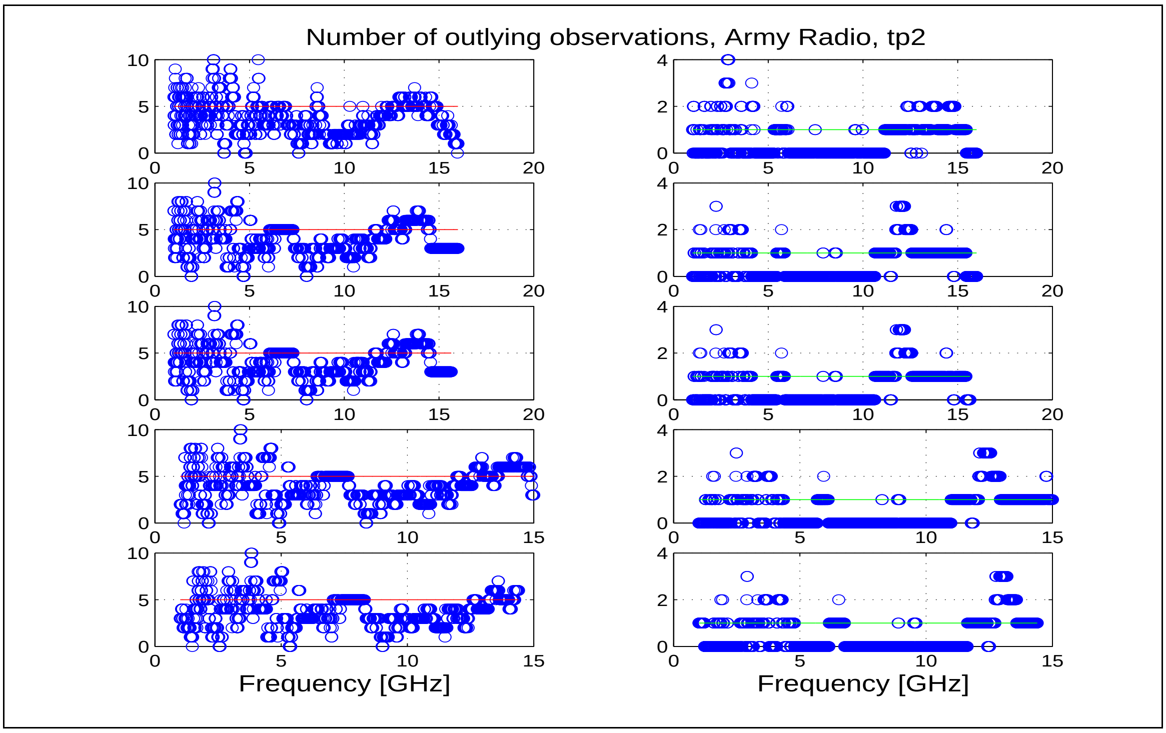

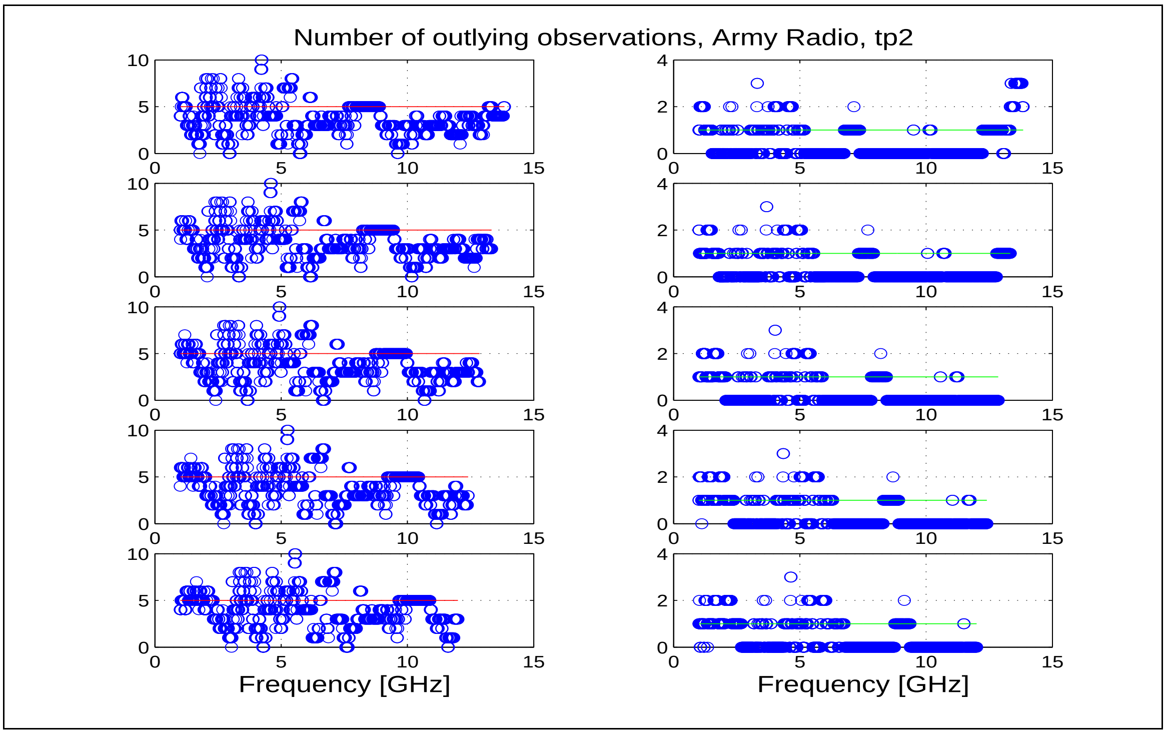

The number of outlying obtained values of EB_{dB} with 95% (left subplots) and 99% statistical limits applied (right subplots). Frequency intervals 1–5 (upper figure) and 6–10 (lower figure). The Army Radio, tp2.

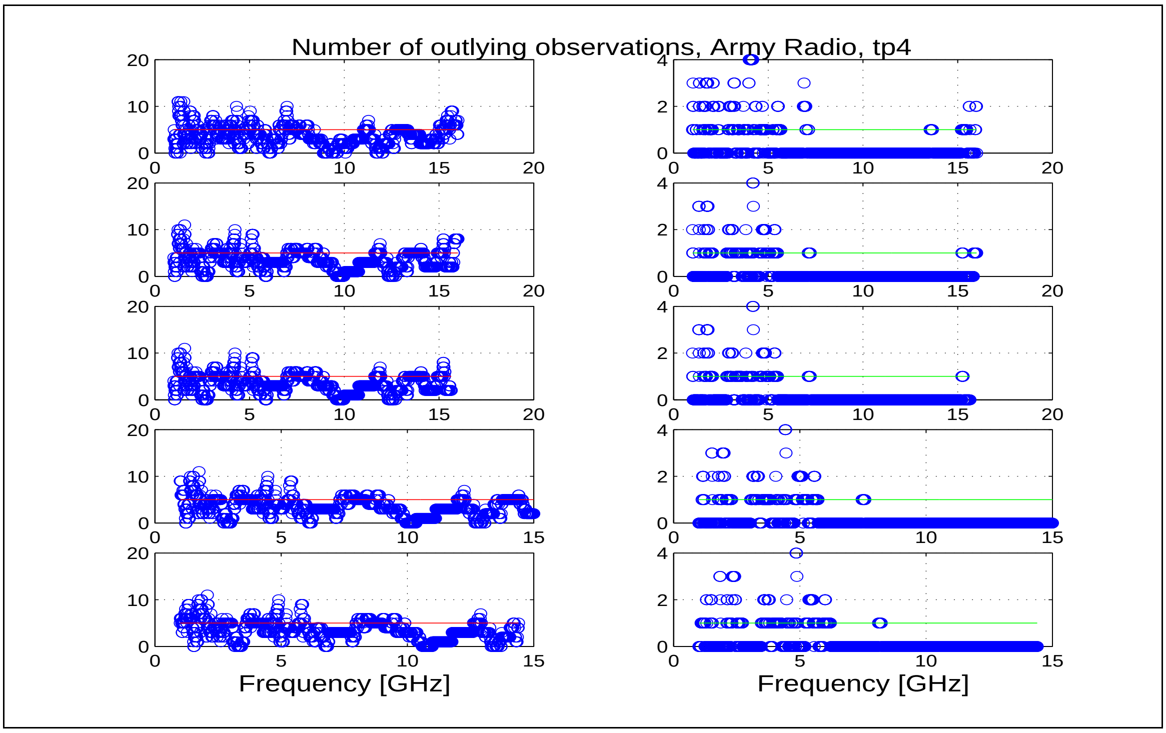

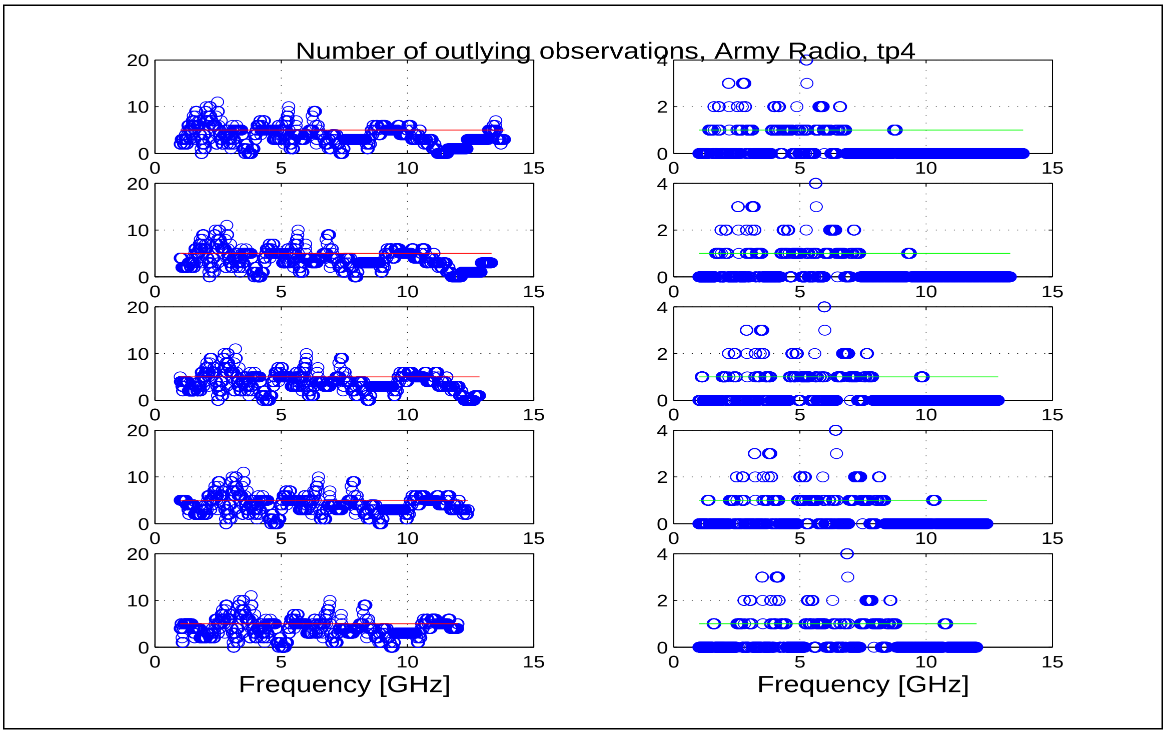

The number of outlying obtained values of EB_{dB} with 95% (left subplots) and 99% statistical limits applied (right subplots). Frequency intervals 1–5 (upper figure) and 6–10 (lower figure). The Army Radio, tp4.

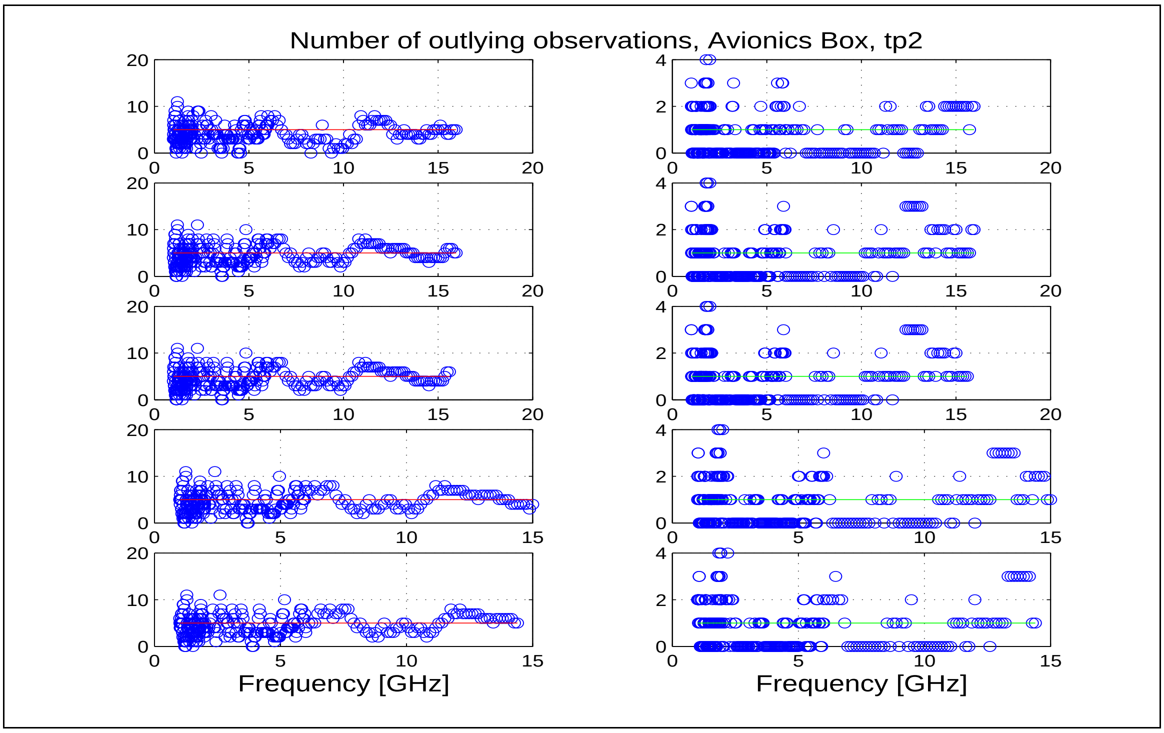

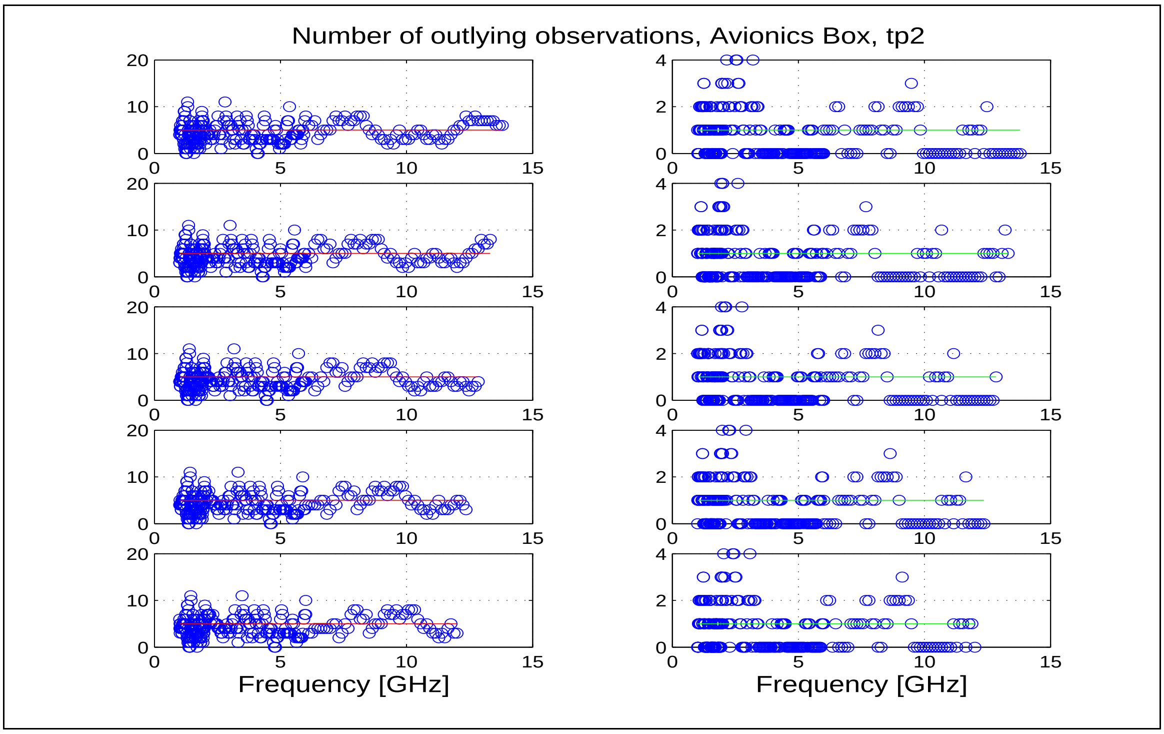

The number of outlying obtained values of EB_{dB} with 95% (left subplots) and 99% statistical limits applied (right subplots). Frequency intervals 1–5 (upper figure) and 6–10 (lower figure). The Avionic Box, tp2.

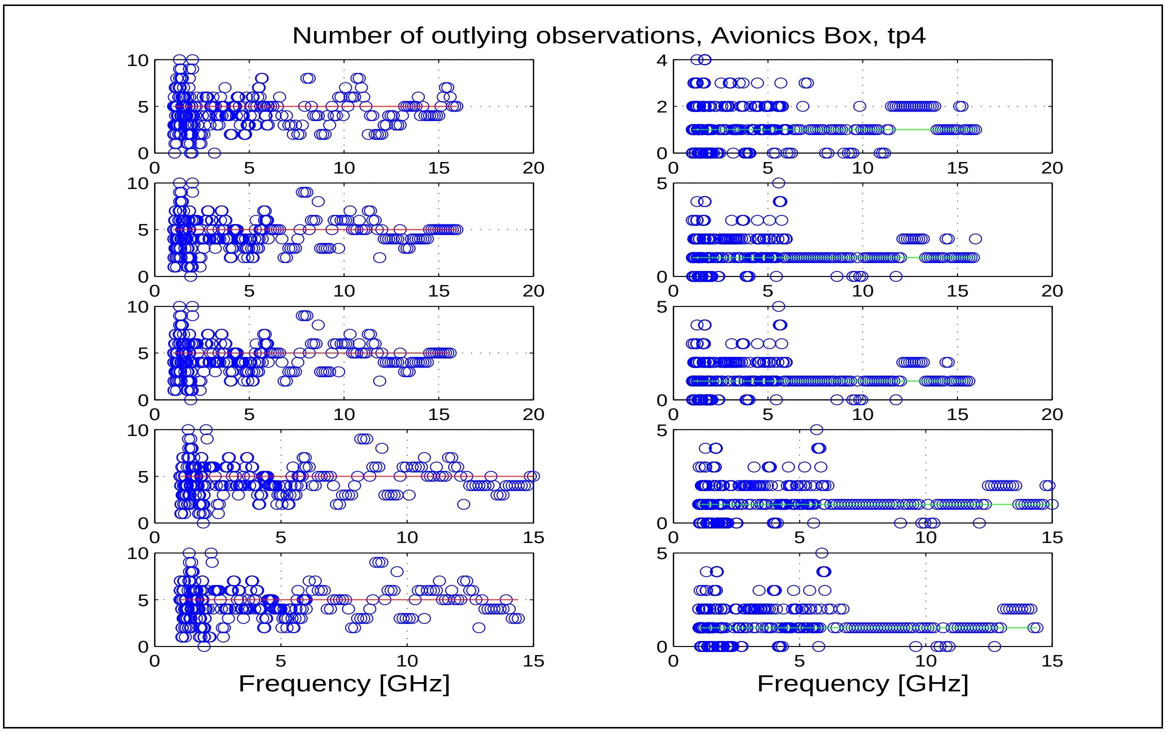

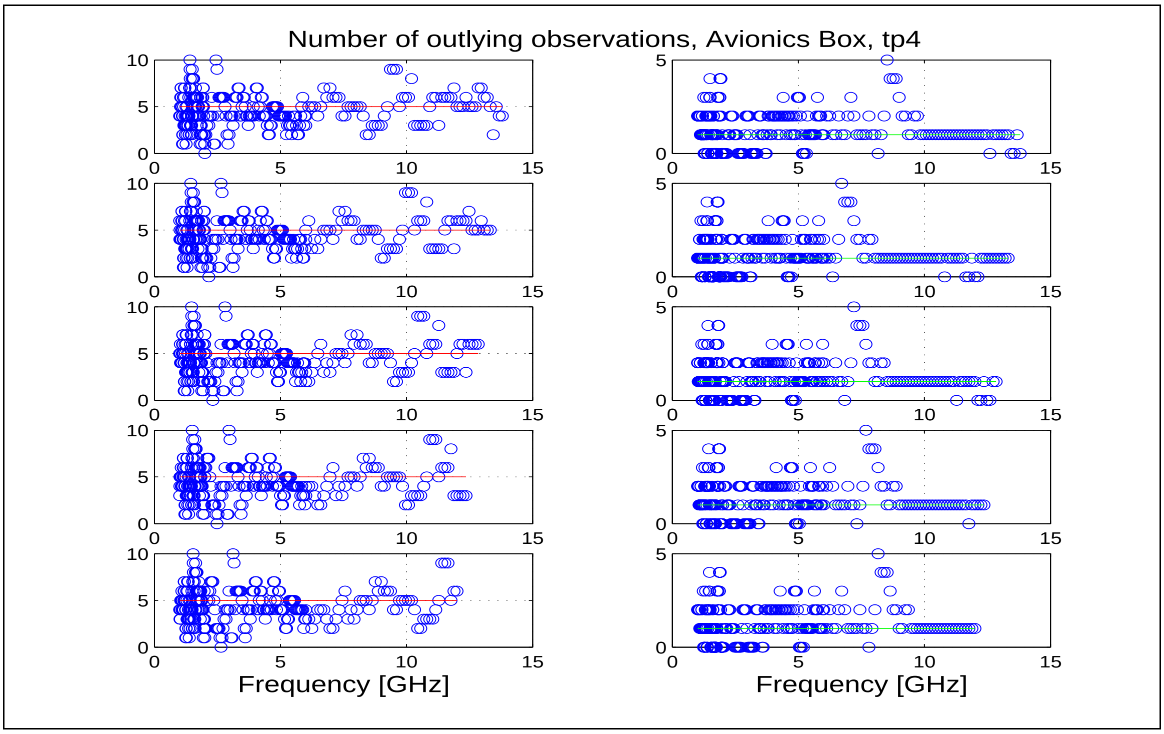

The number of outlying obtained values of EB_{dB} with 95% (left subplots) and 99% statistical limits applied (right subplots). Frequency intervals 1–5 (upper figure) and 6–10 (lower figure). The Avionic Box, tp4.

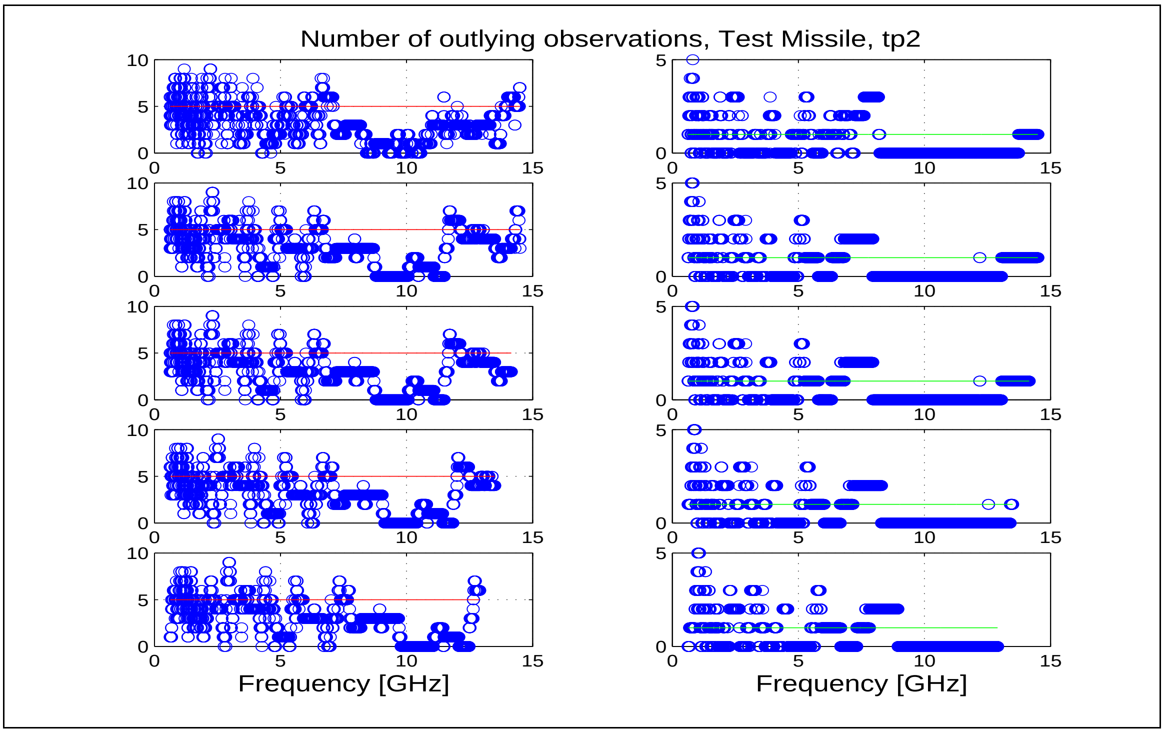

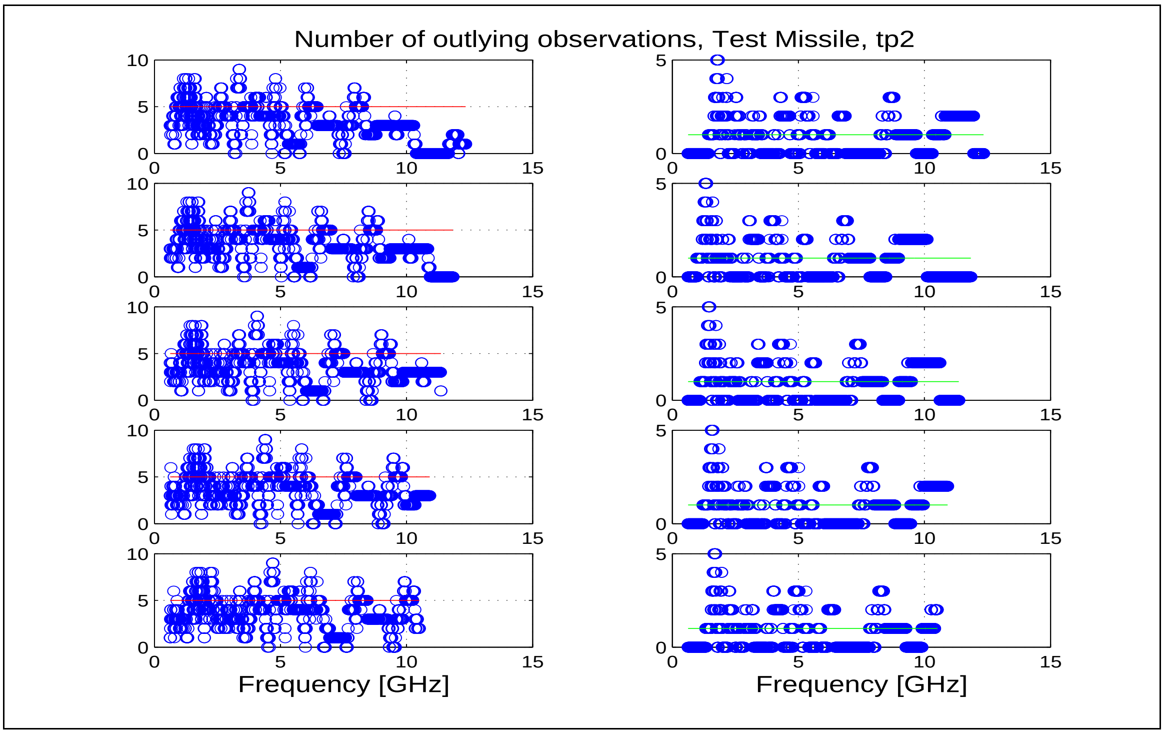

The number of outlying obtained values of EB_{dB} with 95% (left subplots) and 99% statistical limits applied (right subplots). Frequency intervals 1–5 (upper figure) and 6–10 (lower figure). The Test Missile, tp2.

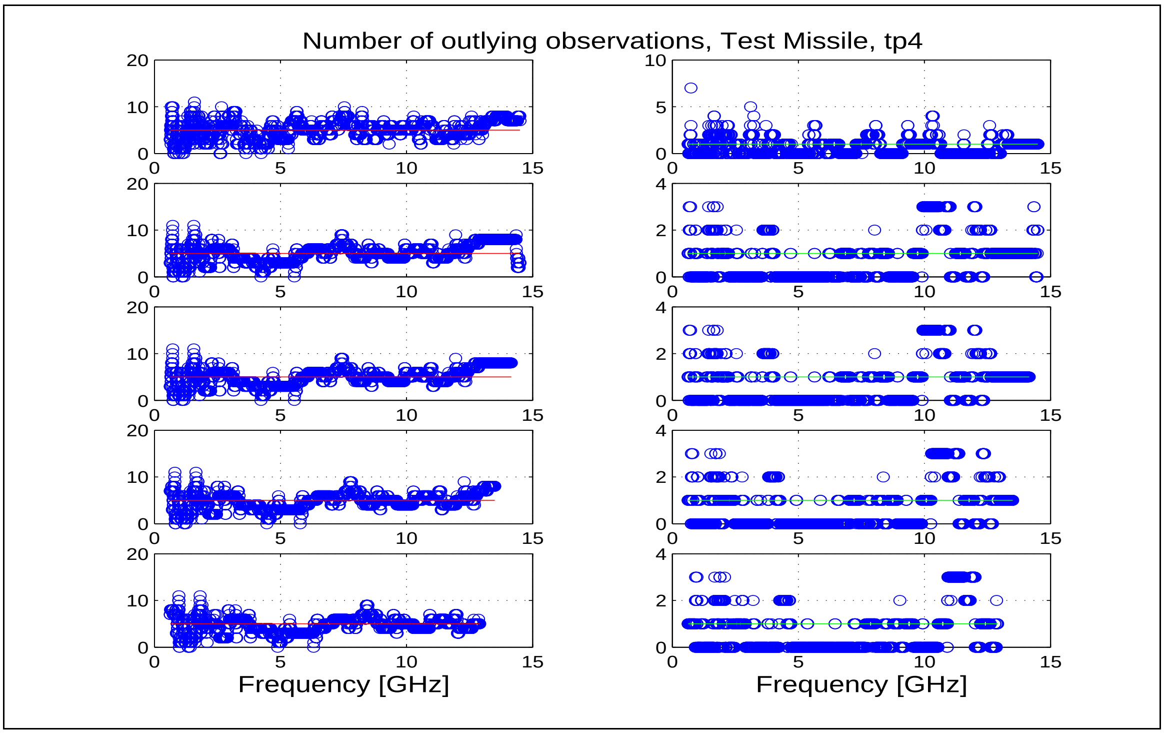

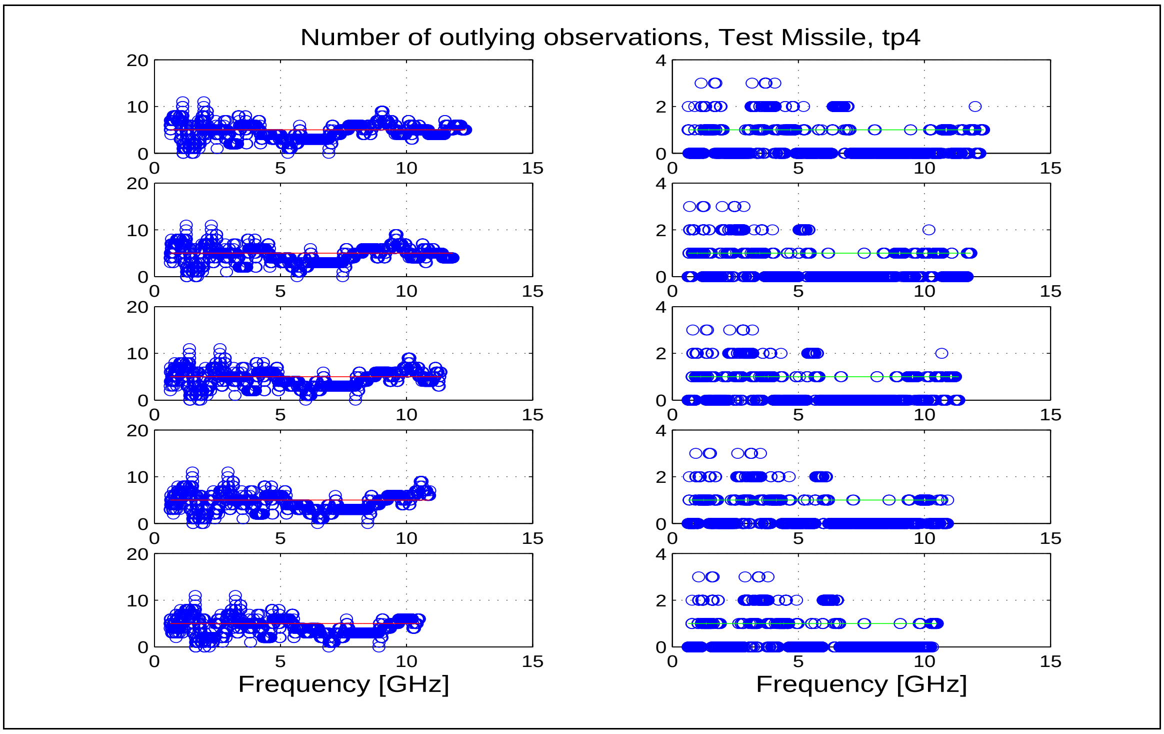

The number of outlying obtained values of EB_{dB} with 95% (left subplots) and 99% statistical limits applied (right subplots). Frequency intervals 1–5 (upper figure) and 6–10 (lower figure). The Test Missile, tp4.

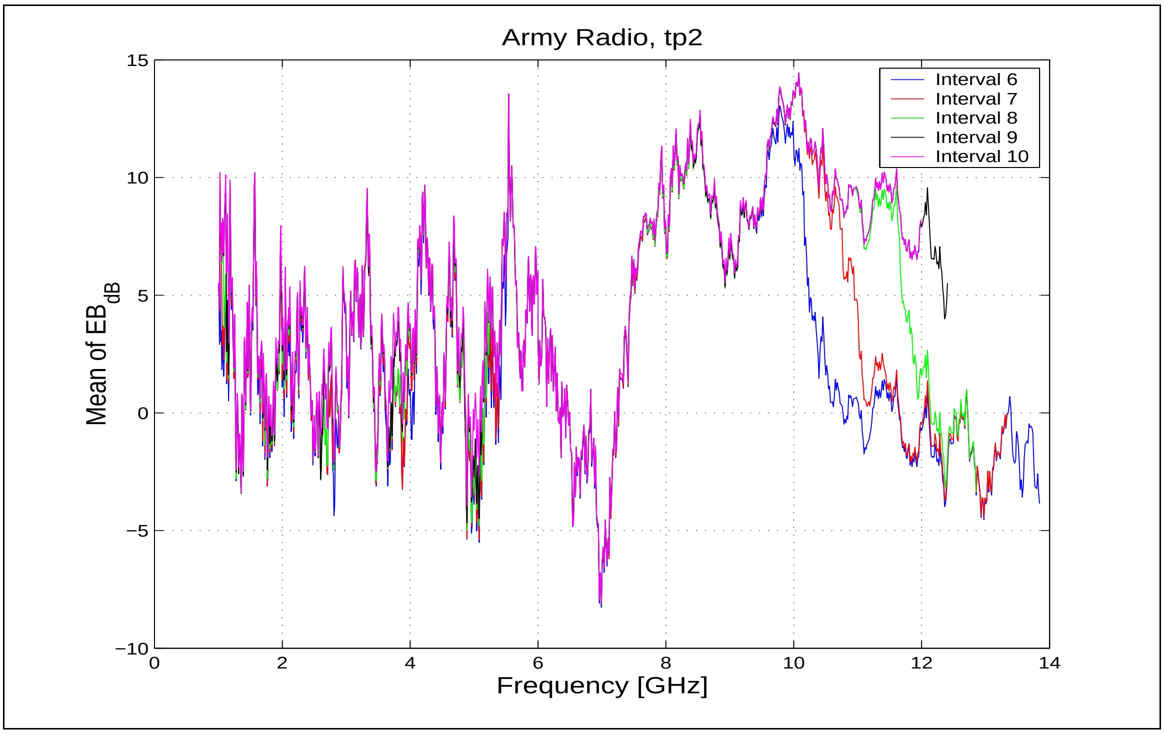

The mean of EB_{dB}, frequency intervals 6 – 10. The Army Radio, tp2.

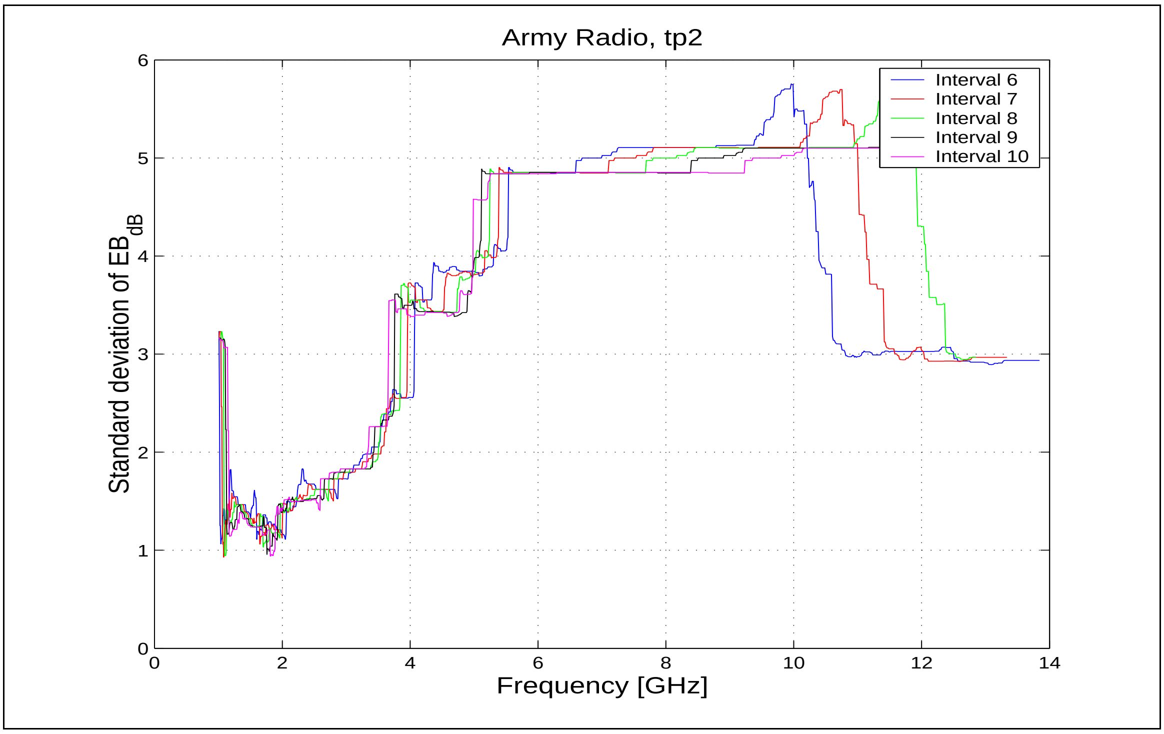

The standard deviation of EB_{dB}, frequency intervals 6 – 10. The Army Radio, tp2.

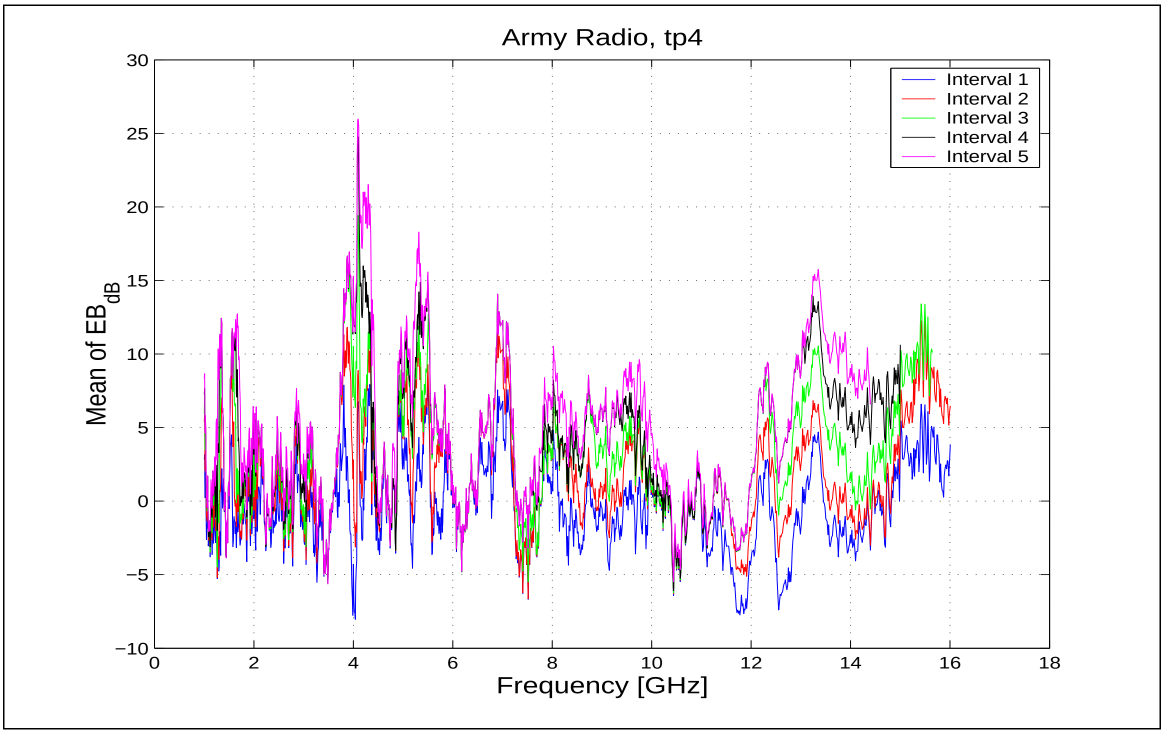

The mean of EB_{dB}**, frequency intervals 1 – 5. The Army Radio, tp4.**

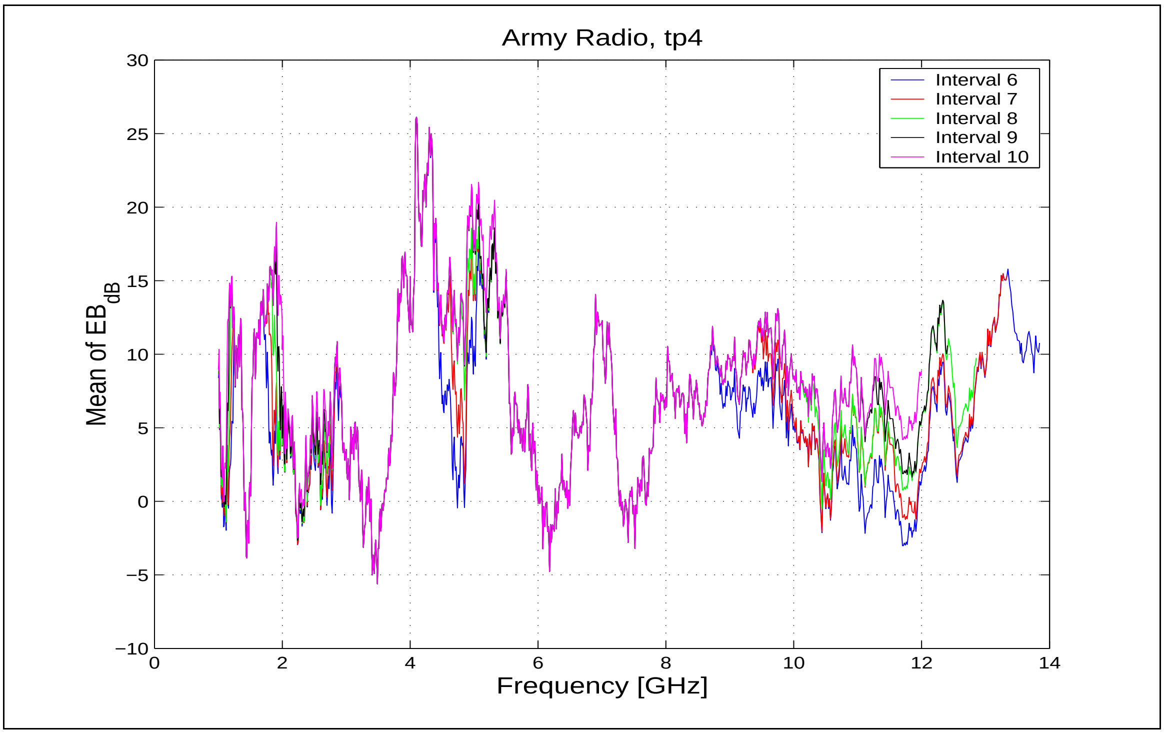

The mean of EB_{dB}**, frequency intervals 6 – 10. The Army Radio, tp4.**

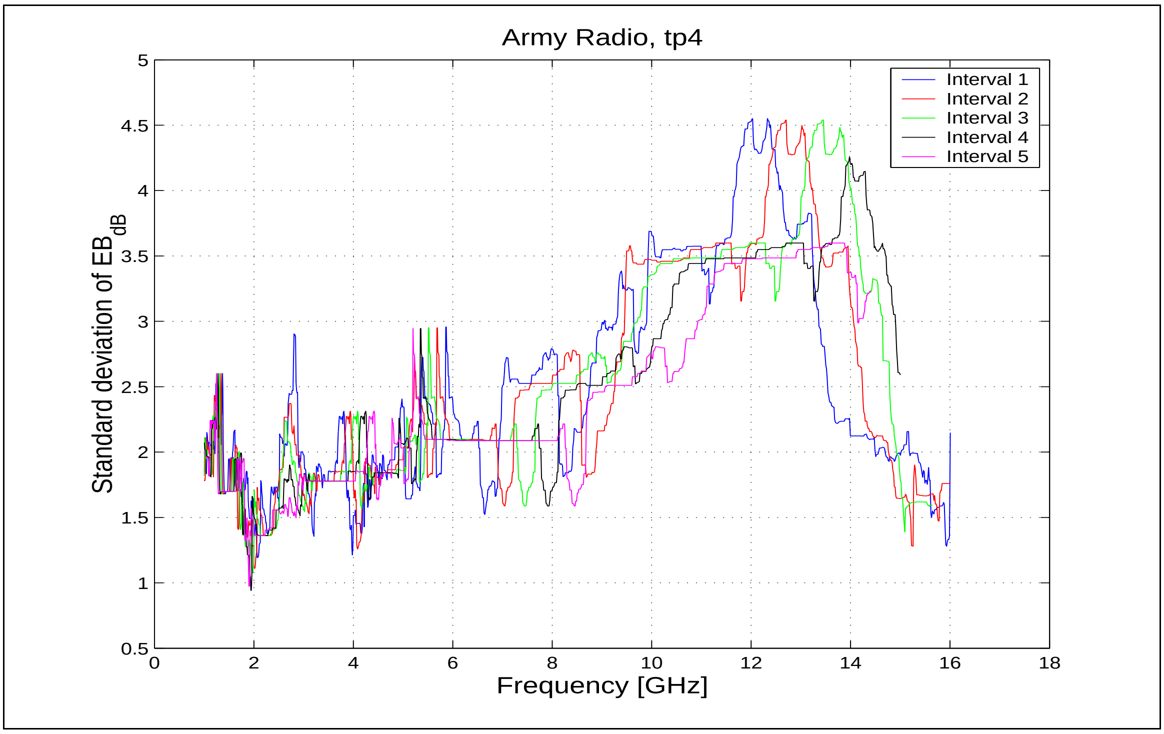

The standard deviation of EB_{dB}, frequency intervals 1 – 5. The Army Radio, tp4.

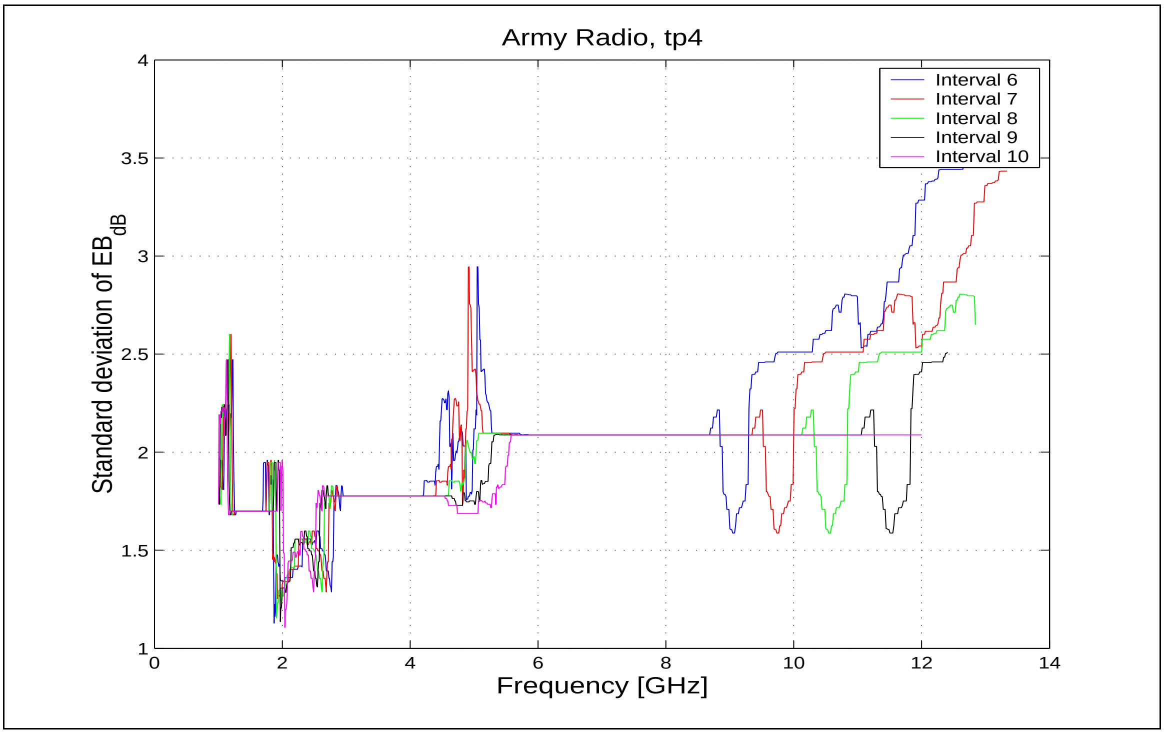

The standard deviation of EB_{dB}, frequency intervals 6 – 10. The Army Radio, tp4.

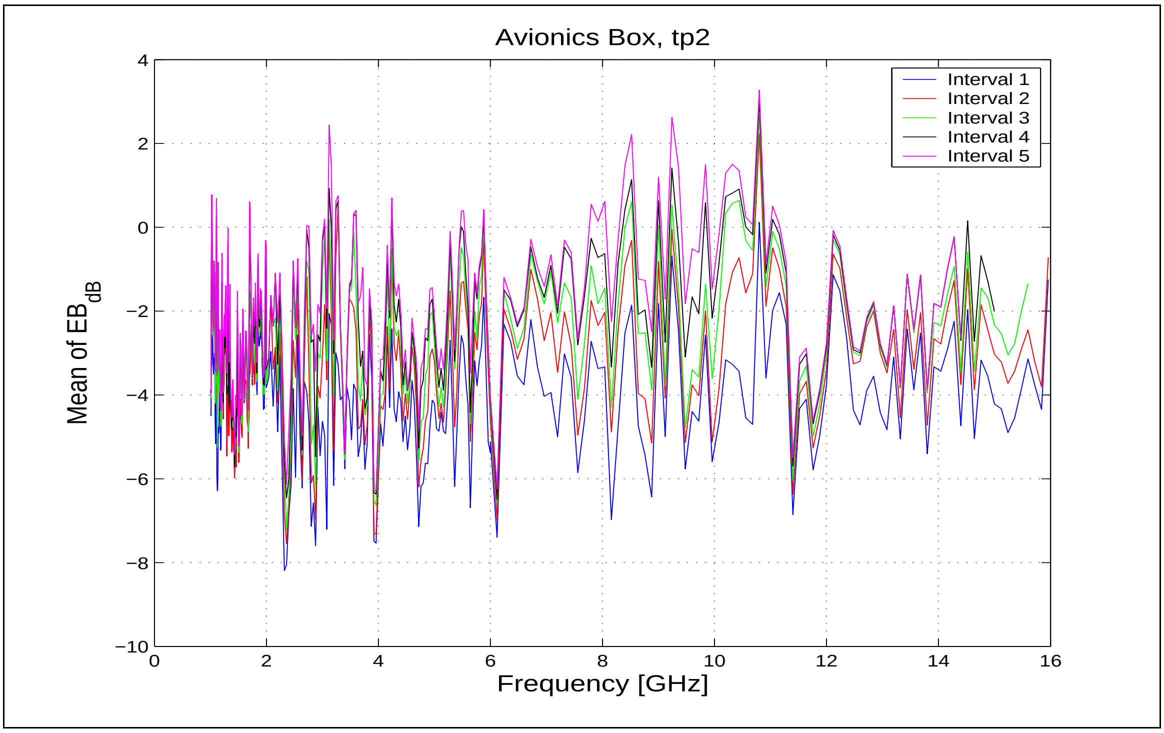

The mean of EB_{dB}, frequency intervals 1 – 5. The Avionic Box, tp2.

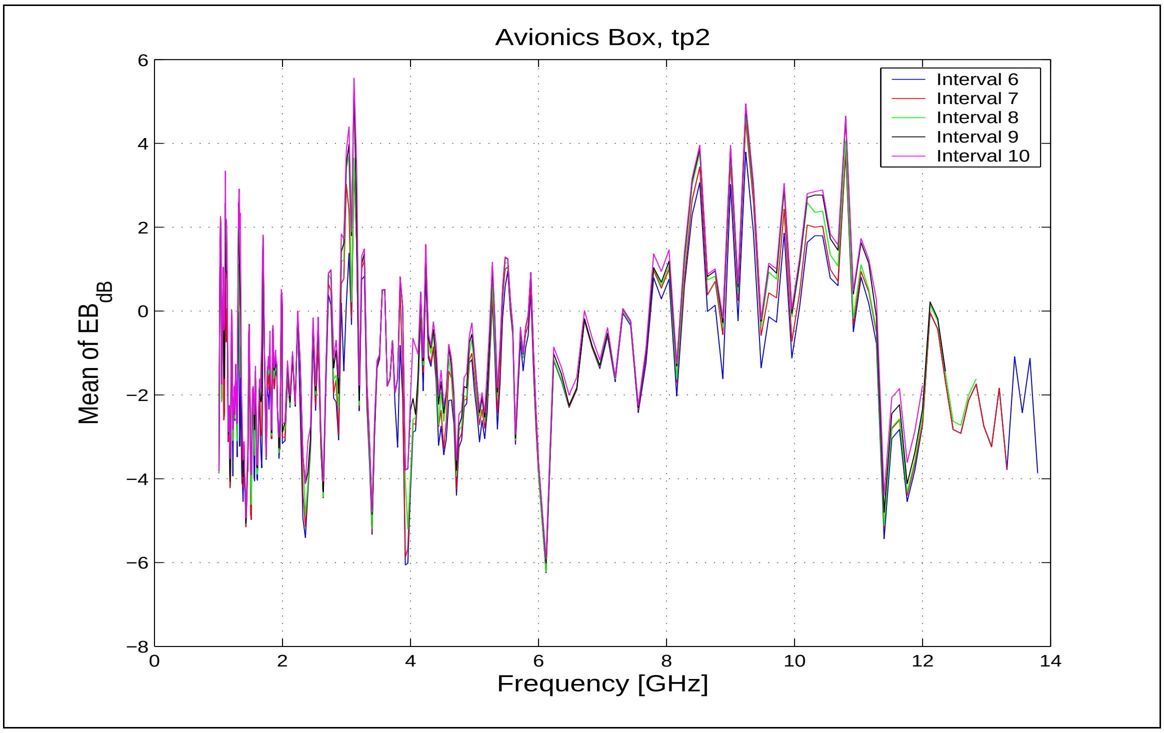

The mean of EB_{dB}, frequency intervals 6 – 10. The Avionics Box, tp2.

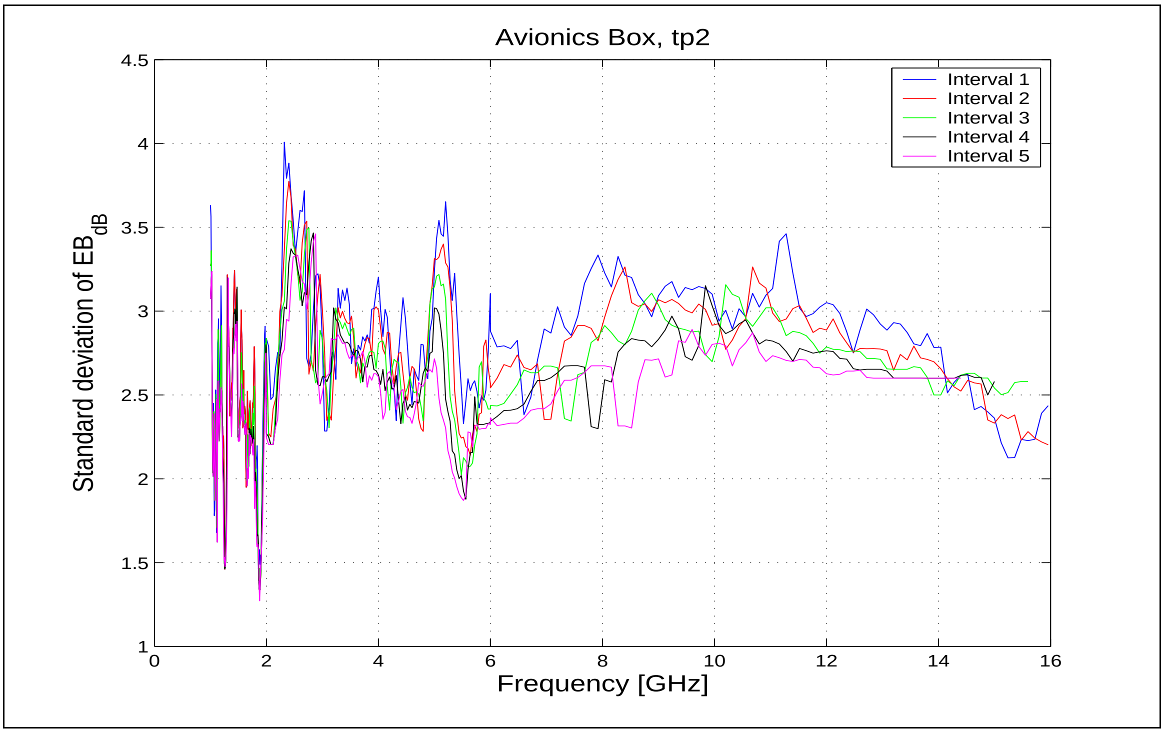

The standard deviation of EB_{dB}, frequency intervals 1 – 5. The Avionics Box, tp2.

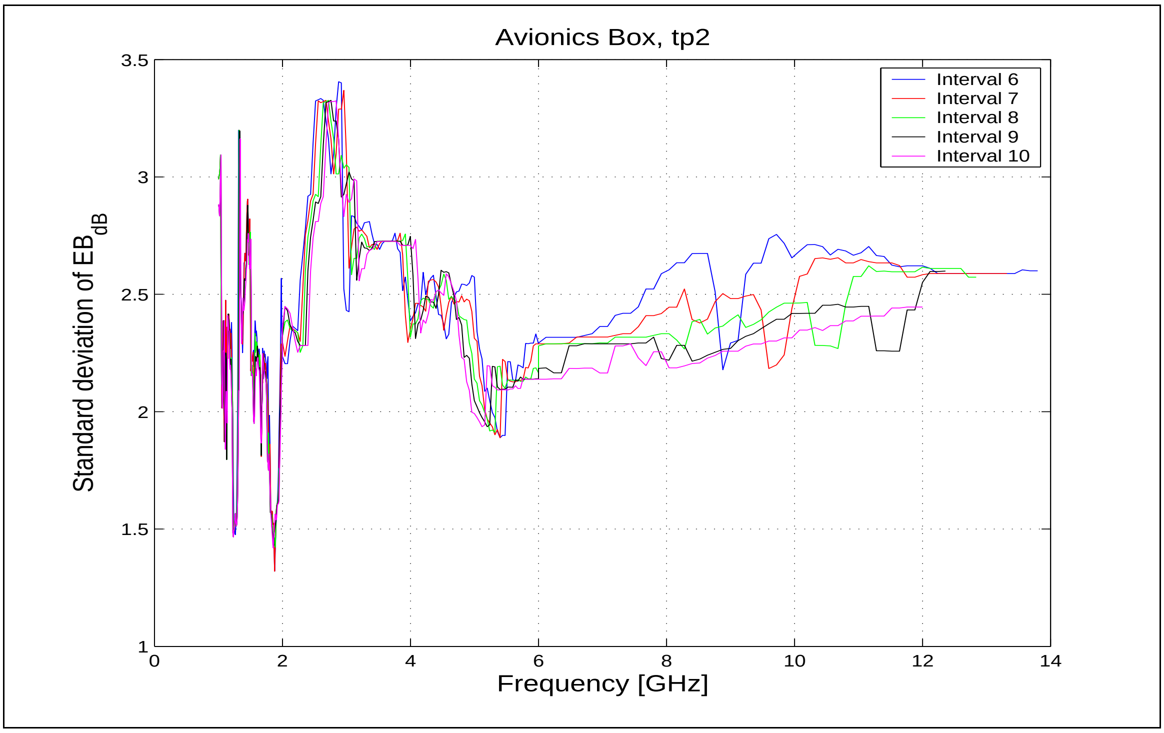

The standard deviation of EB_{dB}, frequency intervals 6 – 10. The Avionics Box, tp2.

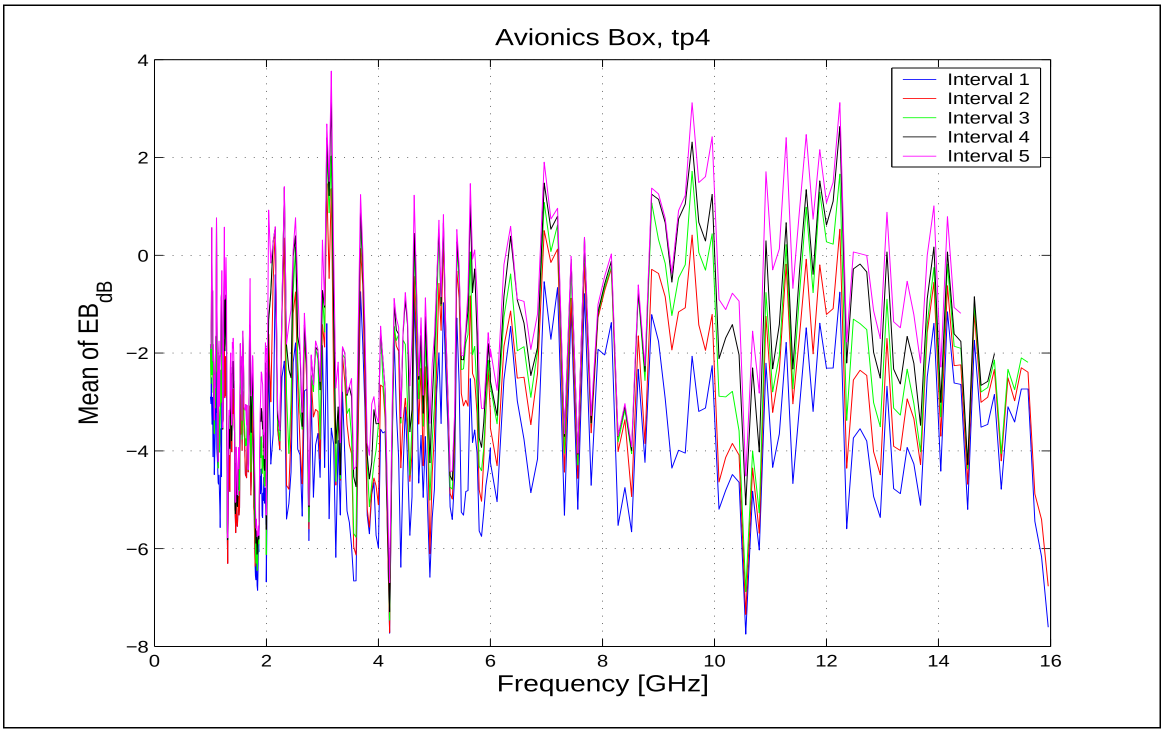

The mean of EB_{dB}, frequency intervals 1 – 5. The Avionic Box, tp4.

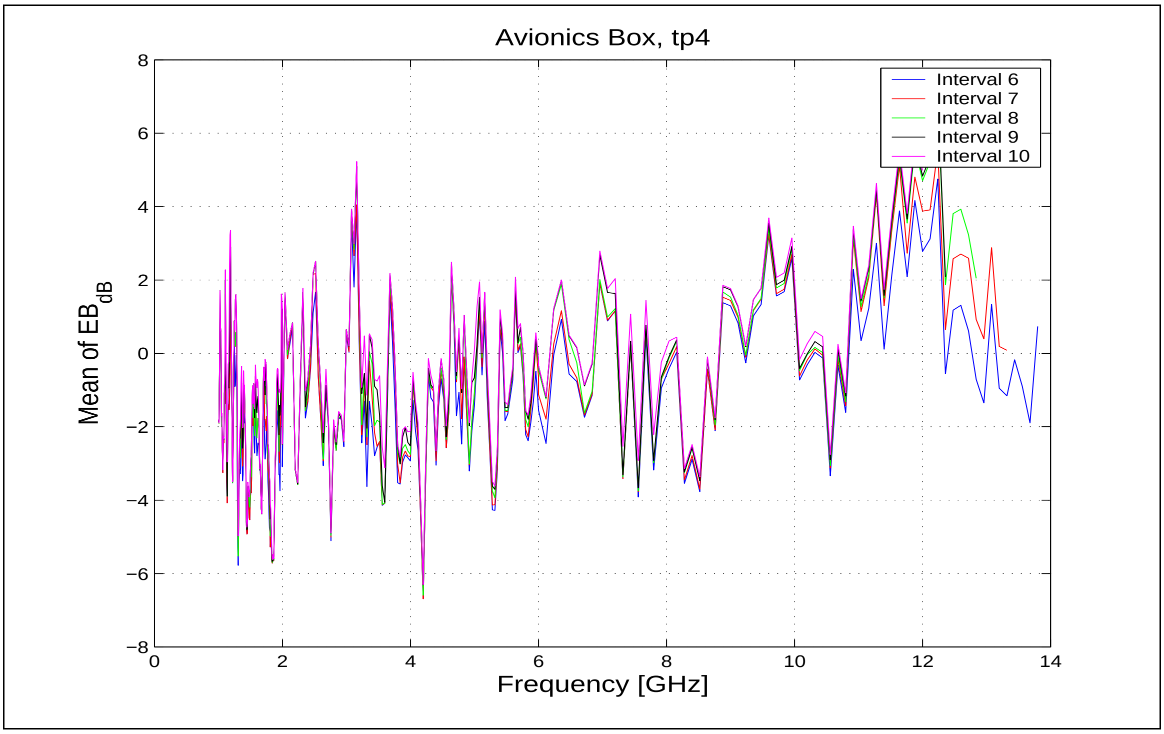

The mean of EB_{dB}, frequency intervals 6 – 10. The Avionic Box, tp4.

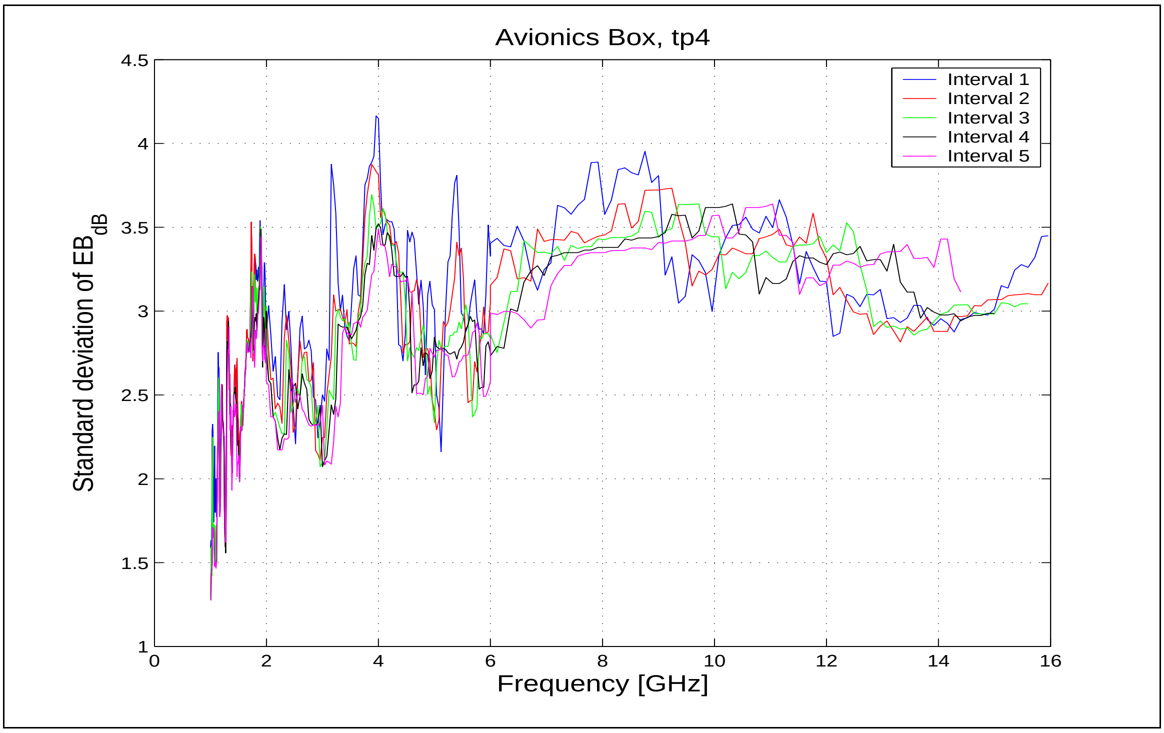

The standard deviation of EB_{dB}, frequency intervals 1 – 5. The Avionics Box, tp4.

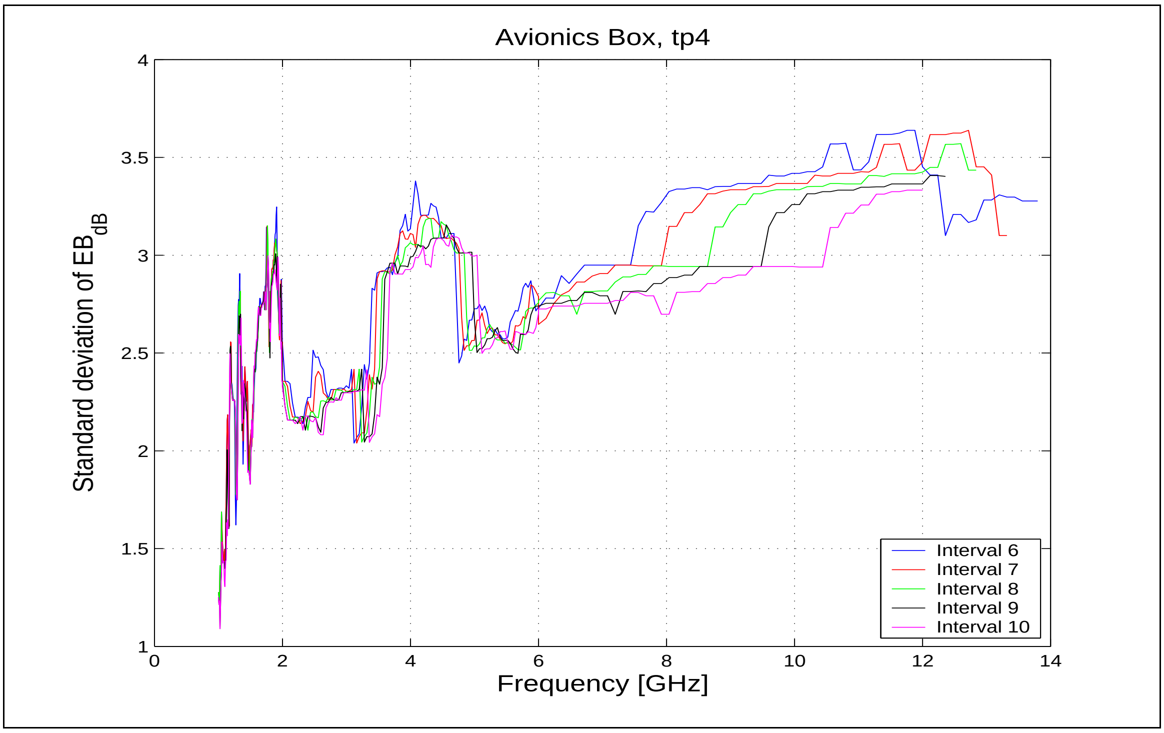

The standard deviation of EB_{dB}, frequency intervals 6 – 10. The Avionics Box, tp4.

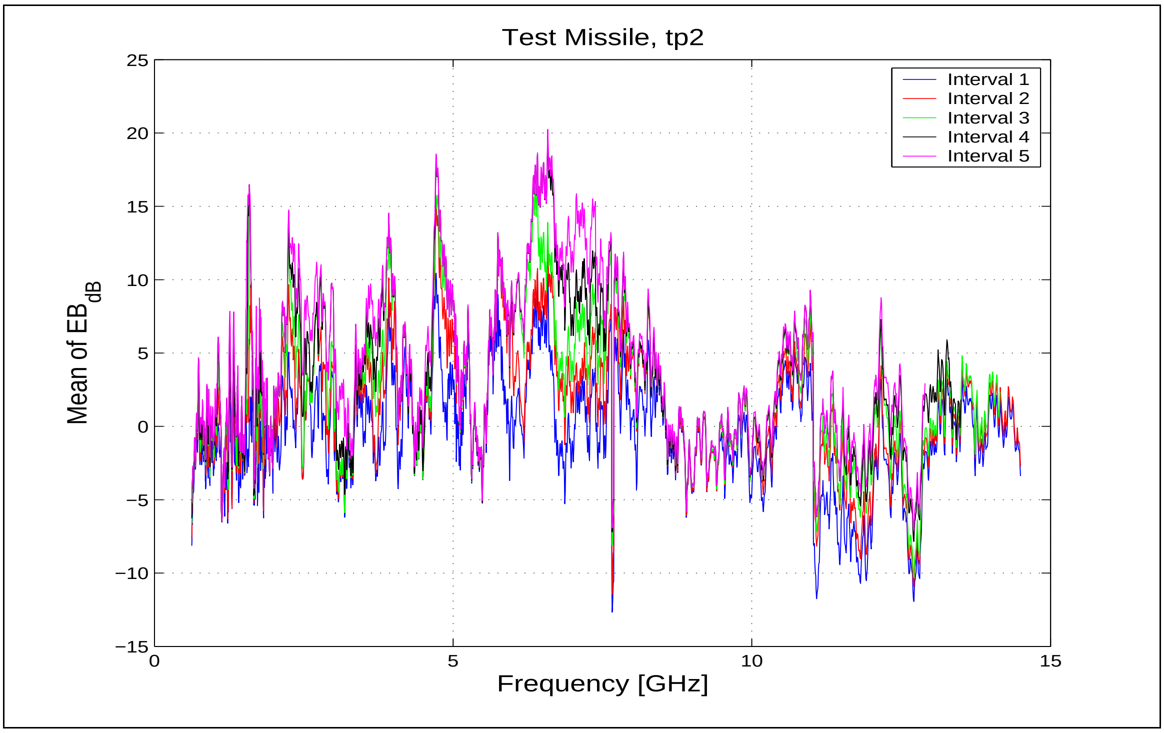

The mean of EB_{dB}, frequency intervals 1 – 5. The Test Missile, tp2.

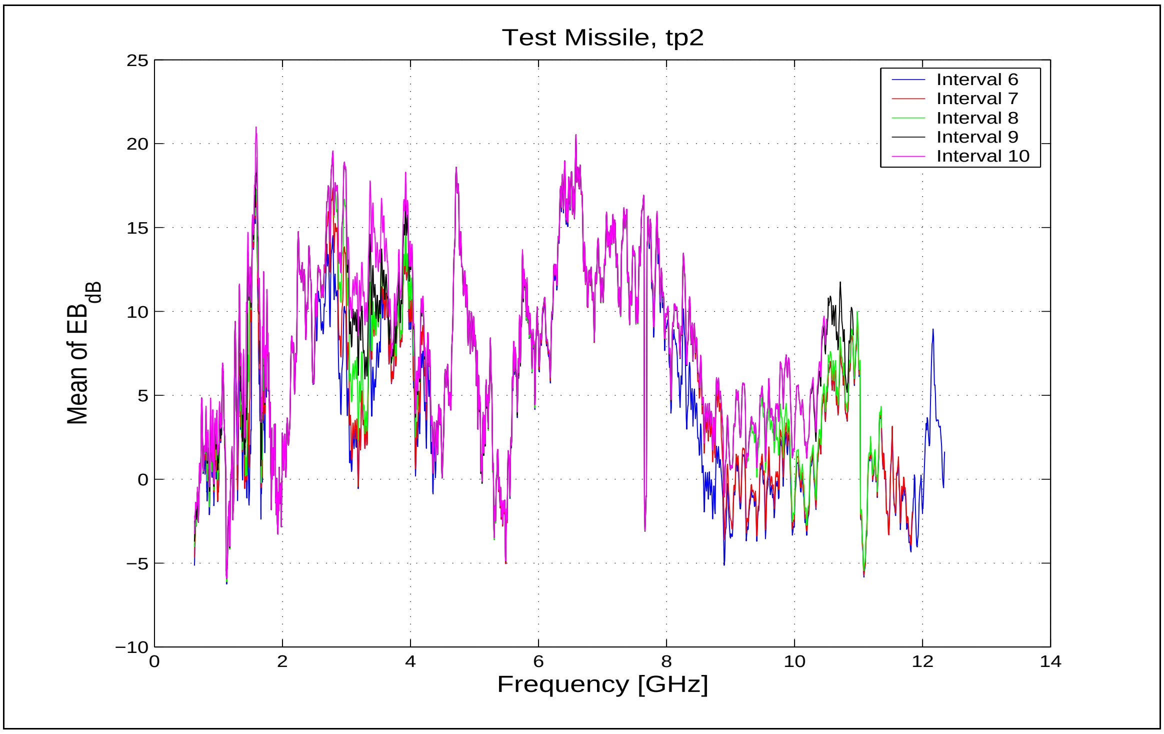

The mean of EB_{dB}, frequency intervals 6 – 10. The Test Missile, tp2.

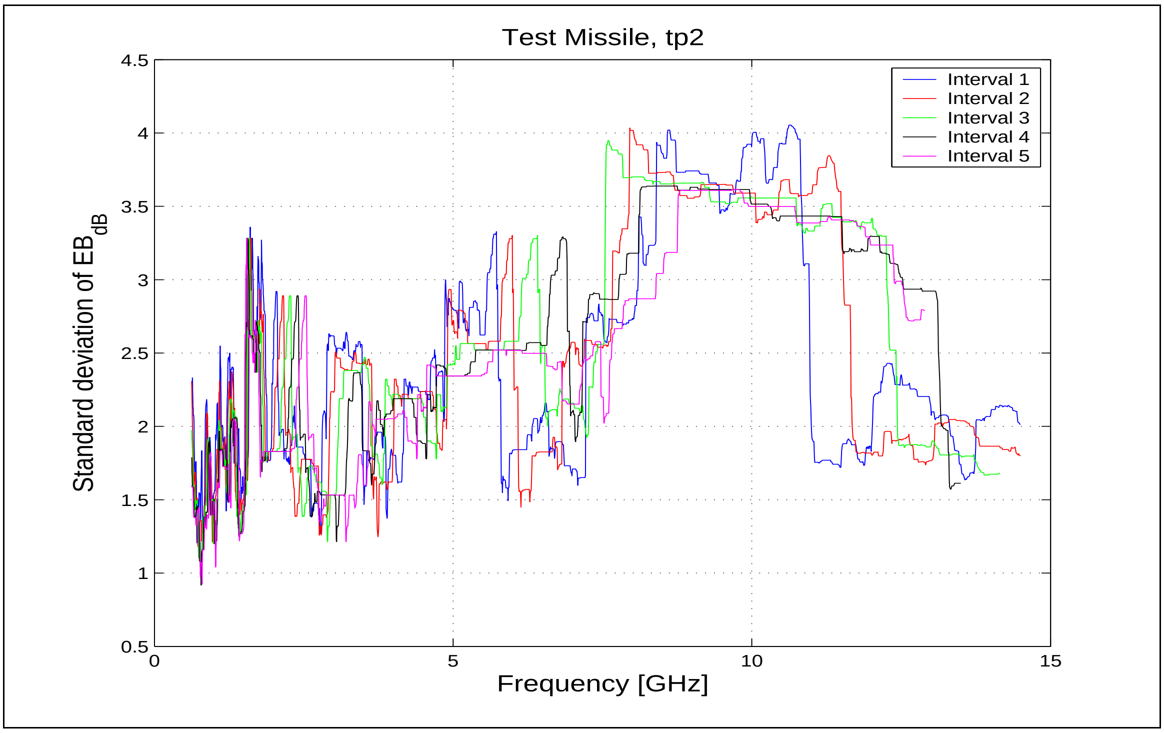

The standard deviation of EB_{dB}, frequency intervals 1 – 5. The Test Missile, tp2.

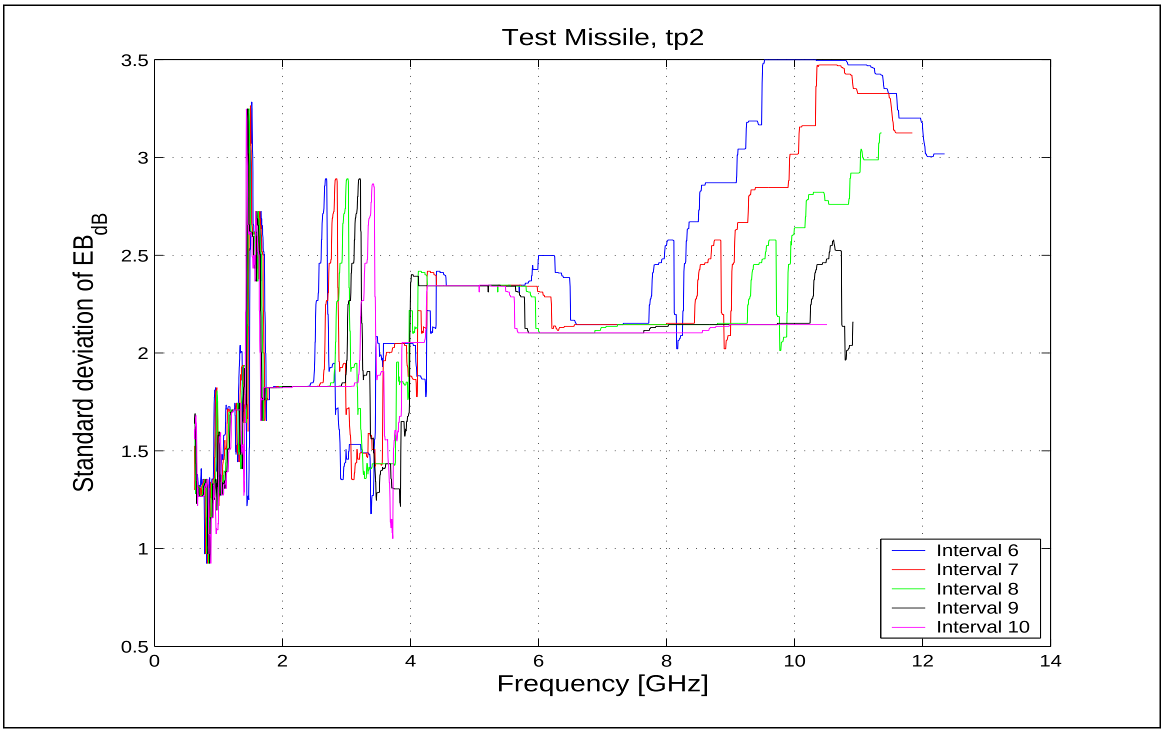

The standard deviation of EB_{dB}, frequency intervals 6 – 10. The Test Missile, tp2.

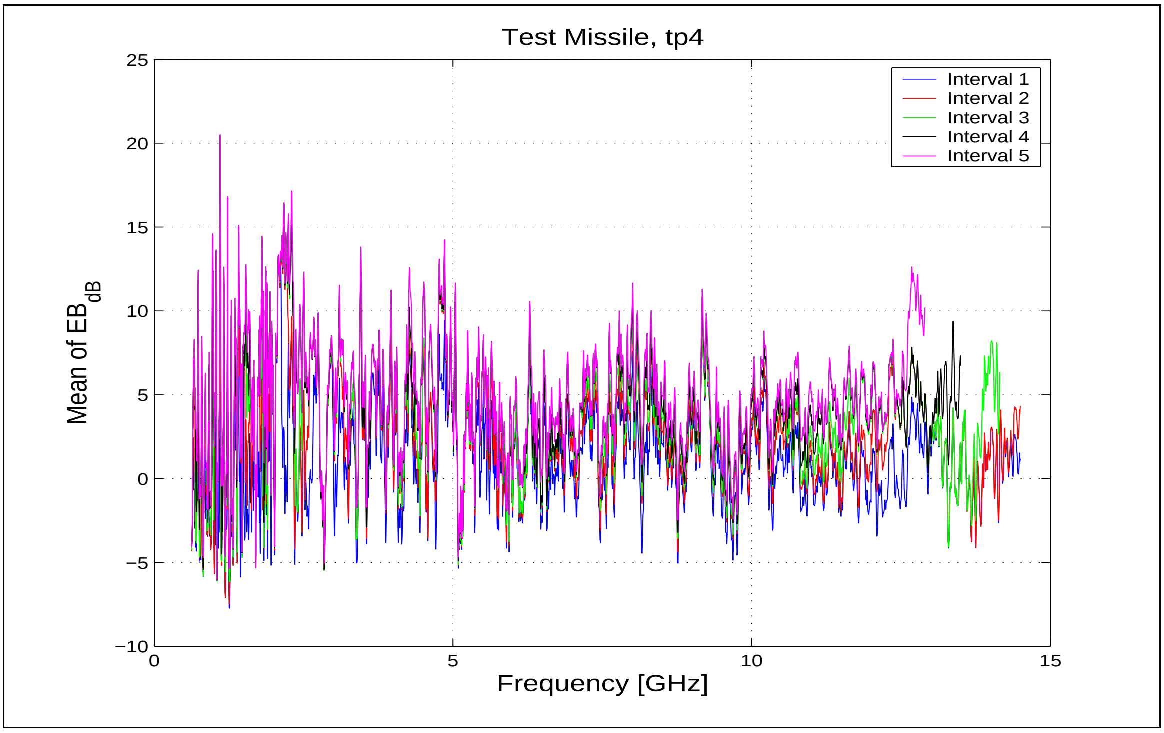

The mean of EB_{dB}, frequency intervals 1 – 5. The Test Missile, tp4.

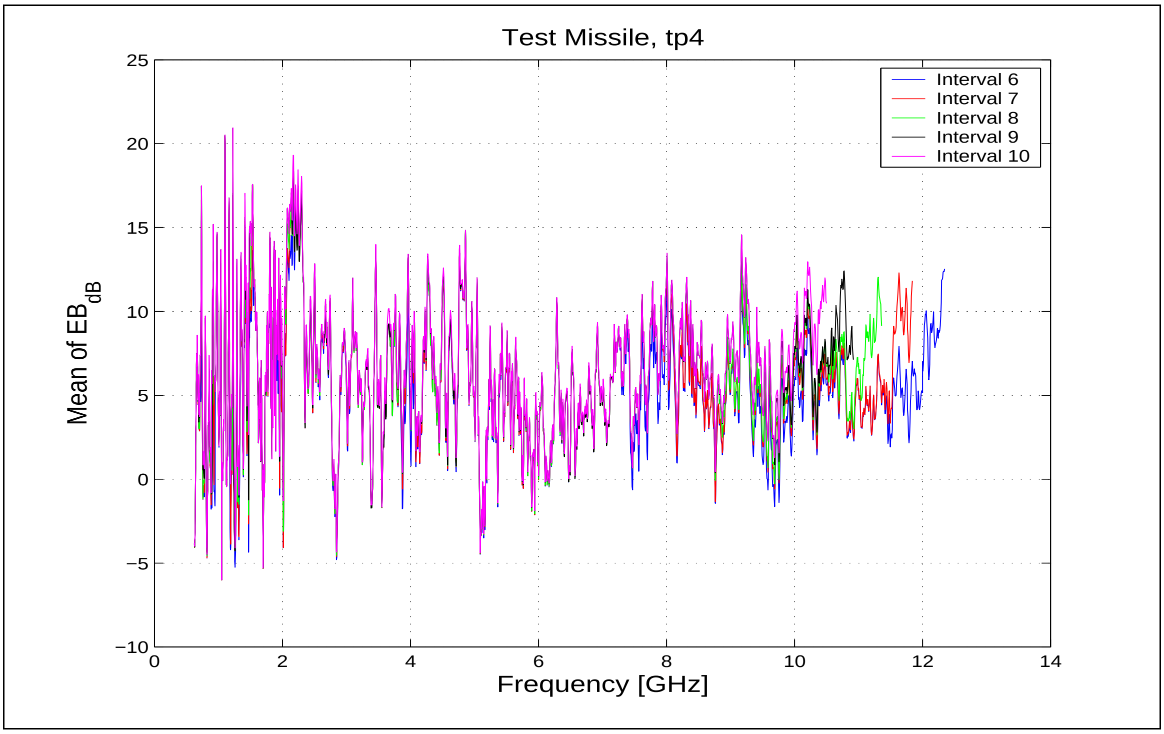

The mean of EB_{dB}, frequency intervals 6 – 10. The Test Missile, tp4.

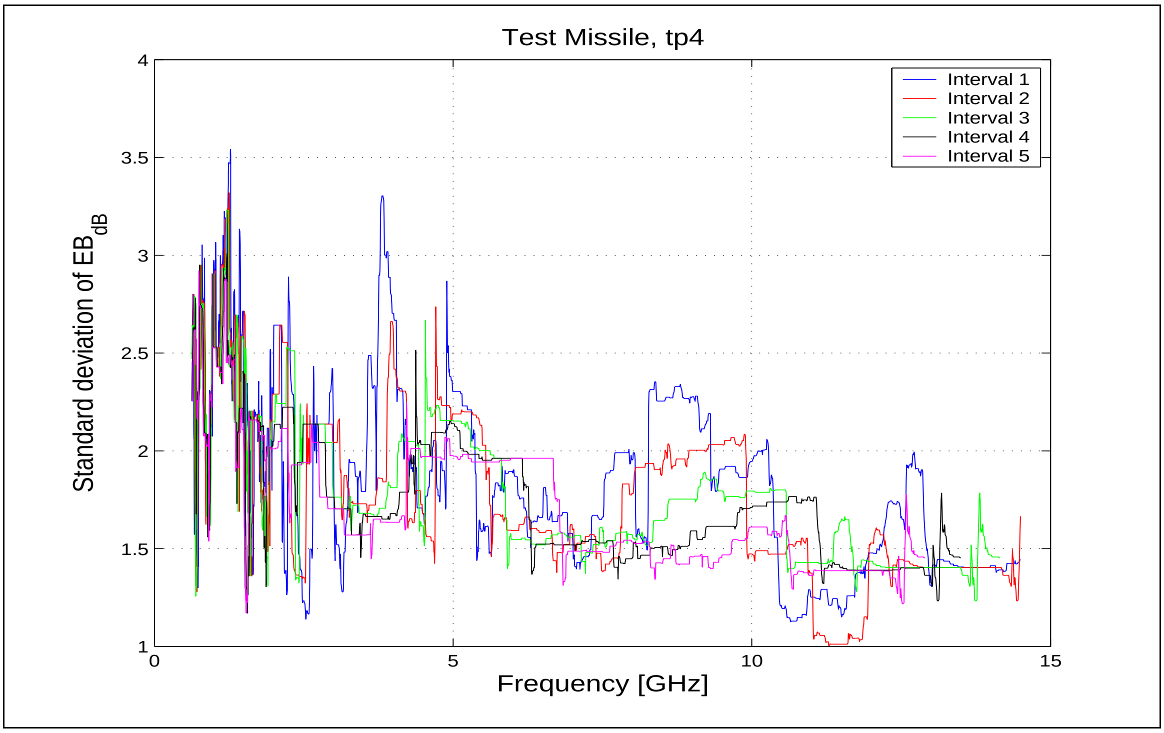

The standard deviation of EB_{dB}, frequency intervals 1 – 5. The Test Missile, tp4.

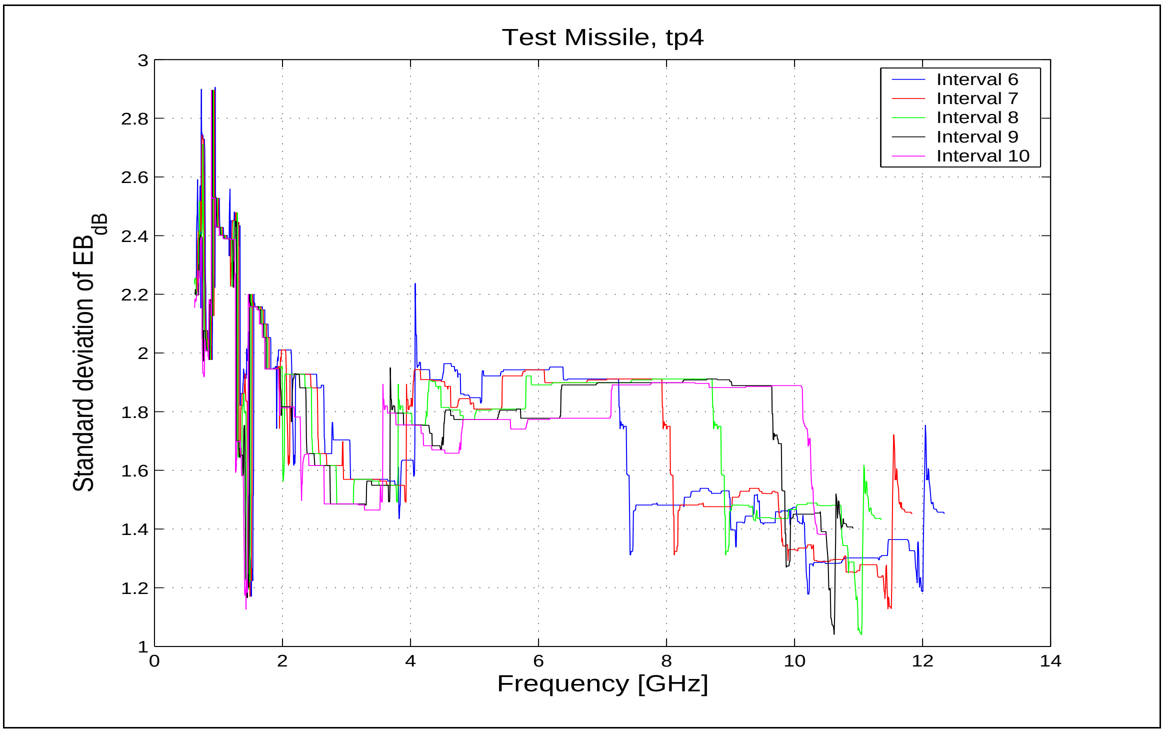

The standard deviation of EB_{dB}, frequency intervals 6 – 10. The Test Missile, tp4.

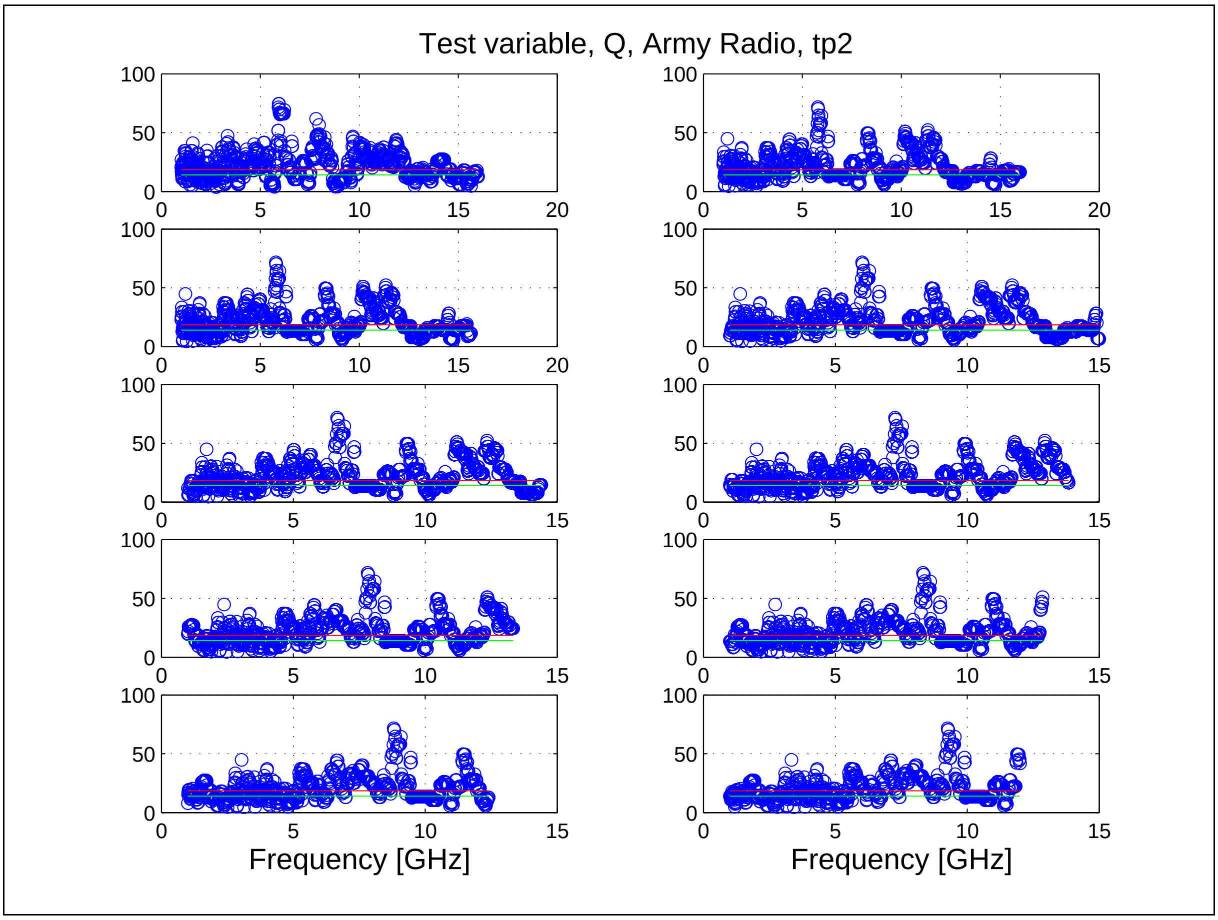

The test variable Q, 1% and 5% significance level for rejection for all tested frequencies. Frequency intervals 1–10 (from the left to the right in the figure). The Army Radio, tp2.

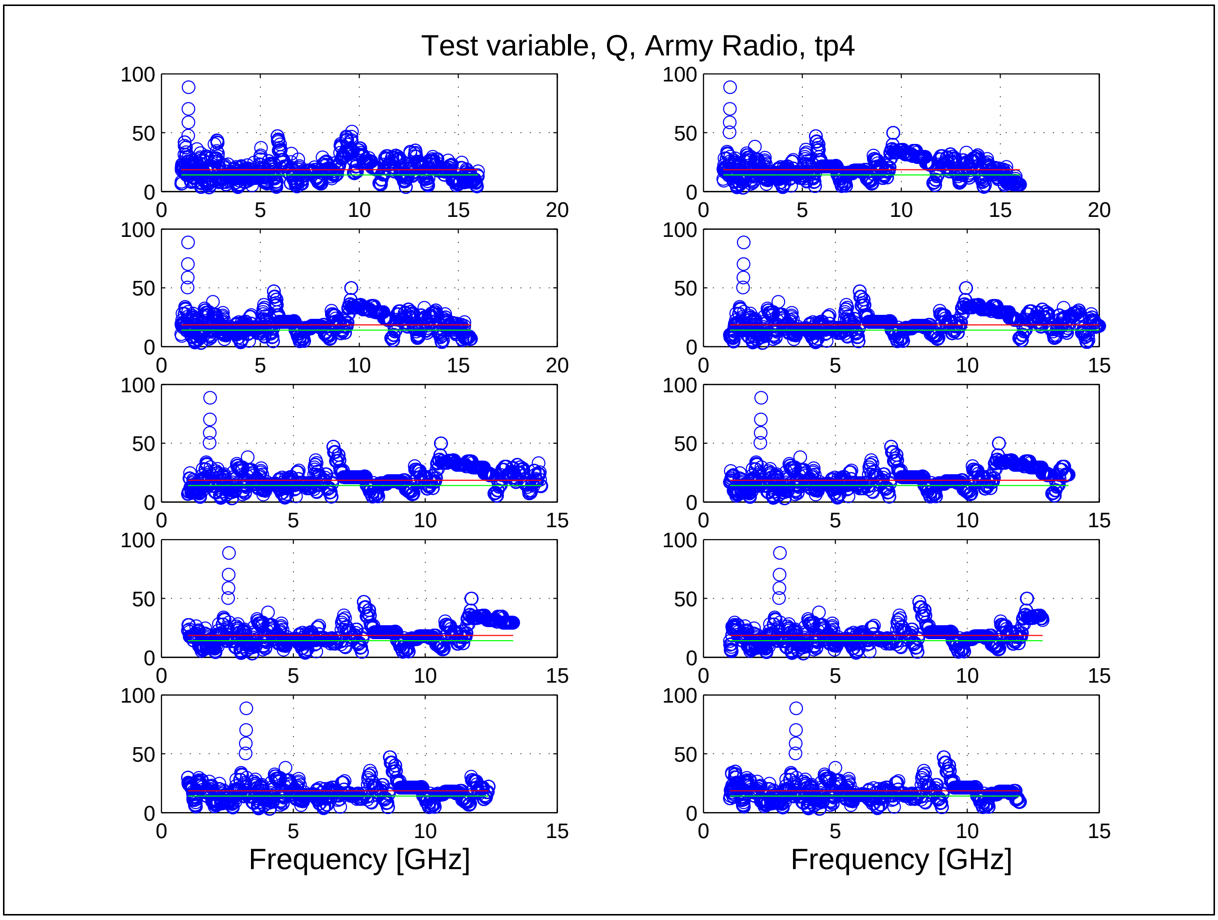

The test variable Q, 1% and 5% significance level for rejection for all tested frequencies. Frequency intervals 1–10 (from the left to the right in the figure). The Army Radio, tp4.

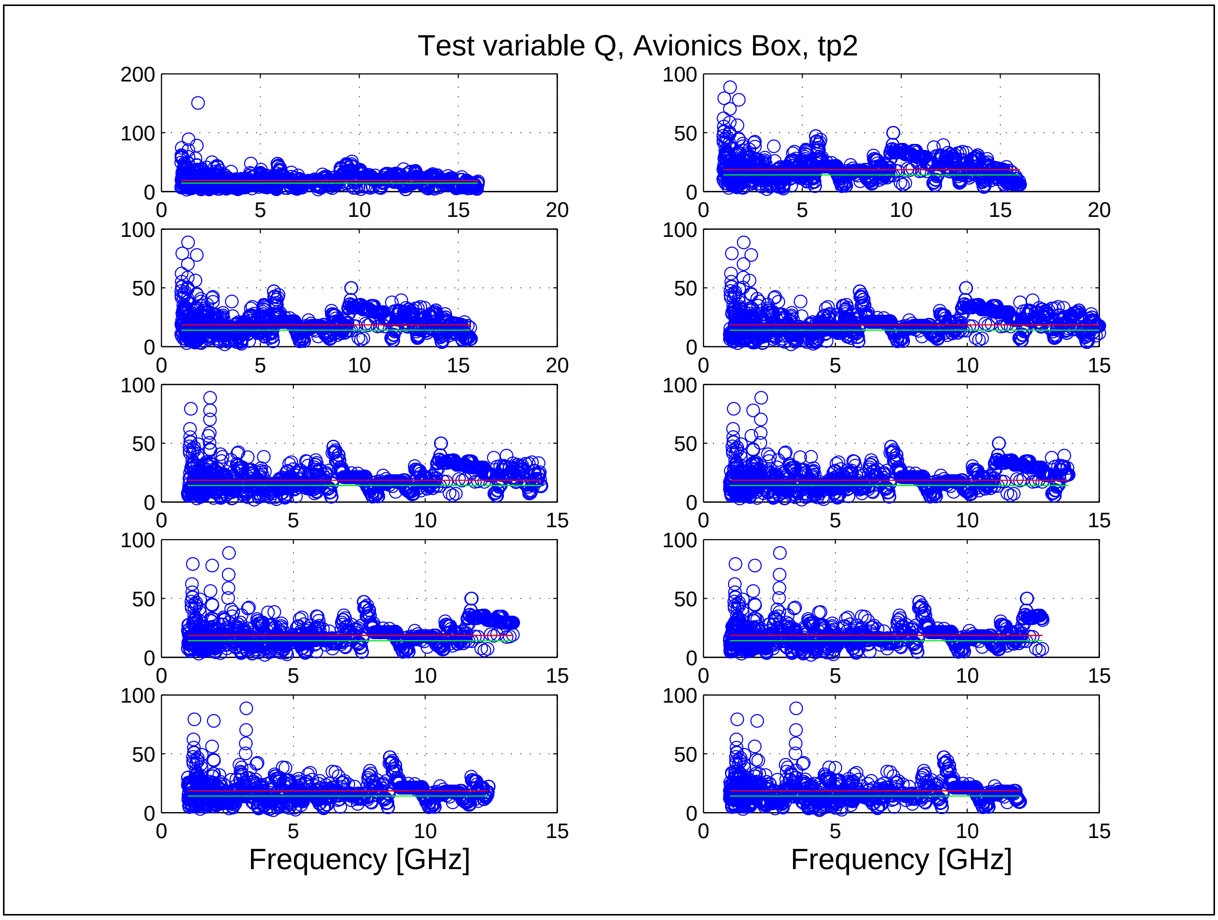

The test variable Q, 1% and 5% significance level for rejection for all tested frequencies. Frequency intervals 1–10 (from the left to the right in the figure). The Avionic Box, tp2.

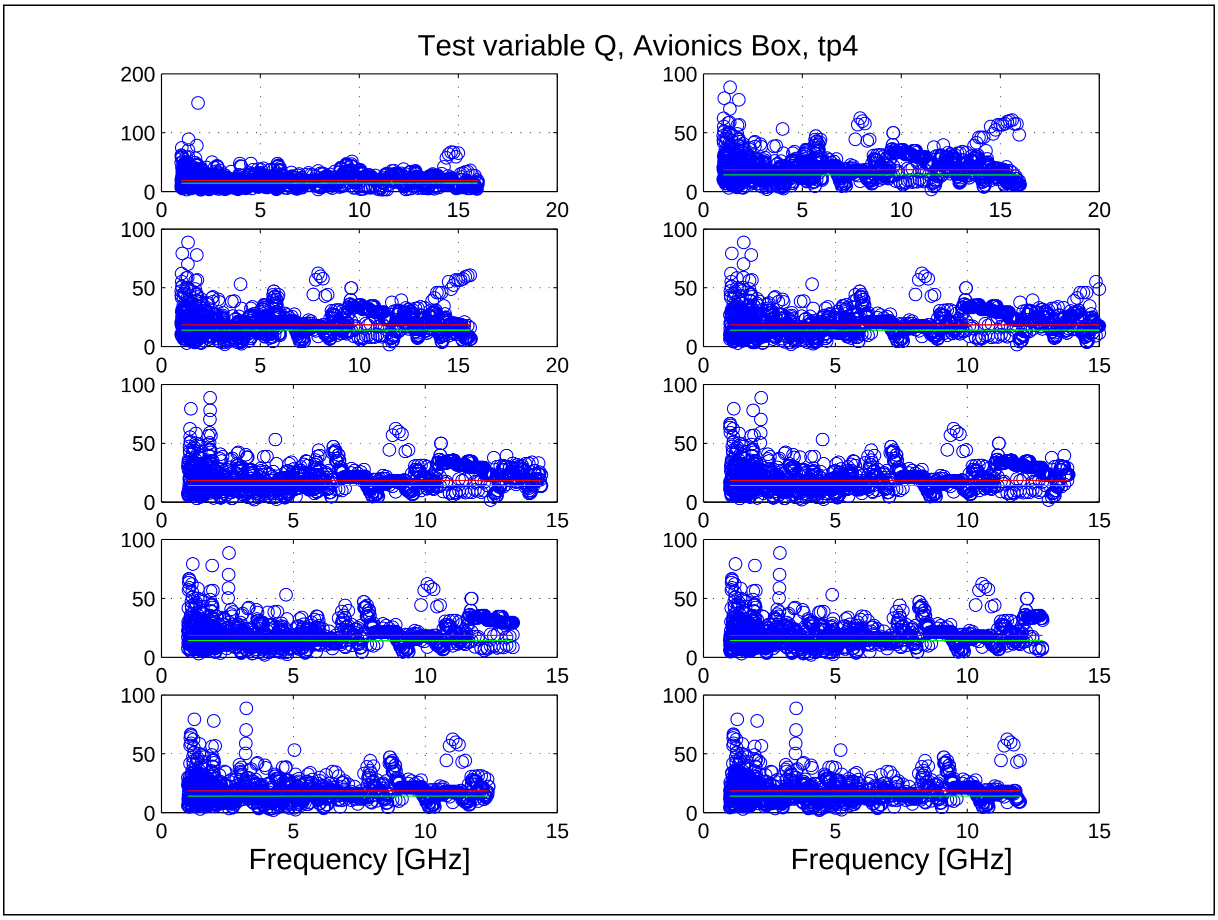

The test variable Q, 1% and 5% significance level for rejection for all tested frequencies. Frequency intervals 1–10 (from the left to the right in the figure). The Avionic Box, tp4.

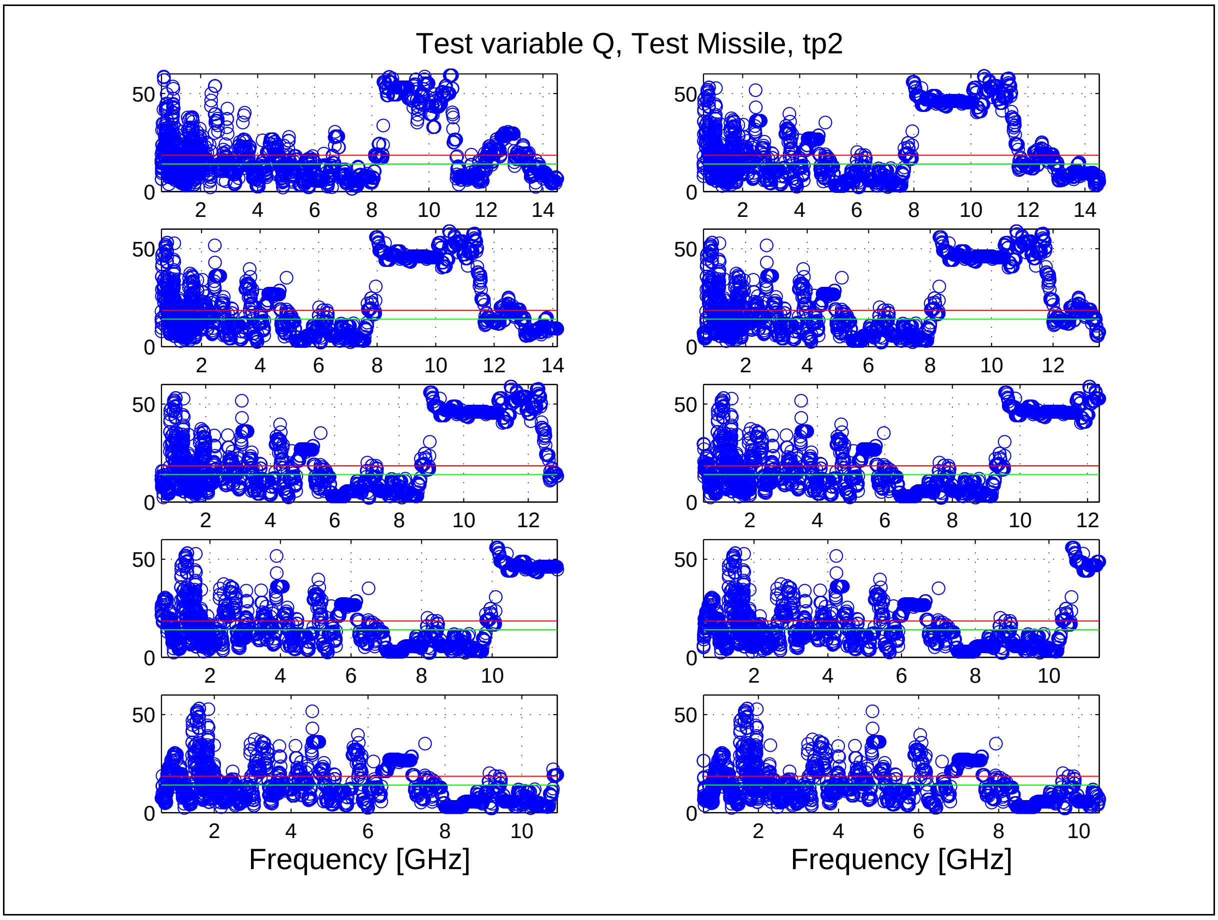

The test variable Q, 1% and 5% significance level for rejection for all tested frequencies. Frequency intervals 1–10 (from the left to the right in the figure). The Test Missile, tp2.

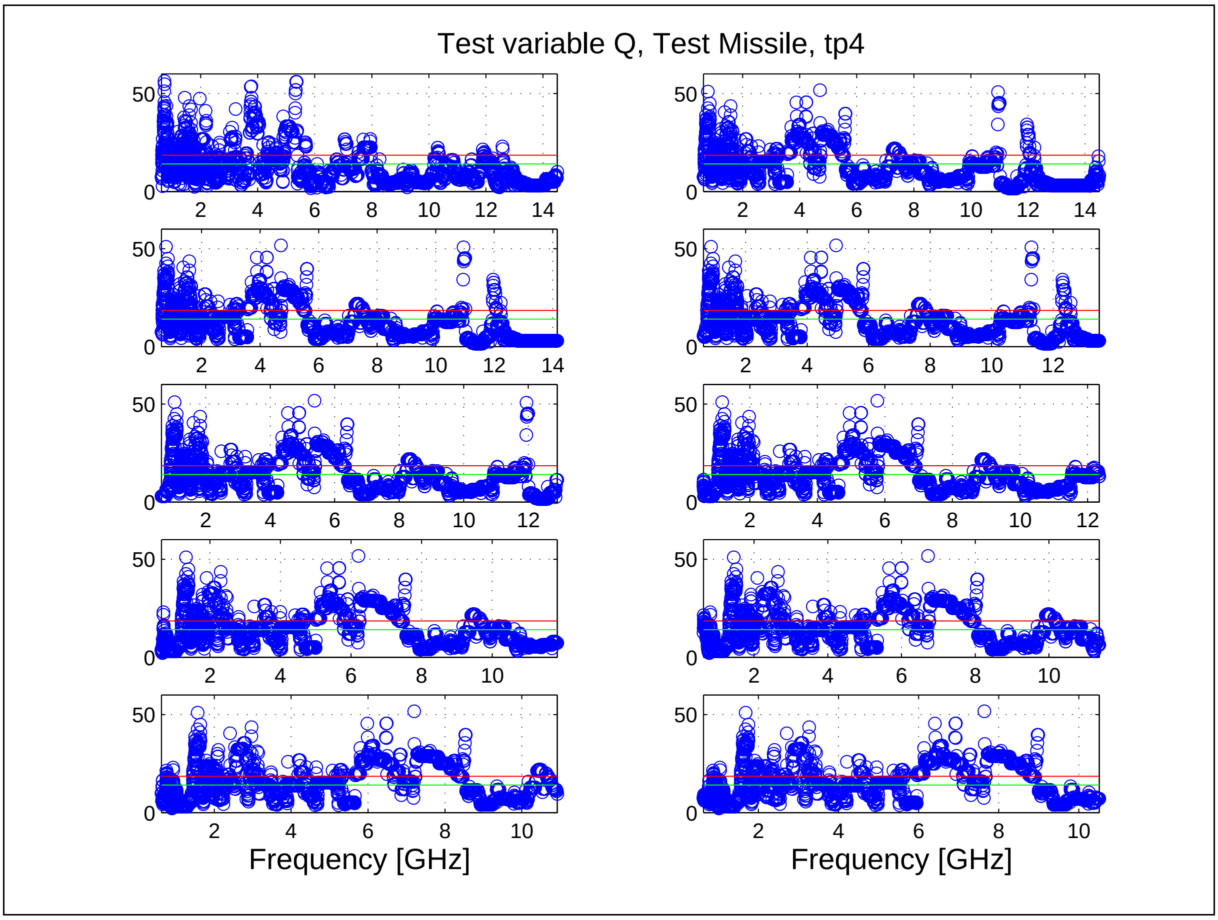

The test variable Q, 1% and 5% significance level for rejection for all tested frequencies. Frequency intervals 1–10 (from the left to the right in the figure). The Test Missile, tp4.

Sample	Angles (degrees)	Sample	Angles (degrees)	Sample	Angles (degrees)	Sample	Angles (degrees)
1	276;324;349	26	177;264;256	51	198;16;84	76	11;127;30
2	327;65;353	27	301;4;18	52	144;44;160	77	22;274;227
3	324;11;102	28	181;106;5	53	19;359;250	78	191;357;110
4	68;220;76	29	286;25;112	54	222;223;299	79	66;205;168
5	360;7;159	30	123;295;2	55	353;158;305	80	142;10;123
6	54;224;272	31	178;221;135	56	143;152;322	81	352;208;278
7	102;190;113	32	72;323;356	57	125;292;358	82	226;264;54
8	66;281;292	33	332;142;239	58	282;307;238	83	150;25;319
9	261;17;221	34	195;76;110	59	98;87;154	84	300;114;324
10	121;211;329	35	5;2;356	60	216;152;277	85	272;55;258
11	181;151;288	36	293;278;326	61	10;250;272	86	303;283;360
12	321;185;141	37	45;35;199	62	344;140;21	87	212;130;135
13	336;102;278	38	3;46;21	63	136;237;253	88	356;320;67
14	262;330;39	39	275;26;259	64	33;342;193	89	88;89;63
15	321;215;5	40	51;222;170	65	328;112;261	90	121;147;225
16	86;45;318	41	184;125;31	66	139;324;25	91	324;245;48
17	293;275;292	42	93;190;51	67	96;225;245	92	171;349;180
18	246;225;133	43	44;181;103	68	266;336;222	93	143;356;277
19	74;100;174	44	41;181;137	69	266;230;62	94	354;87;168
20	145;253;116	45	98;345;165	70	99;293;146	95	13;266;306
21	18;280;200	46	89;299;110	71	238;103;347	96	187;52;280
22	25;179;301	47	12;356;173	72	208;348;186	97	162;60;93
23	166;281;178	48	218;186;352	73	312;82;88	98	263;23;41
24	251;355;128	48	89;241;53	74	324;256;352	99	294;167;328
25	224;186;294	59	146;52;124	75	166;268;241	100	323;75;315

The angle samples.

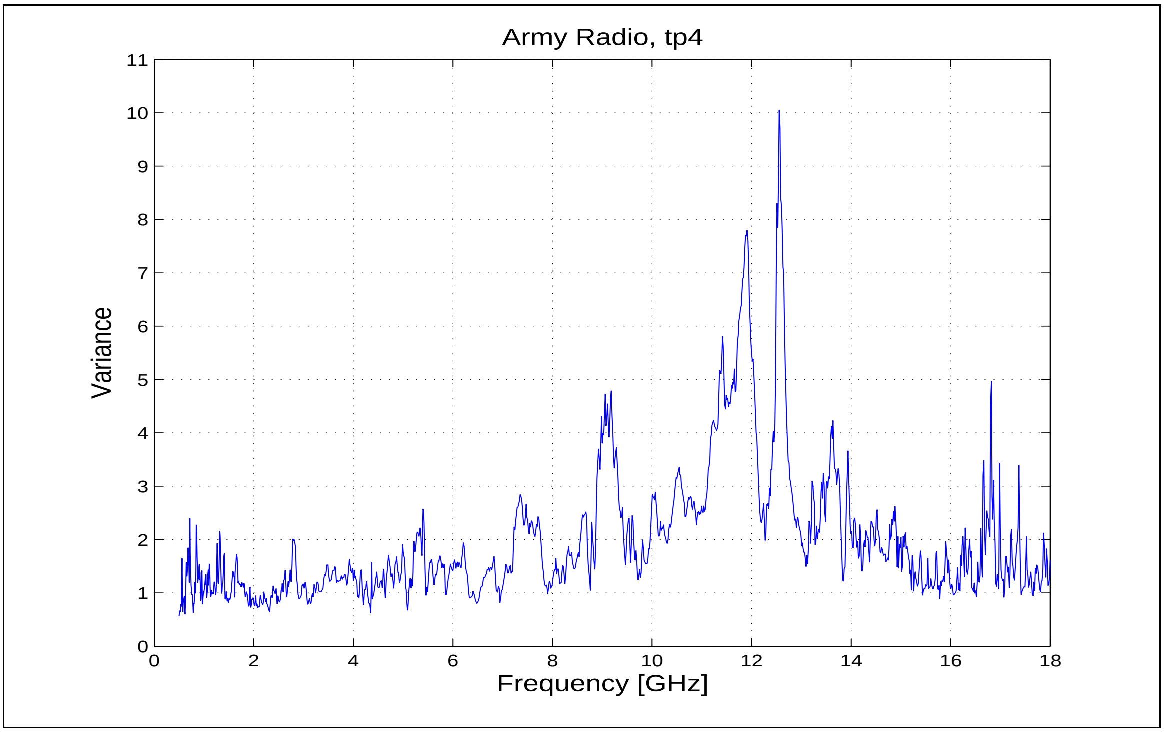

Variance of the received power normalized to mean, taken for all three planes. The Army Radio, tp4.

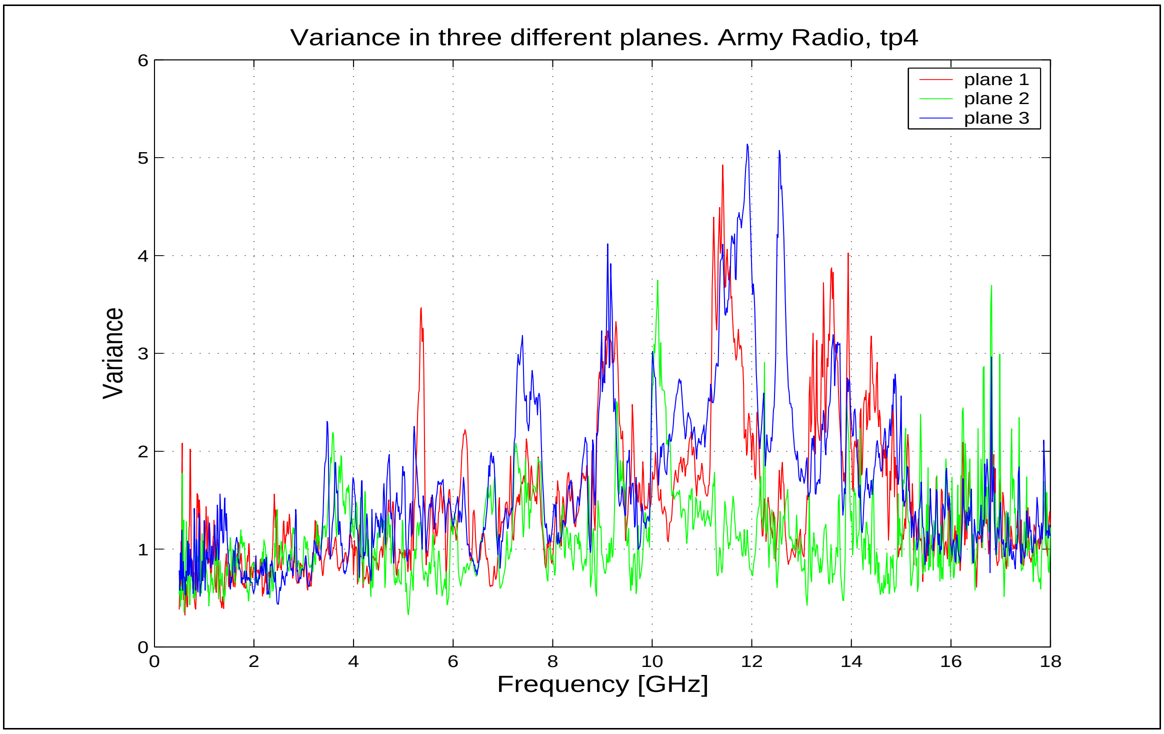

Variance of the received power normalized to mean taken for each plane individually. The Army Radio, tp4.

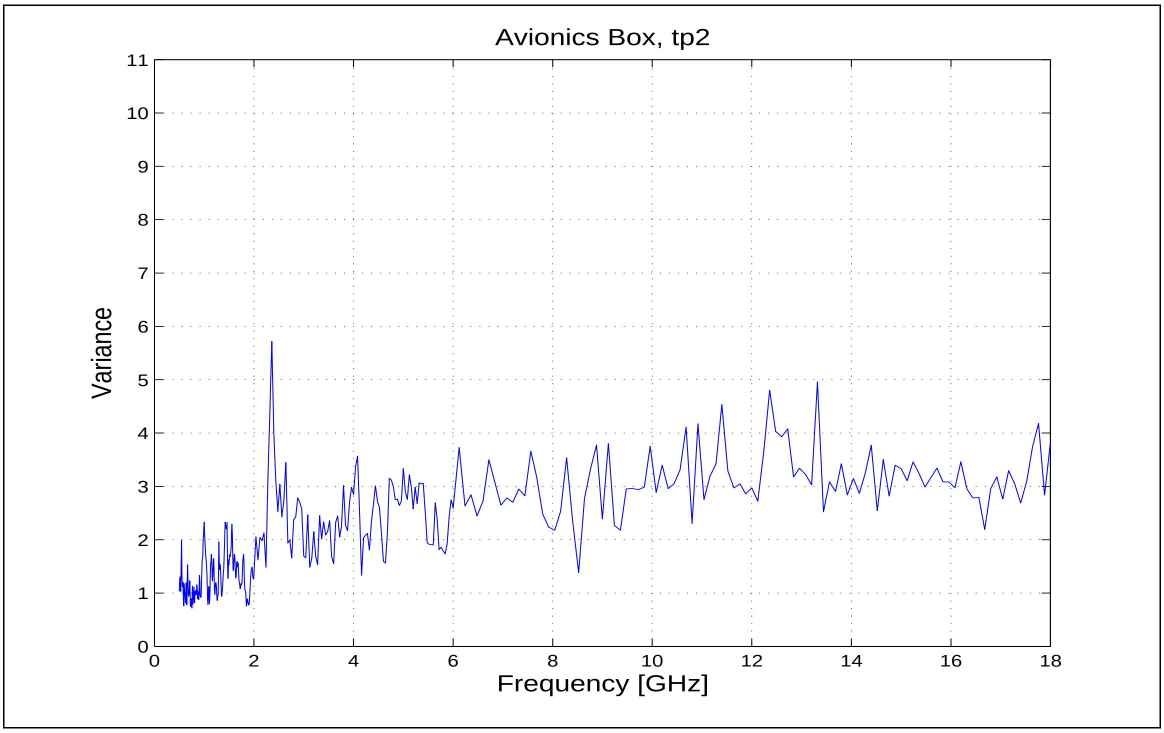

Variance of the received power normalized to mean, taken for all three planes. The Avionics Box, tp2.

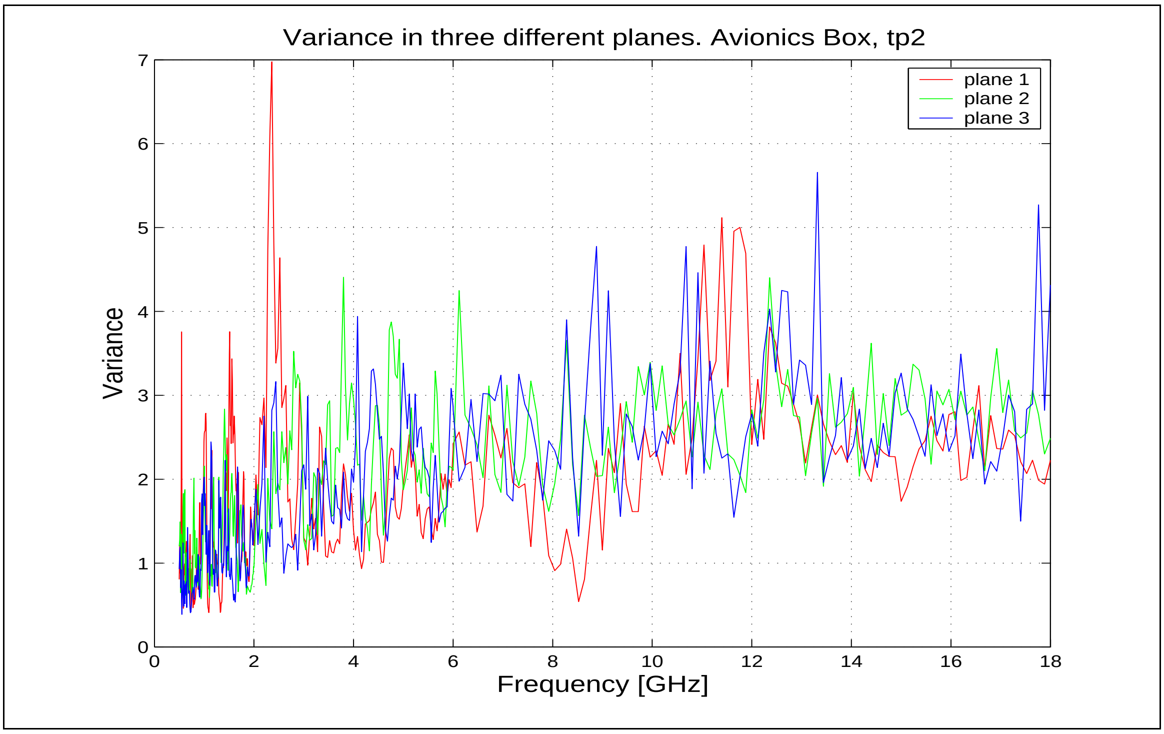

Variance of the received power normalized to mean taken for each plane individually. The Avionics Box, tp2.

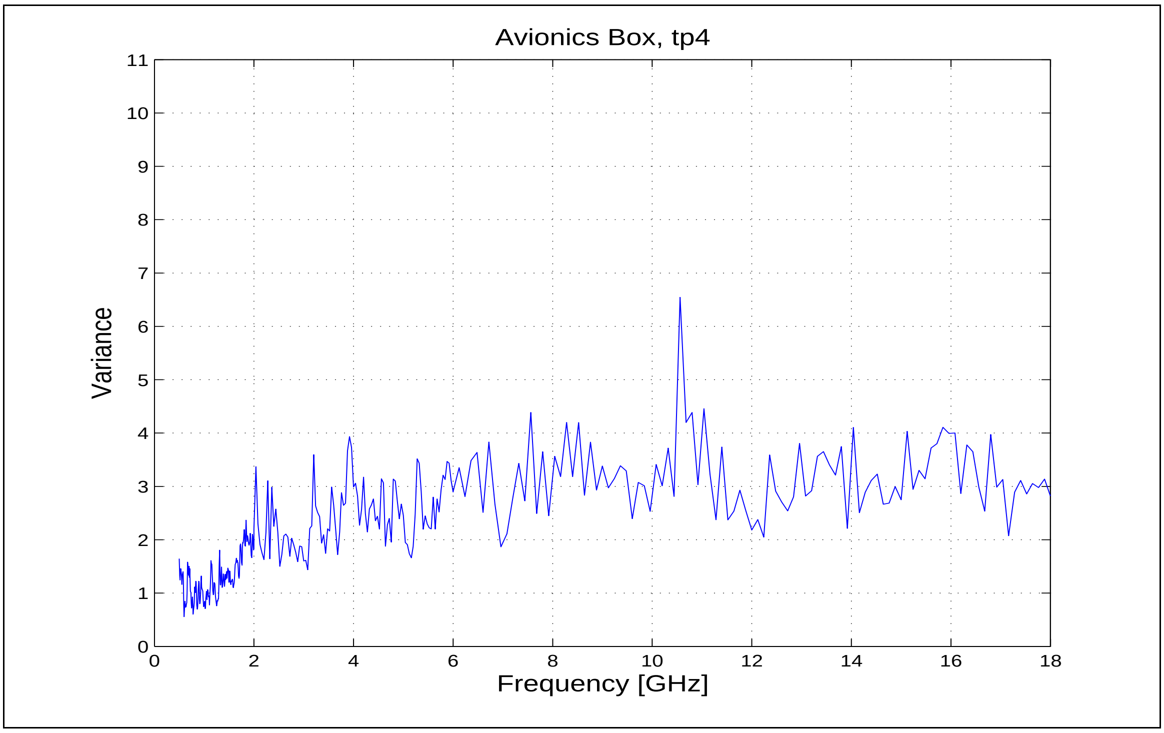

Variance of the received power normalized to mean, taken for all three planes. The Avionics Box, tp4.

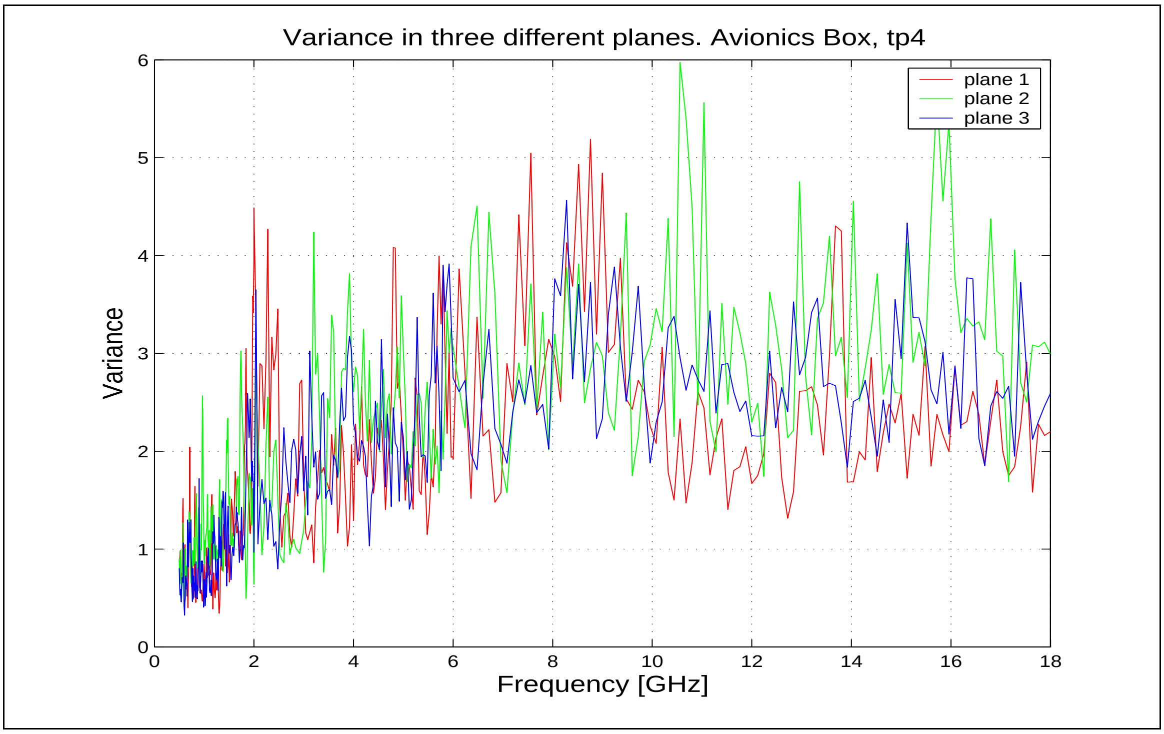

Variance of the received power normalized to mean taken for each plane individually. The Avionics Box, tp4.

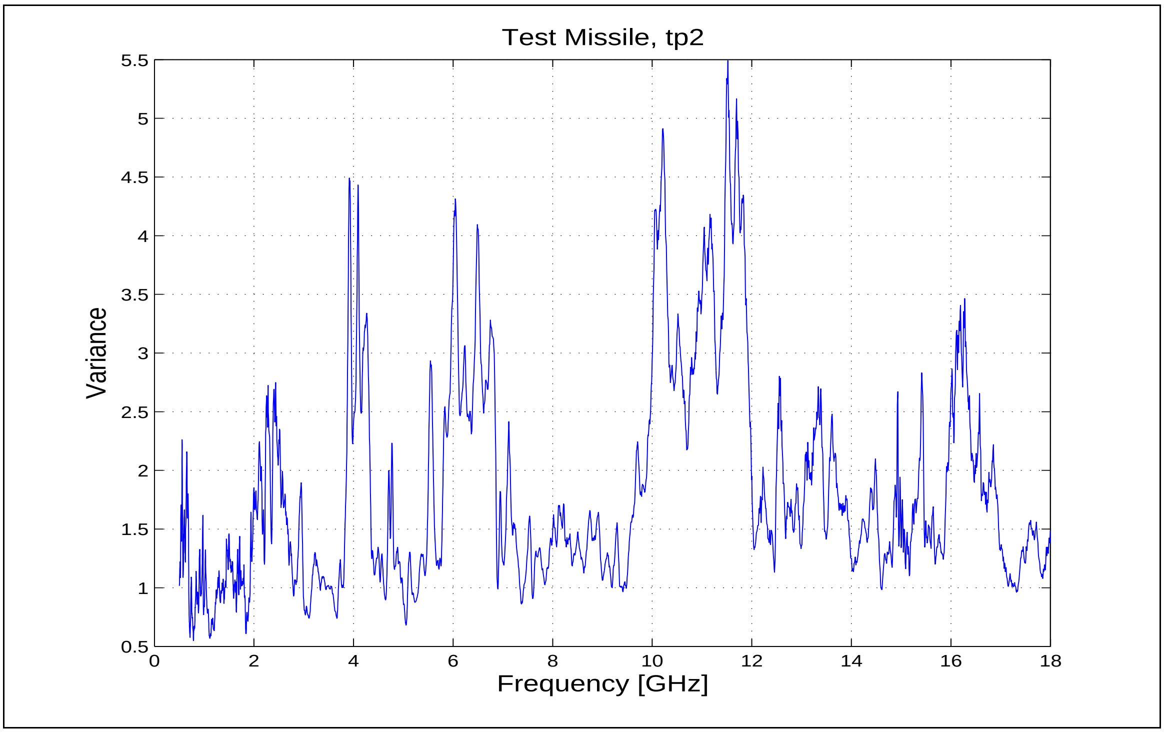

Variance of the received power normalized to mean, taken for all three planes. The Test Missile, tp2.

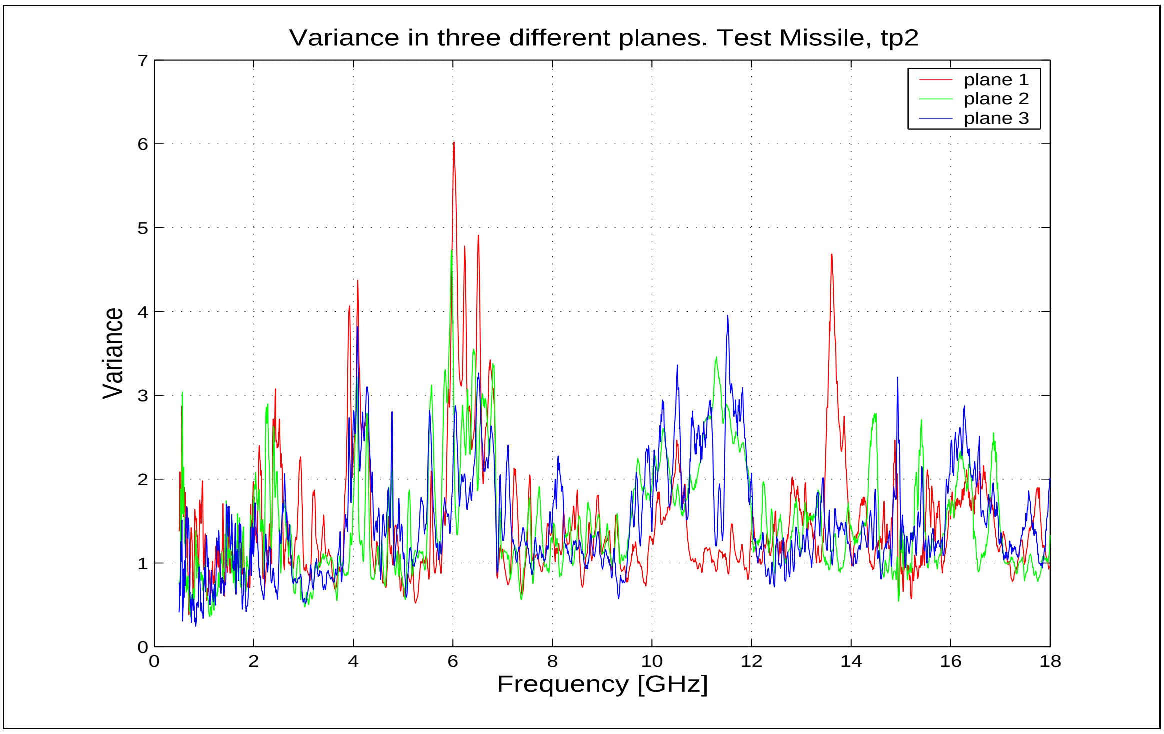

Variance of the received power normalized to mean taken for each plane individually. The Test Missile, tp2.

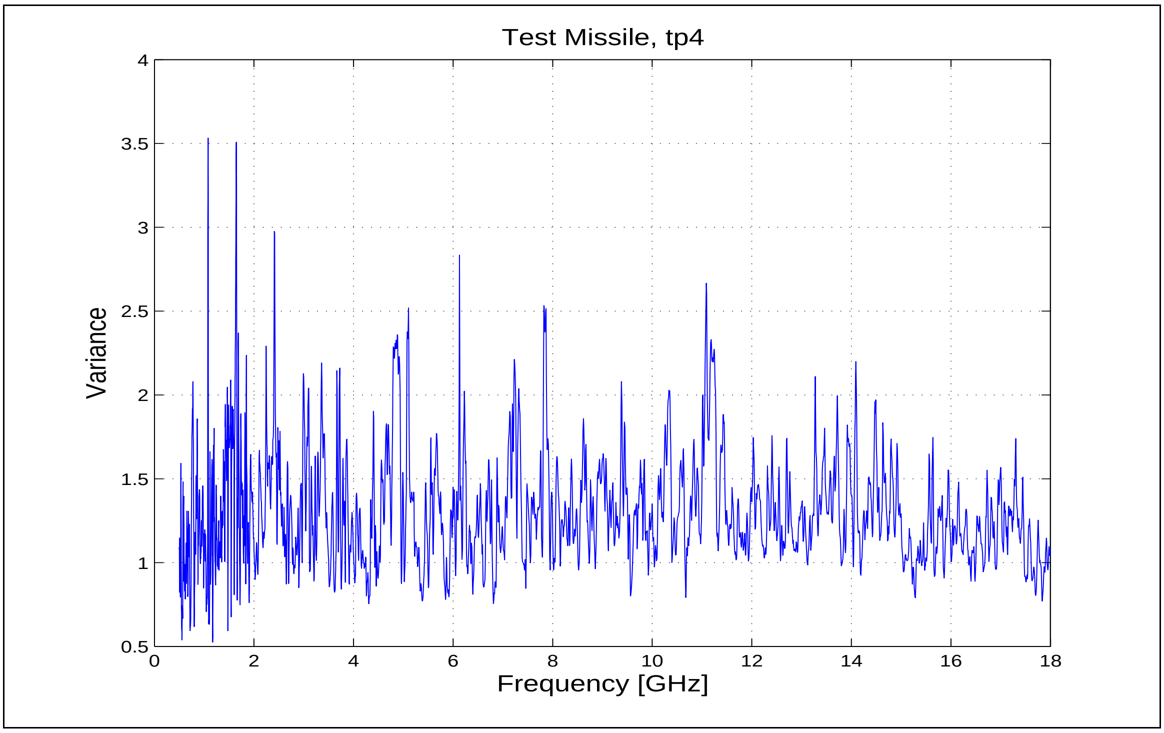

Variance of the received power normalized to mean, taken for all three planes. The Test Missile, tp4.

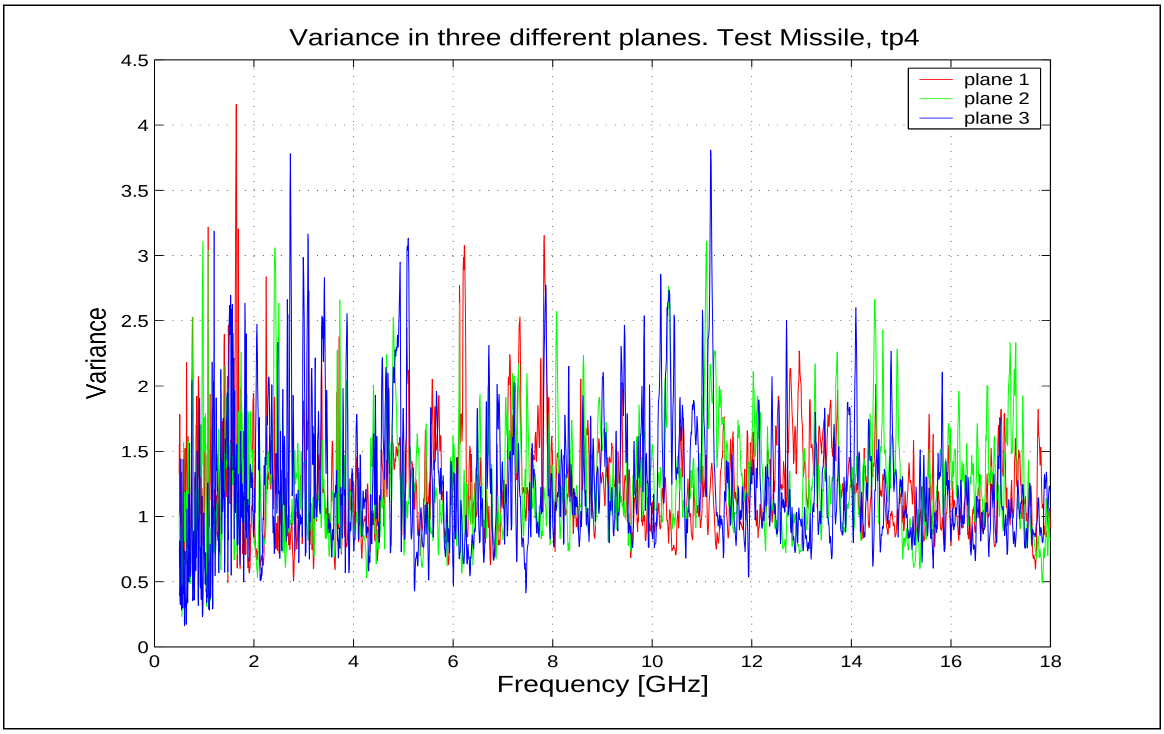

Variance of the received power normalized to mean taken for each plane individually. The Test Missile, tp4.

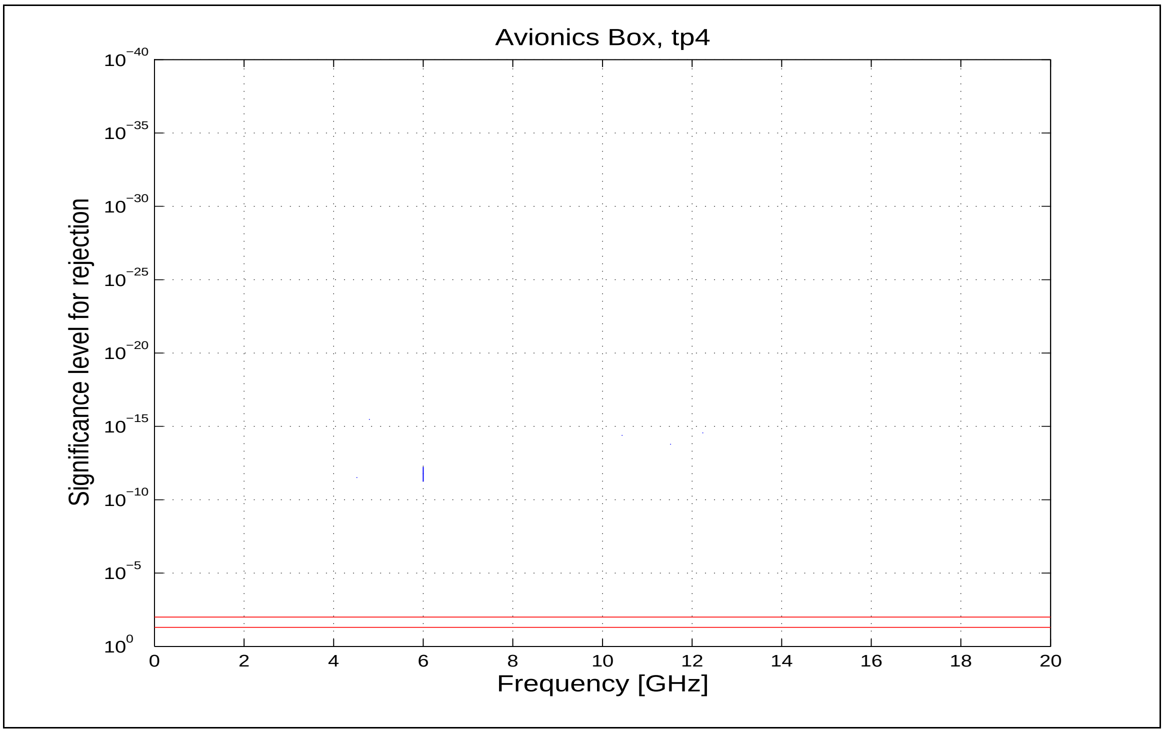

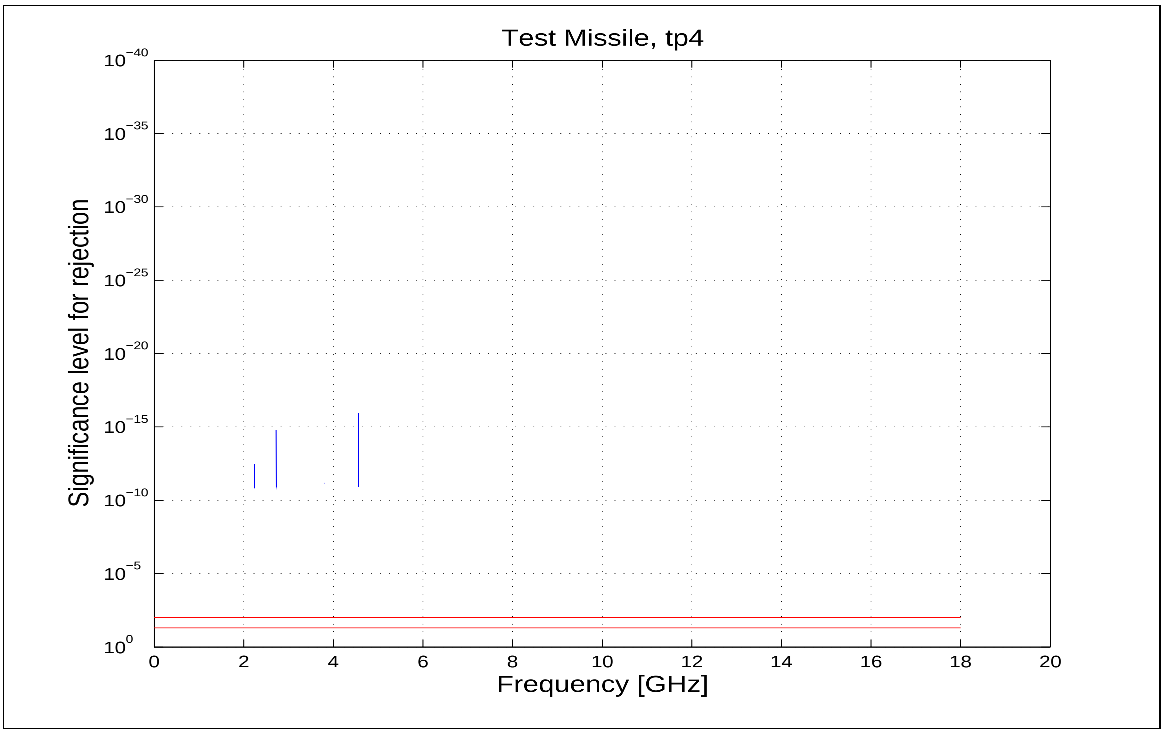

Significance level for rejection for the received power normalized to mean. The Avionics Box tp4 (upper figure) and the Test Missile, tp4 (lower figure). Only a few values of p can be seen; all other values are so small that MATLAB represents them as zeros.